IMPACT OF PROSTATE CANCER GENETIC DRIVERS ON THE DIET-INDUCED TUMOUR MICROENVIRONMENT

M.Sc. thesis presented by

ANDREI FELDIOREAN

Faculty of Medicine

Division of Experimental Surgery

McGill University

April 2020

A thesis submitted to McGill University in partial fulfillment of the requirements of the degree of Master of Science

Abstract

Prostate cancer is the most common cancer in men and a leading cause of cancer-related mortality. Cancer is driven by genetic aberrations that persist and accumulate. Loss of the tumour suppressor gene *PTEN* is frequently observed in early prostate cancer while the additional loss of the *RB1* tumour suppressor gene is associated with more advanced disease. We allografted murine prostate cancer cell lines driven by either loss of *Pten* alone or in combination with *Rb1* in immunocompetent C57BL/6 mice. Critically, combined loss of *Pten* and *Rb1* resulted in a highly aggressive disease with a distinct tumour microenvironment compared to tumour driven by loss of *Pten* alone. Notably, luminex assay showed significant differences in cytokine and chemokine profiles, while flow cytometry data showed altered immune checkpoint ligand expression on tumour cells. Epidemiological studies point to a key role of environmental factors, such as a diet rich in fat, as an etiologic factor in this disease. Accordingly, mice fed a high-fat diet demonstrated an increase in tumour growth irrespective of their genotype. However, analysis of the tumour microenvironment revealed a distinct cytokine and chemokine profile driven by a high-fat diet for each tumour genotype. This suggests that the tumour microenvironment is governed by the cancer cell-intrinsic mechanisms established by the combination of genetic drivers and extrinsic factors such as dietary patterns. Therefore, to fully understand immune infiltration and activation in the tumour microenvironment, additional studies must be performed to dissect the interplay between tumour genetic drivers and diet.

Résumé

Le cancer de la prostate est le cancer le plus fréquent chez les hommes et l'une des principales causes de mortalité liée au cancer. Le cancer est entraîné par des aberrations génétiques qui persistent et s'accumulent. La perte du gène suppresseur de tumeur *PTEN* est fréquemment observée dans le cancer de la prostate précoce tandis que la perte supplémentaire du gène suppresseur de tumeur *RB1* est associée à une maladie plus avancée. Nous avons allogreffé des lignées cellulaires de cancer de la prostate murin entraînées par la perte de *Pten* seule ou en combinaison avec *Rb1* chez des souris C57BL/6 immunocompétentes. De manière critique, la perte combinée de *Pten* et de *Rb1* a donné lieu à une maladie très agressive avec un microenvironnement tumoral distinct par rapport à une tumeur provoquée par la perte de *Pten* seule. Notamment, le test Luminex a montré des différences significatives dans les profils de cytokines et de chimiokines, tandis que les données de cytométrie en flux ont montré une expression altérée du ligand du point de contrôle immunitaire sur les cellules tumorales. Les études épidémiologiques indiquent un rôle clé des facteurs environnementaux, tels qu'un régime alimentaire riche en graisses, comme facteur étiologique de cette maladie. En conséquence, les souris nourries avec un régime riche en graisses ont montré une augmentation de la croissance tumorale quel que soit leur génotype. Cependant, l'analyse du microenvironnement tumoral a révélé un profil distinct de cytokines et de chimiokines entraîné par un régime riche en graisses pour chaque génotype tumoral. Cela suggère que le microenvironnement tumoral est régi par les mécanismes intrinsèques des cellules cancéreuses établis par la combinaison de facteurs génétiques et de facteurs extrinsèques tels que les habitudes alimentaires. Par conséquent, pour bien comprendre l'infiltration et l'activation immunitaires dans le microenvironnement tumoral,

des études supplémentaires doivent être effectuées pour disséquer l'interaction entre les facteurs génétiques tumoraux et l'alimentation.

CONTENTS

LIST OF FIGURES

LIST OF TABLES

LIST OF ABBREVIATIONS

AKT	akt serine/threonine kinase
AR	androgen receptor
BMI	body mass index
CD4	cluster of differentiation 4
CDKN1B	cyclin dependent kinase inhibitor 1B
CTD	control diet
CTL	cytotoxic t lymphocyte
CTLA-4	cytotoxic T-lymphocyte-associated protein 4
DAB2IP	dab2 interacting protein
dKO	double knockout
ERG	ets transcription factor erg
ETS	ets proto-oncogene
EZH2	enhancer of Zeste Homolog 2
G-CSF	granulocyte colony-stimulating factor
GM-CSF	granulocyte-macrophage colony-stimulating factor
GSEA	gene set enrichment analysis
H-2D^{b}	histocompatibility system 2D haplotype b
H-2K^{b}	histocompatibility system 2K haplotype b
HFD	high-fat diet
ICB	immune checkpoint blockade
IFN	interferon
IKK	ikb kinase
IL-2	interleukin 2
Ip10 (CXCL10)	inteferon gamma-induced protein 10
irAE	immune-related adverse event
JAK	Janus kinase
KC (CXCL1)	keratinocyte chemoattractant
KRAS	kras proto-oncogene
LAG3	lymphocyte activation gene 3
LIX (CXCL5)	lipopolysaccharide-induced
MCP-1 (CCL2)	monocyte chemoattractant protein 1
MCP-5 (CCL12)	monocyte chemotactic protein 5
MDC (CCL22)	macrophage-derived chemokine
MDSC	myeloid-derived suppressor cells
MHC	major histocompatibility complex
MIG (CXCL9)	monokine induced by gamma interferon
MIP-1a (CCL3)	macrophage inflammatory protein 1 alpha
MIP-1b (CCL4)	macrophage infammatory protein 1 beta
MIP-2 (CXCL2)	macrophage inflammatory protein 2
MIP-3a (CCL20)	macrophage inflammatory protein 3 alpha
MIP-3b (CCL19)	macrophage inflammatory protein 3 beta
MMP-9	matrix metallopeptidase 9

mTORC2	mechanistic target of rapamycin kinase complex 2
MYC	myc proto-oncogene
MYC	myc proto-oncogene
NF-$_K$B	nuclear factor kappa B
NK	natural killer
NKX3.1	nk3 homeobox 1
OX40L	ligand for OX40 receptor
pAPC	professional antigen presenting cell
PBMC	peripheral blood mononuclear cell
PD-1	programmed cell death protein 1
PD-L1	programmed death-ligand 1
PI3K	phosphoinositide 3-kinase
PIN	prostatic entraepithelial neoplasia
PSA	prostate-specific antigen
pSTAT1	phosphorylated signal transducer and activator of transcription 1
PTEN	phosphatase and tensin homolog
RANTES (CCL5)	regulated upon activation, normal T cell expressed and secreted
RB1	retinoblastoma 1
RICTOR	rptor independent companion of mtor complex 2
SAM	S-adenosyl methionine
sKO	single knockout
SRC	proto-oncogene tyrosine-protein kinase Src
ST2	suppression of tumourigenicity 2
STAT1	signal transducer and activator of transcription 1
TARC (CCL17)	thymus and activation regulated chemokine
TCR	T cell receptor
TGF-β	transforming growth factor beta
Th1	T helper type 1
TIM3	T cell immunoglobulin- and mucin-domain-containing molecule
TMPRSS2	transmembrane serine protease 2
TP53	p53 tumour suppressor
VAT	visceral adipose tissue
VEGF	vascular endothelial growth factor

ACKNOWLEDGEMENTS

I would like to start by thanking Dr. David P. Labbé for the opportunity to study a subject at the crossroads of cancer, immunology and diet through my research project and for the resources required to do so. I felt very fortunate to work on this project. I appreciate the attention provided to support my project and the consistent availability to discuss details of experiments and written work. I would also like to thank my Co-Supervisor Dr. Ciriaco A. Piccirillo, who provided an immunological perspective to the project that helped streamline and focus our efforts. Through the support of my Supervisors, I was offered a learning environment that fostered my scientific thinking.

I would like to take this opportunity to thank Dr. Jacques Lapointe, Chair of my research advisory committee and course Professor, who has often provided me with feedback to develop my understanding of the scientific method and to improve my ability to present scientific works. My Committee Members Dr. Peter Siegel and Dr. Christopher Rudd enthusiastically provided advice to shape future directions of the project – thank you.

I thank the Dr. Labbé Lab. The expertise of Dr. Aurélie Le Page and Dr. Nadia Boufaied in Immunology and Bioinformatics, respectively, made possible the ambitious projects undertaken as part of this thesis. Dr. Le Page served as an additional mentor, teaching me not only techniques necessary to perform my experiments, but *in vitro* and *in vivo* experimental design. Dr. Boufaied was always available to teach and provide valuable input when designing experiments or troubleshooting. I thank Dr. Anna de Polo for freely sharing her knowledge regarding Western blotting, the nuances of protein extraction, and benchwork in general, as well as the useful

conversations regarding various analysis techniques. I thank my labmates Tarek, Janie, and Walaa for being friendly and quick to offer advice and assistance.

I thank the Dr. Piccirillo Lab. I thank Mikhael in particular for his willingness to review and plan experiments related to my own project. Fernando, Roman, Tho-Alfakar, Harry and the entirety of the Dr. Piccirillo Lab were friendly and quick to share their expertise.

I thank Dr. Leigh Ellis for kindly providing the Dr. Labbé Lab with the sKO and dKO murine prostate cancer cell lines that are integral to this study. I also thank the members of the Immunophenotyping Platform, Animal Research Division, and the Small Animal Imaging Labs for their troubleshooting support and expert services.

The work in this thesis was made possible by funding from Canada Foundation for Innovation, Fonds de recherche Santé Québec, Canadian Institutes of Health Research, and McGill University's Division of Experimental Surgery.

The constant and unwavering support of my parents, Daniela and Septimiu Feldiorean, has made possible all that I have accomplished thus far. I thank them for instilling in me a desire to keep learning and growing.

AUTHOR CONTRIBUTIONS

I wrote this thesis and revised it with the aid of Dr. David P. Labbé and Dr. Ciriaco A. Piccirillo.

Experiments were designed with Dr. Labbé, Dr. Piccirillo, and Dr. Le Page. I performed the experiments and interpreted the results. Supervision was provided by Dr. Le Page for experiments with especially challenging technical components. Figures 1-8 are from the literature. Figure 14 food pellet pictures were taken by Dr. Le Page. The data for figure 15B was collected by the Small Animal Imaging Facility. Figures 21-24 were created from the graphs and tables generated by Dr. Nadia Boufaied through R analysis of the Luminex data. I performed the Luminex sample processing and interpreted the R analysis results. I prepared all other figures and the two tables presented.

CHAPTER I

Review of the literature

1.1 Prostate cancer introduction

1.1.1 Prostate function and anatomy

The prostate is a gland of the male reproductive and urinary systems (**Fig. 1**). It is located below the bladder, where it wraps around the urethra [1]. It is roughly the size of a walnut. The structure of the prostate consists of a highly branched network of ducts that are supported by a stroma of connective and muscle tissue. The cells of the ducts produce prostatic fluid, which mixes with sperm and seminal vesicle fluid to produce semen. Hormones such as testosterone and pituitary and adrenal gland secretions help regulate prostate function.

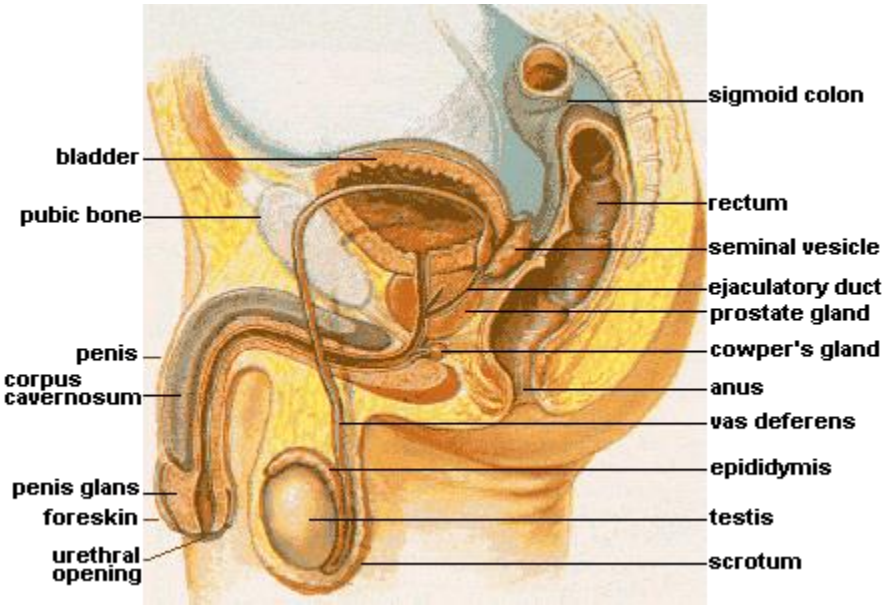

Figure 1: Location of the prostate in the pelvic region [2]. This image is licensed under the Creative Commons Attribution-Share Alike 3.0 Unported license.

1.1.2 Prostate zones

Functionally, the prostate is divided into zones (**Fig. 2**) [3]. The peripheral zone is the largest zone and the point of origin for most prostate cancers. It is checked by a doctor during the rectal examination. The transition zone surrounds the urethra. It expands with age due to benign prostatic hyperplasia, an overgrowth of the prostate cells. The central zone surrounds the ejaculatory ducts originating from the seminal vesicles and malignant transformation rarely occurs there. The fourth zone consists of the anterior fibromuscular stroma. It does not contain any glands and it is rare for malignant transformation to originate there [4].

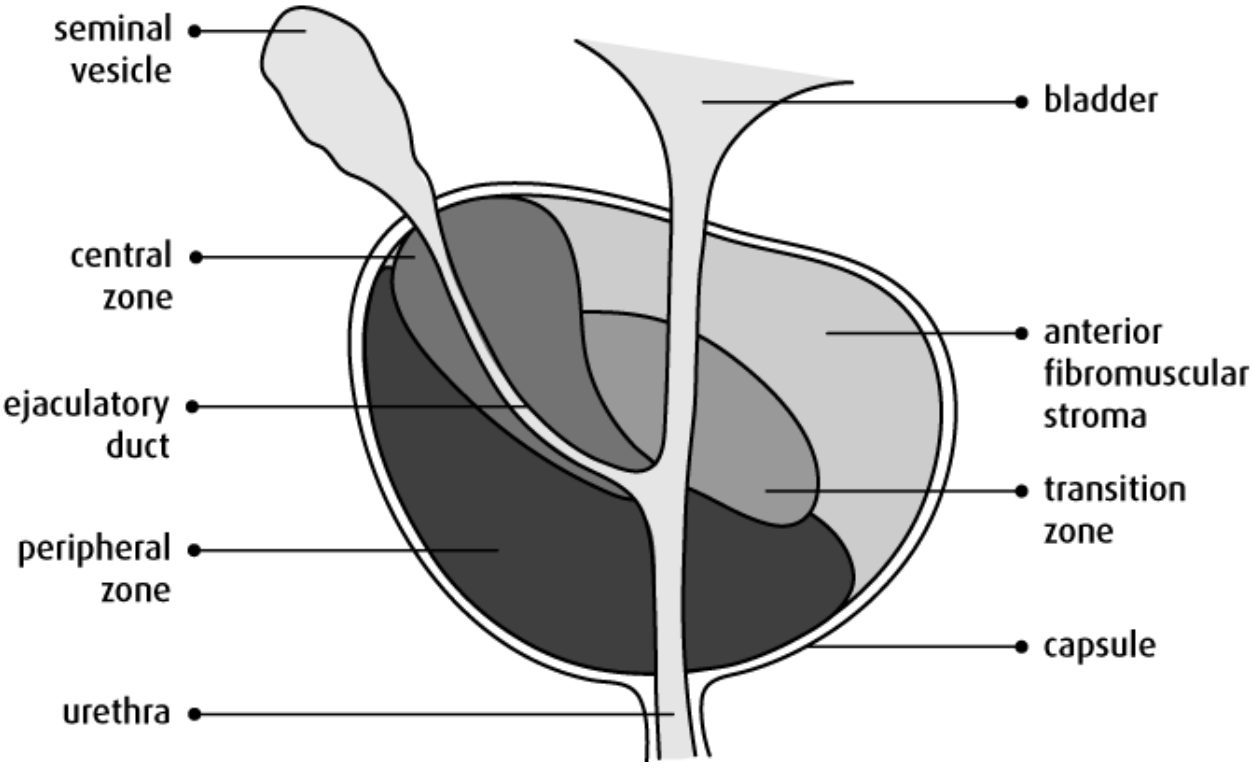

Figure 2: General schematic of the prostate structure [5]. Reproduced for educational and non-commercial purposes. https://www.cancer.ca/en/cancer-information/cancer-type/prostate/prostate-cancer/the-prostate/?region=on

1.1.3 Prostate conditions

There are several conditions that may afflict the prostate and are usually driven by chronic inflammation. Non-cancerous conditions include prostatitis, which can be caused by urinary tract infections or sexually transmitted infections. However, the most common form of prostatic inflammation is non-microbial or in other words, sterile inflammation. Depending on the cause of inflammation, patients may receive antibiotics, alpha-blockers, or muscle relaxants. Benign prostatic hyperplasia is an enlargement caused by overgrowth of the transition zone. It is non-cancerous. Incidence of the condition is correlated with age, abdominal obesity, and lack of physical exercise. Precancerous conditions include prostatic intraepithelial neoplasia (PIN), where epithelial cells lining the secretory ducts look abnormal, but are contained within their tissue type (**Fig. 3**). It may be multifocal: more than one area can be affected. This condition is not treated. Prostate cancer usually begins in the gland cells of the prostate. It is known as prostate adenocarcinoma and it is a multifocal disease[5].

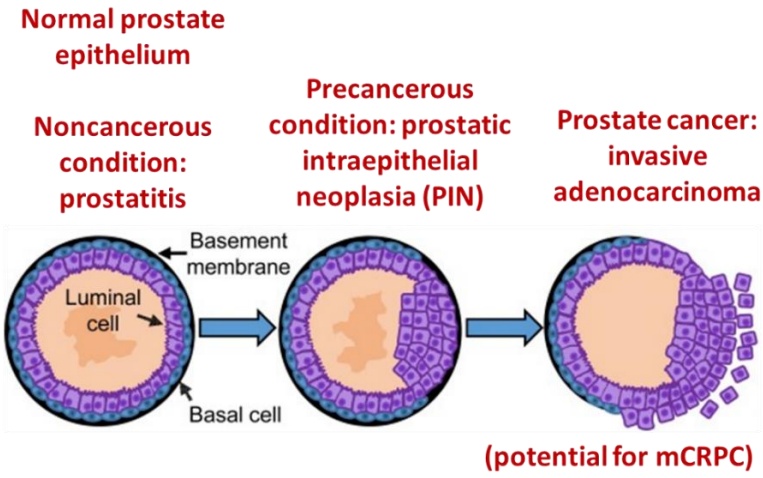

Figure 3: Prostate cancer is generally preceded by precancerous conditions that are driven by chronic inflammation [6]. Original figure modified and used under Creative Commons Attribution 3.0 License. https://creativecommons.org/licenses/by/3.0/legalcode

1.1.4 Prostate cancer statistics

Cancer is the leading cause of death in Canada. About one in two Canadians will develop cancer during their lifetime and one in four Canadians will die from the disease. Lung, breast, colorectal, and prostate cancers are expected to account for nearly 50% of all malignancies diagnosed in 2019. It is estimated that in 2019, 1 in 5 cases of cancer in men were prostate cancer and almost 1 in 10 of cancer-related deaths in men were due to prostate cancer. It has the highest incidence rate of all cancers found in Canadian men and a mortality rate closely trailing that of colorectal cancer [7]. Canadian and American prostate cancer incidence and mortality are predicted to increase from last year. Prostate cancer remains the most common nondermatological malignancy in men and according to American statistics, trails only lung and bronchus cancer in total number of fatalities [8].

1.1.5 Diagnosis of prostate cancer

Diagnosis of prostate cancer has been standardized and screening is routinely performed in Canadian men. The early stage of prostate cancer tends to be asymptomatic. However, tumour growth may put pressure on the urethra, and this has several associated symptoms: increased frequency and urgency of urination, difficulty starting and stopping urination, weak urine flow, and a sensation that the bladder has not fully emptied. There are two widely used screening tools: the digital rectal exam and the prostate-specific antigen (PSA) test. During a digital rectal exam, the physician physically checks the prostate for lumps and hardening. This exam may identify cancer that the PSA test may not identify. However, this method allows the physician to check only part of the prostate [5]. PSA is secreted by prostate gland cells. It is found in both semen and the bloodstream. As the prostate naturally enlarges with age, blood stream levels are higher in older men. However, levels are significantly increased by prostate cancer. While on a per cell

basis, cancerous cells express less PSA than normal prostate epithelial cells, they make up for this by the sheer number of cells that secrete the molecule [9]. PSA serves as an indication of the presence and progression of prostate cancer [10].

1.1.6 Risk factors

Carcinogenesis can be triggered by various intrinsic or extrinsic factors, sometimes combinations of the two. It is believed that roughly only 10-30% of all cancer cases are caused by intrinsic factors such as random DNA replication errors, while 70-90% of cases are caused by extrinsic factors such as exposure to carcinogens [11]. Environmental factors encompass everything that a person is exposed to and ranges from one's eating and exercise habits to the substances that one is exposed to in the workplace. There are several factors of particular importance to increased risk of prostate cancer occurrence [5]:

- Heredity: there is a greater personal risk if the father, brother or son has developed the disease. For example, if the father develops the disease before 60 years of age, risk is increased 2.5-fold [12].
- Bodyweight**:** being overweight or obese increases the risk for prostate cancer occurrence and diagnosis of an elevated stage and grade of disease [13].
- Adult height: the factors that lead to increased growth in childhood may also contribute to the risk of prostate cancer [14].
- Vitamin E and selenium: Vitamin E supplementation increases risk of prostate cancer incidence [15]. Low selenium blood levels increases risk of prostate cancer incidence [16].
- Smoking: may lead to more aggressive or advanced disease [17].
- Androgen levels: increased levels of androgens such as testosterone and dihydrotestosterone are related to prostate cancer growth and development [5].

- Prostatitis: chronic inflammation increases the risk of prostate cancer and metastases formation [18].
- Chemical exposure: contact with pesticides and the heavy metal cadmium has been suggested to increase the risk of prostate cancer [19,20].
- Age: risk rises rapidly after 50 years of age. It is mainly diagnosed in men over 65 years of age [21].

1.1.7 Treatment options

The treatment landscape for prostate cancer is constantly evolving. The sequence of treatment varies with the stage and grade of disease diagnosed. New therapies are being proposed and the sequence of treatment is being modified. However, several treatment modalities are used and will continue to be part of the physician's toolkit for the foreseeable future [22].

- Active surveillance: regular monitoring of the cancer consisting of PSA blood tests twice per year and digital rectal exam once per year. May include biopsies and imaging every 1 to 3 years. This is a common treatment for slow-growing cancer that is confined to the prostate. In older men, the disease may likely never spread, cause symptoms, or lead to death. They will likely die of another condition before the prostate cancer can progress.
- Radical prostatectomy: complete removal of the prostate during early stages of disease. The seminal vesicles are also removed. However, once the lymph nodes are affected, surgery will no longer be effective.
- External radiation therapy: exposure of prostate-confined cancer cells to ionizing radiation gives gradual and cumulative effects. There are generally five sessions per week for seven weeks giving a total dose of 75.6 – 81 Gy of radiation [23]. It may take up to a year before seeing the full results of the therapy. May be combined with prior radical prostatectomy [24].

- Brachytherapy: radiotherapy with either permanent placement of radioactive pellets into the prostate or temporary placement of catheters into the perineum. Effective for relatively indolent disease. May be combined with external radiation therapy [25].
- Cryotherapy: insertion of hollow probes into the prostate and very cold gases are circulated to destroy the prostate tissue. It is not used as a first line treatment, but is an option for men that cannot undergo surgery or radiation therapy [22].
- Hormone therapy: systemic treatment that reduces prostate size and may control spread of metastases. Neoadjuvant hormone therapy consists of hormone therapy followed by another treatment such as radical prostatectomy. Adjuvant hormone therapy is hormone therapy applied after radiation therapy or radical prostatectomy to kill cancer cells that may have been left behind. Hormone therapy consists of regular injections of luteinizing hormone-releasing hormone analogs or antagonists. This impedes the testicles' production of testosterone, the major androgen produced in the body, which leads to a reduction in size of the prostate and the tumour. Orchiectomy is mainly performed when the individual will require hormone therapy for the rest of his life [22].
- Chemotherapy: treatment option for hormone-refractory disease. Docetaxel is given as a first-line chemotherapy. Cabazitaxel, another taxane, is given to patients that fail docetaxel [26]. Taxanes disrupt microtubule formation, therefore inhibiting cell division.
- Second generation hormone therapy: abiraterone acetate inhibits production of almost all androgens, including those produced by the adrenal glands and cancer cells themselves by inhibiting the function of the Cytochrome P450 17A1 enzyme [27]. Enzalutamide reduces the efficiency of androgen receptor translocation to the nucleus and inhibits its binding to DNA and coactivators [28].

1.2 Drivers of disease

1.2.1 Androgen receptor (AR)

AR is a nuclear hormone receptor of great relevance to both normal and transformed prostate tissue. Testosterone, primarily synthesised by the testes, is the most abundant androgen. Testicular androgens are needed for the development and functioning of the prostate, particularly the epithelial cells [29]. Prostate cancer is an adenocarcinoma, so to target these cells in particular, hormone deprivation therapy is a commonly used approach. Androgen deprivation therapy consists of gonadotropin-releasing hormone analogs or surgical castration in combination with antiandrogens such as flutamide. Deprivation leads to rapid cellular apoptosis of the prostate epithelium and involution. Interestingly, paracrine signaling by the prostate stroma is in fact necessary for epithelial apoptosis to occur.

In castration-resistant disease, AR signaling is maintained by an autocrine mechanism. Transformation of the AR signaling pathway is complex. Normal functioning suppresses cellular proliferation, but in transformed tissues, signaling suppresses basal cell proliferation while supporting luminal cell survival [30]. Prostate cancer cell-produced IL-6 mediates androgen-independent AR-related gene activation [31]. Such a prominent role of an inflammatory molecule in a tissue prone to conditions of chronic inflammation suggests the immune system interacts closely with genetic drivers in the development of prostate cancer.

1.2.2 Genetic drivers of disease

Much work has been done towards defining the genetic basis of prostate cancer. Prostate cancer is typically driven by translocations and/or copy number alterations that can ultimately be classified as tumour suppressor loss or oncogene gain. Loss of the prostate-specific tumour

suppressor *NKX3.1* (homeobox protein) leads to PIN and can be used to identify the prostate as the tissue of origin for metastases [32]. Primary prostate cancer is frequently characterized by either the loss of the *PTEN* tumour suppressor gene or amplification of the *MYC* oncogene. Chemical castration is a common first line treatment, but its benefits are only temporary as the disease adapts. Often the cancer recovers through the outgrowth of a castration-resistant subpopulation. As the disease progresses, other mutations tend to accumulate[33].

Copy number alterations and chromosomal rearrangements have been associated with prostate carcinogenesis. In the human genome, *NKX3.1* at 8p21, *PTEN* at 10q23, and *MYC* at 8q24 all undergo copy number alterations: tumour suppressors have copy number loss and oncogenes have copy number gain [34]. It is suggested that complex genome restructuring or "chromoplexy" is able to generate the chromosomal disarray described above with only a few discrete events [35]. While somatic point mutations occur infrequently, abundant DNA translocations and deletions appear in a highly interdependent manner. This suggests copy number loss for tumour suppressors and copy number gain for oncogenes leads to the appearance of disease rather than changes in the proteins themselves [30]. The 8q24 chromosomal region, where *MYC* is located, is amplified in a subset of prostate cancers. It has been demonstrated with a genetically engineered mouse model that *Myc* overexpression forms PIN that progresses to invasive adenocarcinoma [36]. Additionally, overexpression of the MYC protein plays an important role in cancer initiation due to its presence in PIN lesions and carcinomas that lack gene amplification [30].

Most prostate adenocarcinomas undergo chromosomal rearrangements that activate *ETS* family transcription factors such as *ERG*. Seen in 40-50% of prostate tumour foci [37], the *TMPRSS2-ERG* fusion gene creates an ERG protein controlled by an androgen-responsive promoter. The *ETS* family of transcription factors regulate proliferation, differentiation, and apoptosis, among other

processes. This fusion protein is believed to interfere with androgen signaling, disrupting prostate epithelial differentiation [30]. It synergizes with *Pten* loss to create high-grade PIN and carcinoma in mice, suggesting that the genetic event occurs early and may predispose to clinical progression [38].

PTEN (phosphatase and tensin homolog) is mutated or deleted in a variety of cancers, including prostate cancer. Copy number loss of this tumour suppressor is considered an early genetic event in carcinogenesis, but as mentioned before, the accumulation of various mutations appears to be highly interdependent and driven by prostate cell "chromoplexy". Similar to *NKX3.1*, haploinsufficiency may lead to disease, but it also means that there is still some minimal PTEN activity and this may account for why most prostate cancers are relatively indolent [30]. Murine prostate heterozygous *Pten* loss does not progress past development of PIN[39]. Loss of *PTEN* also leads to activation of senescence mechanisms, another reason why prostate cancer tends to be indolent [30]. However, it has been demonstrated in mice that combined *Pten* and *p53* loss leads to invasive prostate cancer due to bypass of the senescence induced by *Pten* loss [40].

Loss of the *RB1* tumour suppressor drives second-line resistant, neuroendocrine differentiated CRPC. It is characterized by downregulation of the androgen receptor and upregulation of several general neuroendocrine markers such as synaptophysin and chromogranin A [33]. Interestingly, loss of *RB1* also reduces senescence, making it a potent second hit to tissues that have already lost *PTEN* [41]. The different genetic alterations described above cooperate to promote the progression of human prostate cancer [42].

Characterization of prostate cancer has highlighted the role of epigenetic modifiers such as *EZH2* in disease initiation and progression [43,44]. Prostate tumours undergo chromatin modifications concurrent with cancer progression. Loss of *Rb1* appears to activate *Ezh2*, leading to the trimethylation of lysine residue 4 (active) instead of lysine residue 27 (repressive) of histone H3.

The change in trimethylation leads to transcription of nearby genes, creating a stem cell-like state that facilitates metastasis, neuroendocrine differentiation, and resistance to androgen deprivation in murine prostate cancer cells [33].

1.2.3 Signaling pathway molecules

Development of cancerous cells requires changes in the genetic material and how that genetic material is expressed, but the impact must translate to a phenotype. mTORC2 and PI3K are important signaling molecules for *PTEN*-loss-driven cancers. Loss of the PTEN protein is indicated to drive up-regulation of the AKT/mTOR pathway in prostate cancer, while stimulation of IKK from the NF-κB pathway is implicated in advanced disease. SRC tyrosine kinases are involved in a positive feedback loop with AR that leads to both castration resistance and cellular proliferation [30].

It was shown that nude mice injected with human prostate epithelial cells lacking *PTEN* could not form tumours if the cells did not have intact mTORC2. Additionally, *Rictor* is a haploinsufficient gene: loss of one copy prevents prostate cancer formation in mice that are *Pten* heterozygous. The demonstration that mTORC2 is necessary for prostate cancer formation in prostate epithelium with *Pten* deletion, but unnecessary for normal function of prostate epithelial cells presents an attractive treatment target for prostate cancer [45].

The PI3K-Akt is a highly conserved signaling pathway involved in cell metabolism, proliferation, and survival. Binding of growth factors to their cognate receptors triggers PI3K to convert PIP_2 to PIP_3. PI3K binds PIP3 to allow PDK1-mediated phosphorylation of T308, leading to partial activation of Akt. This is enough to activate mTORC1, which acts on a plethora of substrates including 4EBP1 and S6K1. mTOR may phosphorylate Akt at S473 to complete its activation. Full Akt activity has consequences on processes ranging from cell growth and

proliferation to apoptosis. PTEN serves to antagonize Akt signaling by converting PIP_3 back to PIP_2 [46].

Similar to PTEN, RB1 acts to prevent the transmission of potentially oncogenic signals to the transcription machinery of the cell. RB1 functions include suppression of tumours, regulation of the cell cycle, apoptosis, and differentiation. RB1 is regularly phosphorylated by the action of proteins such as cyclinD and Cdk4 during cell cycle progression. Hypophosphorylated RB1 acts to inhibit cell proliferation by binding E2F activating proteins such as E2Fs, E2F1, E2F2, and E2F3 that serve to promote progression into S phase. The activity of RB1 also regulates the activity of further downstream, pro-apoptotic proteins such as Arf, p73, and APAF-1. Additionally, the regulation of E2F by RB1 can help stabilize p53 expression to further promote apoptosis [47].

1.3 The immune response

1.3.1 Tumour microenvironment

The accumulation of mutations and outgrowth of different subclonal populations means distinct tumour phenotypes develop that the immune system must recognize [48-50]. The original cancer hallmarks, as described by Hanahan and Weinberg in their seminal review article published in 2000 [51], include self-sufficiency in growth signaling, insensitivity to anti-growth signaling, sustained angiogenesis, evasion of apoptosis, and tissue invasion/metastasis. Immune evasion gained recognition as an emerging cancer hallmark approximately a decade later and increased attention was paid to the interaction of the cancer cells with the immune system [52]. This led to the recognition of another hallmark: evasion of immune destruction. A successful antitumour immune response consists of recognition and elimination of cancer cells. Tumour antigens must be captured

and presented to the immune system [53,54]. Additionally, stimulatory signals must be present for the recruitment and proliferation of effector lymphocytes. These cells must travel into the tumour microenvironment to perform their function. The tumour microenvironment consists of cancer cells, immune cells, and various other cell types such as endothelial cells and fibroblasts. The tumour microenvironment is shaped in part by the cancer[55]. Tumours can modulate the immune response that they encounter [56-59]. The immune compartment of the tumour microenvironment consists of several cell types:

- Cytotoxic T lymphocytes (CTL) kill MHCI+ tumour cells by granule exocytosis and induction of apoptosis by FasL [60]. Secretion of interferon-ɣ (IFN-ɣ) and tumour necrosis factor α (TNFα) produce cytotoxic effects as well.
- Helper T cells contribute to CTL activation through CD40-CD40L interaction and promote proliferation through IL-2 secretion [61]. Additionally, helper cells contribute to the formation of memory CTLs.
- Regulatory T cells control the activity of effector T cells and so, constitutively express PD-1 and CTLA-4. While control of amplitude and duration of immune response limits severe tissue damage as seen with autoimmune disease, it limits effective CTL response to cancer cells [62].
- NK cells represent about ten percent of circulating lymphocytes and perform similar duties to CTLs. NK cells produce perforin and granzymes to kill target cells. They also secrete cytokines such as TNF-α and chemokines such as CCL5 to support the immune response[63].
- Dendritic cells are professional antigen-presenting cells (pAPC) and provide co-stimulation through CD80 and CD86 (signal 2) necessary for effective T cell activation.

They also secrete chemokines such as CXCL9 and CXCL10 that directs activated CXCR3+ T cells into inflamed tissues [61].

- M1-polarized macrophages produce inflammatory cytokines and reactive oxygen and nitrogen species to kill tumour cells in addition to their ability to phagocytose [64].
- M2-polarized macrophages produce anti-inflammatory cytokines to suppress immunosurveillance. They also contribute to angiogenesis and matrix remodeling though release of metalloproteinases that contributes to tumour progression and metastasis formation [64].
- Neutrophils are capable of phagocytosis, release of various cytotoxic compounds, and formation of extracellular nets [65]. They also produce inflammatory cytokines. Macrophages and neutrophils are the most abundant immune cells in the tumour microenvironment.
- B cells contribute to both antigen-presentation and antibody-dependent cellular cytotoxicity. However, through their production of cytokines they have the potential to contribute to tumour progression [66].
- Myeloid-derived suppressor cells (MDSCs) produce MMP9 and VEGF, which enhance angiogenesis and suppress the immune cells infiltrating the tumour microenvironment. Mainly consist of M2 macrophages and granulocytes [66].

Xenograft murine models have been employed in the study of prostate cancer and they demonstrate the importance of the immune system in controlling tumour growth [67]. The first xenotransplantation of human prostate cancer was done in athymic mice of BALB/c background[68]. Nude mice are T cell deficient due to lack of a thymus. Athymic models have been able to recreate in mice the development of lymph node and bone metastases seen in progressive human disease.

Severe combined immunodeficiency (SCID) mice are deficient in mature B and T cells due to a defect in the genetic recombination necessary for lymphoid development. As in the nude mice, NK cells and the myeloid subset are still intact. These mice were used to demonstrate that LNCaP (prostate cancer cell line) engineered to overexpress the tyrosine kinase HER2 could induce androgen independent tumour growth [69]. An alternative to SCID mice, recombination activating gene (RAG) mice lack active RAG1 or RAG2 and are therefore fully B and T cell-deficient [70]. Breeding of the SCID mice with non-obese diabetic (NOD) mice led to the creation of a strain which lost NK cell, complement system, and APC functionality. These mice were used to demonstrate the potential of human prostate cancer to metastasize to subcutaneously implanted human bone in mice [71]. Generally, the more severely immunocompromised the mouse is, the better the prostate cancer will grow. Additional loss of IL2Rγ, found in NOD *scid* gamma (NSG) mice, adds complete NK cell loss to the other deficiencies mentioned. In contrast to human prostate cancer in nude mice that may stop growing and regress after as few as 6 weeks of growth, NSG tumours grow at an accelerated rate and do not regress [72]. The more deficient the immune response is, the better the prostate cancer tumours grow.

Therefore, the immune compartment of the tumour microenvironment in an immunocompetent host is essentially a dysbalanced immune response where subsets of effector and regulatory cells are both present, but effector cells have their cytotoxic subsets suppressed and they differentiate to phenotypes supporting tumour growth. As the tumour develops, the balance may continue shifting in support of the tumour [73]. Genetics, diet, and immunotherapy are among the factors that alter this balance.

The tumour microenvironment of prostate cancer is generally perceived as being poorly infiltrated by effector immune cells [74]. However, comparison of the immune infiltrate of normal

and transformed prostate tissue has identified several populations that are changing along with the prostate microenvironment [75].

- Lymphocyte studies have mixed results indicating the presence of CD4+ and CD8+ T cells, but no consensus whether there is increased infiltration relative to normal tissue. No clear correlation with prognostic markers. Studies have focused on correlations between infiltrating populations and clinical outcome rather than characterization of the functionality of the infiltrating cells [76].
- Presence of T regs, Th1 cells, and Th17 cells. T reg infiltration is increased in transformed prostate tissue. T reg infiltration is significantly associated with reduced progression-free survival and overall survival [77].
- M2 macrophages are associated with advanced disease and higher infiltration than in benign tissue. Recurrence-free survival was reduced in patients with high tumour-associated macrophage counts. These macrophages express high levels of immunosuppressive cytokines, especially TGF-β2 [78].
- Intratumoural and peritumoural mast cells have been implicated in prostate cancer [79].
- No clear prognostic value of neutrophil to lymphocyte ratio in prostate cancer [80].

Several tumour-intrinsic factors contribute to the immune compartment profile of the prostate tumour microenvironment. Prostate cancer has a relatively low somatic mutation burden and therefore low neoantigen expression. The mean mutation frequency in prostate cancer is approximately one-tenth of that of melanoma [81]. MHC-I, needed for neoantigen presentation, is silenced by epigenetic modification in prostate cancer [82]. *Pten* tumour suppressor loss in prostate cancer drives infiltration of the tumour by Gr1+ CD11b+ MDSCs. The phenotype of these MDSCs

can be modulated by the presence of other genetic alterations in the tumour. This points to a role for genetic drivers in the composition of the immune infiltrate in the prostate tumour microenvironment [48].

1.3.2 Interferons

Regulation of the immune system is a complex system in which interferons are important drivers of the immune response. Interferons (IFN) are important modulators of the immune response playing a pivotal role in combatting viral infections. For example, Hepatitis C is treated with IFN-α. The IFN type 1 class includes IFN-α and IFN-β. Most cells can express this class in order to resist viral infections, but plasmacytoid dendritic cells in particular produce large amounts of type 1. The IFN type 2 class includes IFN-ɣ. It is secreted primarily by NK cells and T cells in the context of infection or cancer leading to increased cytotoxicity. While IFNs have been used in the clinical treatment of cancer, evidence suggests that IFN-ɣ may have protumourigenic activities depending on the tumour microenvironment [83]. IFN-ɣ induces TH1 polarization, cytotoxic lymphocyte activation, and dendritic cell tumouricidal activity. However, it stimulates tumours to downregulate MHC expression and upregulate PD-L1 expression [84]. There is much interest in the role of IFN-α and -γ as a bridge between innate and adaptive immunity [85]. The interaction of IFN-α and -γ with dendritic cells may serve as a potent mechanism of anti-tumour immunity [86]. Prostate cancer tumours generally have high inflammation levels driven by interferons [73]. However, lack of immune infiltration coupled with potentially reduced JAK1 signaling in prostate cancer cells[87] means the tumour is protected from the direct (anti-proliferative) and indirect (immune response-stimulating) effects of interferons [88]. IRF7 regulates the immunomodulatory effects of IFN-α. Overexpression of IRF7 in mice with prostate cancer reduces bone metastasis. Additionally, prostate cancer cells upregulate IFN-α signaling pathway-related genes such as *STAT1* when

treated with fractionated doses of radiation. It is believed that upregulation of these genes contributes to the development of radio-resistance [88]. Interferons are known to drive the antitumour immune response[89-91], but the downstream impacts of IFN-γ and IFN-α signaling in the tumour microenvironment of human prostate cancer is not fully known. Better understanding will allow improved application of cancer immunotherapies.

1.3.3 Cancer immunotherapies

Owing to the central role of the immune system in keeping most individuals cancer-free, there is much interest in manipulating the immune system in cancer patients so that it becomes "competent" and targets the disease for destruction. Immunotherapy is one of the latest approaches in cancer treatment and joins more traditional approaches such as surgery, radiotherapy, and chemotherapy. Several immunotherapeutic strategies have emerged for the treatment of cancer:

- Nonspecific immune stimulation is one strategy for generation of an anti-tumour immune response. This is based on systemic administration of interleukins such as IL-2 or interferons such as (IFN-α) [88]. Bacille Calmette-Guérin (BCG) has also been used as an adjuvant in select cancers such as bladder cancer.
- Immune checkpoint blockade consists of inhibiting or modulating the ligand-receptor interactions that regulate the immune system. The immune checkpoints are the multitude of inhibitory pathways of the immune system, particularly of T cells, that ensure self-tolerance is maintained (prevention of autoimmunity) and collateral tissue damage is minimized during an immune response [62]. The ultimate amplitude and quality of the T cell response, initiated through antigen recognition by the T cell receptor, is a balance between costimulatory and inhibitory signals (immune checkpoints) [92]. However, tumours co-opt these mechanisms to evade the immune response. Dampening these mechanisms enhances

antitumour immunity, particularly in melanoma [62]. PD-1, CTLA-4, and their cognate ligands (discussed further in section 1.3.5 beginning on page 20) are often the targets of immune checkpoint blockade.

- Adoptive cell transfer consists of infusing autologous immune cells with antitumour traits. These immune cells can be natural T or NK cells, genetically engineered T cells with tumour antigen-specific TCR, or chimeric antigen receptor (antibody binding domain fused to T cell signaling domain) [88].
- Cancer treatment vaccines help the immune system recognize tumour-associated antigens to be able to attack existing cancer cells.
- Oncolytic virus therapies introduce a virus directly into the tumour. The virus can be cleared by healthy cells of the host, but the cancer cells cannot and die during the life cycle of the virus as it spreads. For example, T-VEC is a therapy based on a modified herpes simplex type-1 virus and has durable responses against melanoma. It is being tested in other cancer types and in combination with checkpoint blockade [93].

Prostate cancer-specific immunotherapies have also evolved:

- Sipuleucel-T is an active cellular immunotherapy. Autologous peripheral-blood mononuclear cells (PBMCs), particularly APCs, are extracted, incubated with antigen prostatic acid phosphatase (present in 95% of prostate cancer cells) and GM-CSF (maturation factor). Treatment increased overall survival of patients with metastatic castration-resistant prostate cancer. No significant difference in disease progression [94].
- Pembrolizumab is an immune checkpoint blockade treatment. It is an antibody that binds to PD-L1, a ligand for PD-1, to avoid the onset of T cell exhaustion. It is accepted as

treatment for metastatic castration-resistant prostate cancer after other therapies, such as Docetaxel and Sipuleucel-T, have failed [95,96]. The highest objective response rate found from the three cohorts of the phase II Keynote-199 study performed on treatment-refractory, metastatic, castration-resistant prostate cancer was 5%, while 60% of all patients developed adverse events [95]. To understand why immune checkpoint blockade is not highly effective in prostate cancer, immune checkpoint blockade must be discussed in more detail.

1.3.4 Immune checkpoint blockade

Immune checkpoint modulation involves suppressing inhibitory checkpoints or activating stimulatory checkpoints using antibodies. Two common treatments are CTLA-4 blockade with Ipilimumab and PD-1 blockade with Nivolumab. Immune checkpoint blockade (ICB) has transformed the therapeutic landscape of several cancer types, especially melanoma [97]. However, immune-related adverse events (irAEs) are a concern due to the more rare, severe reactions, such as colitis, toxic epidermal necrolysis, and endocrinopathies [98], that lead to prolonged hospitalization or even death [99]. Immune checkpoint blockade helps the immune system overcome the tumour's defense mechanisms, but it also removes the regulation that avoids immune-mediated collateral damage of healthy tissues. Another issue with this treatment option, many patients demonstrate resistance to treatment that may be due to poor immune infiltration of the tumour microenvironment or upregulation of other immune checkpoints [100]. Because ICB targets cell-cell interactions, resistance can stem from different cells and their interactions in the tumour ecosystem. Infiltration of the tumour with T cells has been associated with patient survival and improved immunotherapy responses [101], but the determinants that dictate if a tumour will have high (''hot'') or low (''cold'') levels of T cell infiltration are only partially understood. Among multiple factors, malignant cells may play an important role in determining this phenotype.

Immune checkpoint blockade as monotherapy has not been effective against prostate cancer [102,103]. Prostate cancer is known as a cold tumour. This means that the tumour is poorly infiltrated by T cells. ICB efficacy is dependent on the presence of an immune population in the microenvironment that it then allows to become active. However, evidence from other cancers suggests that obesity increases the efficacy of ICB. Mouse data demonstrates that obesity leads to a greater frequency of CD8+ T cells expressing PD-1, TIM3, and LAG3. Researchers identified leptin, a hormone produced by adipose cells and enterocytes that inhibits hunger, as an intermediary for high-fat diet (HFD) disrupting the immune response in the context of melanoma. It appears that leptin signaling under the high-fat condition leads to tumours where PD-L1 and PD-L2 expression predominates as the tumour's mechanism of immune suppression. This makes these tumours particularly sensitive to ICB therapy [104]. PD-1, and other molecules such CTLA-4, serve as checkpoints regulating immune activity that normally aim to limit collateral tissue damage. Blockade of these checkpoints in the context of cancer removes the suppression experienced by effector T cells so that they may kill the cancer cells. This discovery highlights how the environmental factors that lead to carcinogenesis can be leveraged to identify treatments for patients. To understand ICB, it is important to know how T cell activation is regulated.

1.3.5 T cell activation and regulation

T cell activation requires binding of the T cell receptor to peptide-major histocompatibility complex (signal 1), binding of CD28 to CD80 or CD86 (signal 2), and cytokine stimulation (signal 3) that defines the role of the activated T cell. Signal 2 provides both co-stimulation and control of T cell activation. Immune checkpoints refer to the group of pathways that regulate the duration and intensity of immune responses. A successful immune response will clear a pathogen with minimal collateral tissue damage. Immune checkpoints therefore can either promote or suppress

the immune response and can sometimes do both depending on the checkpoint ligand. Being shaped by their environments, tumours will express immune checkpoint profiles that contribute to their continued survival. Activation of these pathways is based on ligand-receptor interactions and therefore are susceptible to blocking with antibodies [62]. It is not known how HFD and diet-induced obesity impact checkpoint ligand expression in prostate cancer and there are many ligands of interest:

- Major histocompatibility complex class 1: MHC class 1 molecules can be expressed by all cells but are not regularly expressed at baseline. They appear on the cell surface during intracellular infection. Cytotoxic T cells recognize the receptor and kill the cell [61].
- Major histocompatibility complex class 2: expressed primarily by professional antigen presenting cells (pAPCs): B cells, macrophages and dendritic cells. Recognition of the receptor by a naive T helper cell primes it [61].
- Programmed Death – Ligands 1 and 2: only one ligand needed for engagement of PD-1. The PD-1 receptor is expressed when T cells become activated. Its role is to limit effector T cell activity in tissues. Persistent expression leads to a state of exhaustion or anergy in antigen-specific T cells. PD-1 also appears on activated B cells, and NK cells. PD-1 is highly expressed on T reg cells and engagement will enhance proliferation of these cells[62].
- CD80 and CD86: provide costimulatory signaling through binding with the CD28 receptor, which provides signal 2. However, they may instead provide inhibitory signaling by binding Cytotoxic T-Lymphocyte Associated Protein 4 (CTLA-4), which regulates the amplitude of T cell activation. CTLA-4 has greater affinity for the ligands than CD28. It both sequesters CD80 and CD86 and delivers a negative signal upon binding. The two

main consequences of CTLA-4 engagement are a decrease in T helper cell activity and an increase in T reg cell activity. CTLA-4 is constitutively expressed on T reg cells [62].

- CD40: costimulatory receptor for APCs that is bound by CD40L on T helper cells. CD40L is transiently expressed on cells under inflammatory conditions. A wide variety of roles in the initiation and progression of cellular and humoral immunity including IgG class switching and germinal centre formation. Depending on the type of cancer, the CD40 pathway can promote proliferation and survival of the tumour cells [105].
- OX40L: expression is induced on pAPCs and engages the OX40 receptor to augment the clonal expansion of effector and memory T cell populations. OX40 suppresses the differentiation and activity of T reg cells. Found to play a role in the development of several inflammatory and autoimmune diseases. Promotes tumour suppression through a mechanism that may include both NK and NKT cells [106].
- Galectin-9: expressed by APCs and interacts with its receptor, T cell immunoglobulin- and mucin-domain-containing molecule (Tim-3, expressed on T helper 1 cells. The interaction appears to negatively regulate Th-1-mediated immune responses by promoting T-cell senescence. This was seen in Hepatitis B virus-associated hepatocellular carcinoma. Galectin-9 is upregulated in the presence of IFN-ɣ [107].

The interaction of PD-L1 and PD-L2 with PD-1 and the interaction of CD80 and CD86 with CTLA-4 have been attractive targets for checkpoint blockade across cancer types. Pembrolizumab and Ipilimumab, respectively, have been applied in the treatment of prostate cancer with limited efficacy and so, continue to be tested in combination with other therapies [74].

Despite the variety of checkpoints that could be targeted, immune checkpoint blockade is only effective if effector immune cells infiltrate the tumour microenvironment.

1.3.6 Cytokines

Cytokines are a broad group of small proteins secreted by immune cells in particular to modulate the behaviour of receptive cells in an autocrine, paracrine, or endocrine fashion [108]. As peptides, they cannot freely cross the lipid bilayer of cells and cells must express receptors in order to respond to encountered cytokines. Specificity of cytokine-mediated cell stimulation induces the recruitment of an immune population with the appropriate functionality for the particular context. Cytokines are considered to be immunomodulatory agents and can be subdivided into several groups including interleukins, interferons, and tumour necrosis factors [108]. Cytokine signaling can be quite complex as one cytokine can be produced by several cell types. Inversely, several cytokines may be needed for the differentiation of a particular cell type. For a CD4+ T cell, antigen presentation and costimulation activate the cell, but the cytokines it is exposed to determines the phenotype [109]. While the exact profile of cytokines needed for the differentiation of a specific T cell subset varies in the literature, for a general example, TGF-β contributes to T reg differentiation (a regulatory T cell subset) while TGF-β combined with IL-6 contributes to Th17 differentiation (an inflammatory T cell subset).

1.3.7 Chemokines

Chemokines are cytokines that govern immune cell chemotaxis to maintain homeostasis and to create inflammation when necessary to eliminate infectious agents or cancerous cells. There are four main subgroups based on the structure of the amino acid chain: CXC, CC, CX3C, XC. The C denotes a cysteine residue while the X means any other amino acid may be present. Several chemokines are recognized for playing specifically inflammatory or homeostatic roles. The

inflammatory chemokines: CXCL1, CXCL2, CXCL3, CXCL5, CXCL7, CXCL8, CXCL9, CXCL10, CXCL11, and CXCL14. The homeostatic chemokines are constitutively expressed and involved in homeostatic leukocyte trafficking: CCL14, CCL19, CCL20, CCL21, CCL25, CCL27, CXCL12 and CXCL13 [110]. Chemokines have been implicated in the antitumour immune response as well as autocrine cancer cell signaling and metastatic niche formation:

CXC Chemokines

- CXCL1/CXCL2/CXCL5 – recruit MDSCs [111]
- CXCL8 (IL8) – the potent recruiter of neutrophils to sites of inflammation [112] also has potential as an autocrine growth factor [113]. Implicated in several processes including angiogenesis.
- CXCL9 (MIG), CXCL10 (IP-10), CXCL11 (ITAC) – known for attracting T cells, signaling from the premetastatic niche facilitates migration of cancer cells to that site [114].
- CXCL12 – while capable of attracting most leukocytes [115], may be involved in tumour progression in obesity and metastasis formation [116].
- CXCL14 – attracts dendritic cells to tumour tissue and contributes to their maturation [117].

CC Chemokines

- CCL2 (MCP-1) – inflames microenvironment and found to promote prostate cancer growth and invasion [118].
- CCL5 (RANTES) – attracts several leukocytes and correlates with prostate cancer metastases [119].
- CCl11 (Eotaxin-1) – known for attracting eosinophils and supports the formation of breast cancer metastases [119].

- CCL19 (ELC) and CCL21 (SLC) – recruitment of lymphocytes and dendritic cells to lymphoid tissues

CX3C Chemokine

- CX3CL1 (neurotactin) – macrophage polarization that promotes tumour growth [120].

Focusing on prostate cancer, CCL2 has been identified as an inflammation-promoting chemokine through its response against tumours mediated by the migration of monocytes and macrophages. The CCL2-dependent STAT3 activation induces EMT, and inhibition of the CCL2 axis leads to an enhanced suppression of the migratory and invasive properties when compared with AR targeting alone. CXCL8 also leads to increased expression of the AR; the CXCL8/CXCR1 axis leads to proliferation, whereas the CXCL8/CXCR2 axis leads to angiogenesis. CXCL6 and CXCL8, the ligands for CXCR1, regulate angiogenesis by promoting the recruitment of neutrophils that are responsible for matrix degradation [121].

1.3.8 Impact of obesity on the immune system

The hallmarks of cancer, established at the turn of the century, were updated a decade later and introduced metabolic dysregulation and immune evasion as emerging cancer hallmarks[52]. Carcinogenesis requires an incompetent immune system that is unable to detect and destroy aberrant cells. Obesity has been shown to modify immune cell populations. Obesity contributes to an immune aging effect known as inflammaging. In practice, affected tissues appear to have aged significantly further than warranted by their chronological age. HIV patients are known to suffer from this phenomenon, however that is driven by infection rather than diet[122]. Lean adipose tissue harbors various anti-inflammatory immune cells, such as eosinophils, M2 macrophages, T helper 2 (Th2) cells, induced natural killer T (iNKT) cells, and T regulatory cells. These immune cells

help in maintaining insulin sensitivity and store extra energy in the form of triglycerides. In obese adipose tissue, the numbers of pro-inflammatory immune cells, including neutrophils, M1 macrophages, mast cells, Th1 cells, and CD8 T cells, are greatly elevated. Th1 cells and CD8 cells produce IFN-γ [123]. Adipocytes, hepatocytes, and macrophages produce type 1 interferons under HFD conditions [124]. Interferons are important drivers of the immune response and contribute to the creation of an inflammatory state. Additionally, T cells, B cells, and monocytes are all known producers of IL-6, another important inflammatory cytokine.

The prostate, like the breast and ovarian tissues, is surrounded by fat tissue. Prostate cancer is often associated with earlier chronic inflammation occurring in the prostate. This suggests that the immune system may play an important role in the onset of disease and subsequent progression. One well described immune system-prostate cancer axis involves the IL-6 cytokine and the androgen receptor. IL-6 is an inflammatory cytokine typically mediating its effects by signaling through the Janus kinase / signal transducer and activator of transcription (STAT) pathway. Il-6 has been shown to cause androgen independent activation of the androgen receptor (AR)-mediated gene activation, an important component of androgen independent prostate cancer progression. IL-6 signals through STAT3, which associates with AR in an androgen-independent, but IL-6-dependent fashion. Blocking STAT3 inhibits AR-mediated gene activation [31]. Adipose tissue is a major source of inflammatory cytokines such as IL-6. Elevated IL-6 levels have been described in obese patients, as well as the adipocytes and adipose tissue-resident macrophages that produce IL-6 [125]. This knowledge of how the immune system is impacted by obesity may be leveraged to fight cancer.

1.4 Role of diet in prostate cancer

1.4.1 Diet and obesity

The importance of diet and diet-induced obesity in carcinogenesis has gathered much attention in recent years and for good reason. In the United States, where more than two thirds of the population are at least overweight, 15-20% of cancer deaths are believed to be caused, at least in part, by being overweight or obese [126]. Very obese women have breast cancer death rates three times greater than women who are very lean according to body mass index (BMI). The relative risk of developing colon cancer doubles in obese men [126]. Similarly, an unhealthy diet, broadly defined in a meta-analysis by Grosso *et al* as consisting of increased meat and alcohol consumption and decreased vegetable consumption relative to healthy diet controls, is found to double the risk of colon cancer in men [127]. Men were also found to generally have higher increases in their risk of developing cancer across tissue types due to being part of the unhealthy diet group than women [127]. This suggests that diet may especially impact males' incidence of cancer.

Since 1980, the worldwide prevalence of obesity has doubled. Obesity is generally defined as a BMI of $\geq$30 kg/m^2. Overfeeding with a high-fat and/or high-calorie diet while engaging in less physical activity results in an energy imbalance and adiposity. Obesity causes insulin resistance, type 2 diabetes, cardiovascular diseases, and several malignancies via systemic inflammation. Obesity also increases insulin-like growth factor 1 (IGF-1) serum levels [126]. Higher IGF-1 levels increase the risk of certain cancers, including prostate [128].

1.4.2 Epidemiological link between diet and prostate cancer

To highlight the importance of environmental and lifestyle factors in the incidence of prostate cancer, a study was performed that compared the incidence of prostate cancer of Japanese

migrants to the incidence in the United States and their ancestral homeland. Incidence was approximately 4 times higher in the US compared to Japan. Japanese immigrants to the United States were found to have an increased prostate cancer incidence relative to men in Japan. The earlier in life that Japanese men immigrated to the US, the higher their risk of prostate cancer became (**Fig. 4**). Japanese men that immigrated to the US early in life, had incidence rates comparable to that of the US-born male population. Interestingly, even men that immigrated late in life saw their risk more than triple [129]. Clearly, hereditary and familial factors alone are not responsible for the increase in prostate cancer incidence and lifestyle factors such as diet must be contributing.

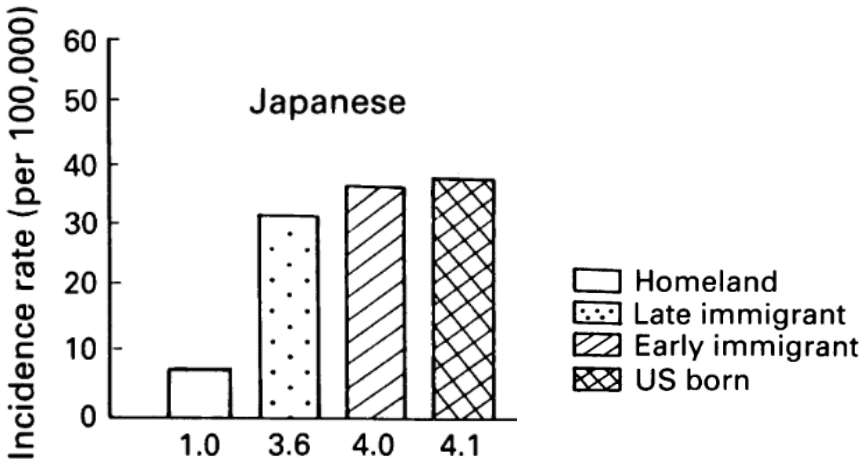

Figure 4: Prostate cancer incidence in Japanese emigrants compared to the general United States-born male population [129]. Incidence increases inversely with age of immigration to US. Adapted by permission from Springer Nature on behalf of Cancer Research UK. Shimizu, H., *et al.* Cancers of the prostate and breast among Japanese and white immigrants in Los Angeles County. *British journal of cancer* **63**, 963-966 (1991).

Epidemiological studies show that HFD increases prostate carcinogenesis and progression. In a study of men with non-metastatic prostate cancer, it was found that a 5% increase in calories coming from saturated fat intake and a 5% decrease in calories coming from carbohydrates gives a hazard ratio of 1.8 for all-cause death and 2.8 for death caused by prostate cancer. Switching 10% of calories from carbohydrates to vegetable fats led to a 33% decrease in all-cause mortality [130]. Similarly, obesity, as defined by elevated BMI, is associated with prostate cancer-specific mortality and biochemical recurrence. A 5kg/m^2 increase in BMI was found to be significantly associated with at least a 15% increase in risk of prostate cancer-related death or biochemical recurrence (**Fig. 5**) [13].

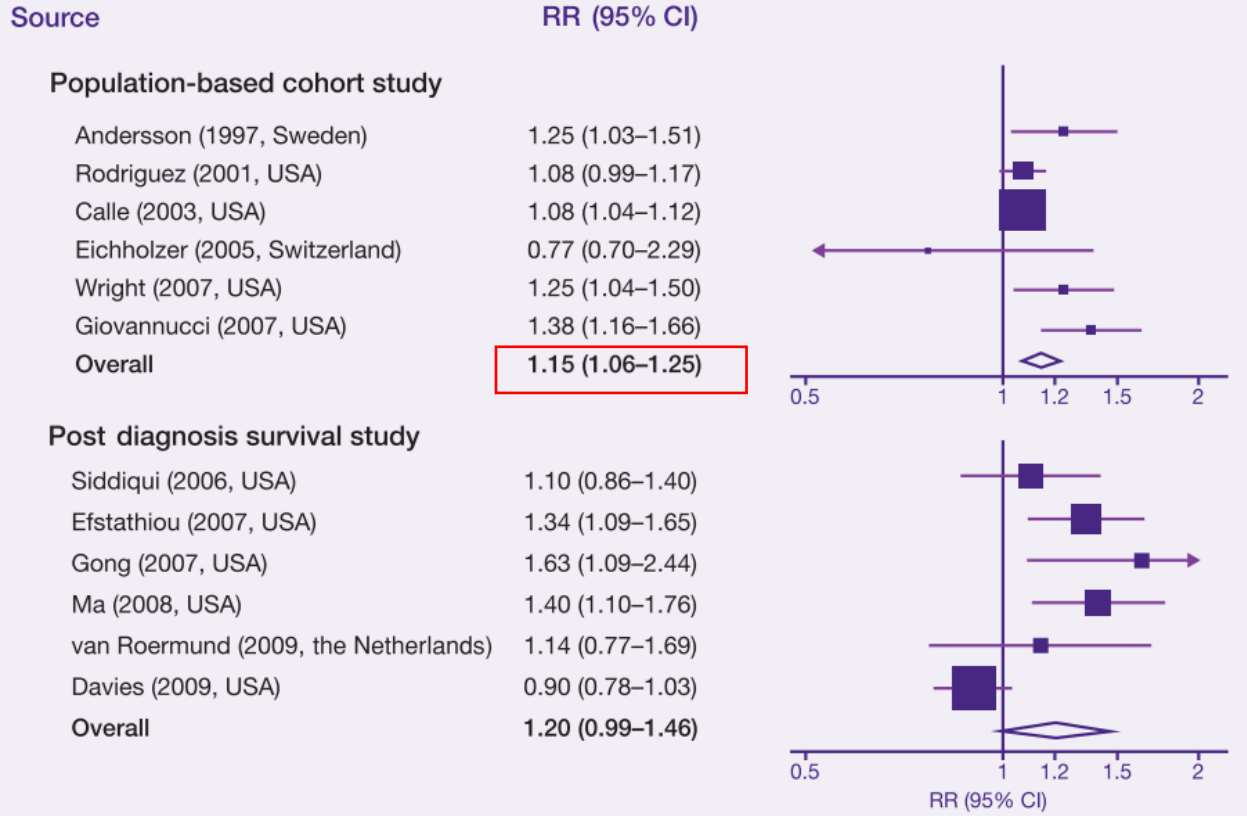

Figure 5: Meta-analysis reveals relative risk for prostate cancer-specific mortality increases by 15-20% per 5 kg/m2 increase in BMI [13]. Adapted with permission from AACR. Cao, Y. & Ma, J. Body mass index, prostate cancer-specific mortality, and biochemical recurrence: a systematic review and meta-analysis. Cancer prevention research (Philadelphia, Pa.) 4, 486-501 (2011).

1.4.3 Biological evidence linking diet to prostate cancer

While a great number of solid tumours exhibit the Warburg effect, prostate cancer does not display this phenotype. The Warburg effect refers to the reliance of most cancer cells on aerobic glycolysis, an inefficient method of generating ATP, instead of mitochondrial oxidative phosphorylation [131]. Early prostate tumours rely on lipids rather than the increased glucose uptake seen with many malignancies [132]. The prostate is known to be surrounded by fat tissue and so may be particularly sensitive to changes in body fat due to diet. It is only after significant disease progression where several mutations have accumulated that the Warburg effect appears in prostate tumours[132]. Identifying the differences between the metabolic processes of benign prostate tissue and prostate cancers will lead to increased understanding of cancer initiation.

Biomolecules obtained through the diet may serve as substrates or cofactors for the epigenetic remodeling supporting prostate carcinogenesis [133]. Epigenetic marks such as DNA methylation and histone modification regulate the state of a cell. In prostate cancer, DNA methylation is widely impaired and leads to transcription of sections of the genome normally left unexpressed. This can lead to genomic instability, an important driver in many cancers as well as the activation of proto-oncogenes such as *MMP2*, a metalloproteinase. Enrichment of histone acetylation (e.g. H3K9ac) is also a feature of prostate cancers. A cyclic metabolic process known

as one-carbon metabolism is central to epigenetic modification because it generates SAM, the primary methyl group donor (**Fig. 6**). The Hi-Myc model, a genetically engineered mouse model of *MYC* oncogene overexpression, was used to study the effects of methyl-rich diets (enrichment of choline, betaine, folic acid, etc.) on prostate cancer. Mice fed the diet with increased methyl donors in utero do not develop higher grades of prostate cancer while their control diet (CTD) counterparts do [134]. While this data demonstrates the role of the diet in prostate cancer progression supported by epigenetic modification, it does not draw a molecular link to lipids [133].

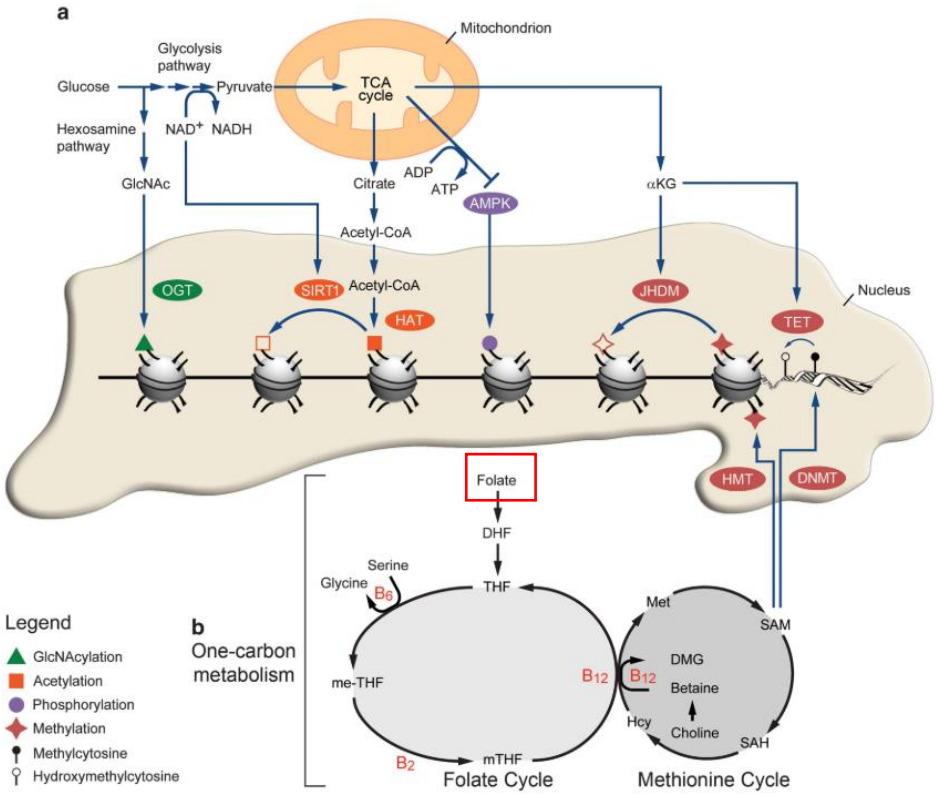

Figure 6: Metabolites provided by the diet, such as folate, contribute to the maintenance and remodeling of the epigenome [133]. A) The metabolism has a broad impact on epigenetic regulation. B) Folate is essential to one-carbon metabolism and DNA methylation. Original figure modified and used under Creative Commons License 4.0. http://creativecommons.org/licenses/by-nc-sa/4.0/

Various mouse models have been developed to study the role of diet in prostate cancer. The TRAMP mouse model has been used to demonstrate that an increase in both dietary fat and dietary cholesterol, representative of a Western diet, significantly accelerates prostate tumour progression [135]. The TRAMP prostate cancer mouse model is driven by pRb, p53, and PP2A inactivation caused by SV40 Large T and small t antigen expression in the prostate tissue [136]. However, this study did not identify the exact contributions of fat and cholesterol to the observed tumour phenotype. Another study using the Hi-Myc model demonstrated that a low-fat diet delays tumour progression. This study also found that a calorie-restricted diet reduced the incidence of localized adenocarcinoma when compared to overweight mice (fed a 10% fat diet) and obese mice (fed a 60% fat diet). The tumour progression seen with the TRAMP model is also attributed to excessive calorie intake. Work was also done to identify specific molecules driving the diet-caused phenotype. This led to a study comparing Omega-3 fatty acid-rich diet with Omega-6. Mice with prostate cancer driven by *Pten* loss in the prostate epithelium demonstrated that the Omega-3-enriched diet led to a relative reduction in prostate cancer growth and progression and increased mouse survival [137]. Interestingly, insertion of an Omega-3 desaturase (converts Omega-6 to Omega-3) into mice fed the Omega-6 diet leads to the less aggressive tumour phenotype seen with the Omega-3 diet.

More recently, it has been shown that saturated fat consumption mimics overexpression of the *MYC* oncogene [138]. MYC (c-Myc) is a master regulator of both cellular growth regulation and cellular metabolism. MYC makes it possible for the transformed cell to support the increased need for nucleic acids, lipids, and proteins that occurs with increased cellular proliferation. At the same time, MYC overexpression causes changes in gene expression that leads to the increased cellular proliferation. In prostate cancer, *MYC* oncogene gain is a prominent driver of the disease. The

protein is overexpressed at early stages of the disease and so, overexpression of the protein in the ventral lobe of the Hi-Myc FVB mouse prostate faithfully recreates the primary disease seen in men. The dorsolateral and anterior lobes also express the protein to some degree, but the ventral experiences complete penetrance in this mouse strain. Since this is a spontaneous disease model, mice will eventually develop the disease as they age, but with different diets provided to these animals, it was possible to examine diet-dependent onset of disease and its progression (**Fig. 7**). Mice were fed either CTD with 10% of calories coming from fat or HFD where 60% of calories came from animal fat, rich in saturated fat. Mice on the HFD developed the hallmarks of diet-induced obesity: increased body weight, liver steatosis, hyperinsulinemia, and hyperglycemia. Researchers identified a fat-induced MYC-related transcriptional signature associated with disease aggression (**Fig. 8**). The MYC-driven metabolic and epigenetic reprogramming driving prostate carcinogenesis can be amplified by HFD, highlighting their possible contribution to the development of a more aggressive disease [138].

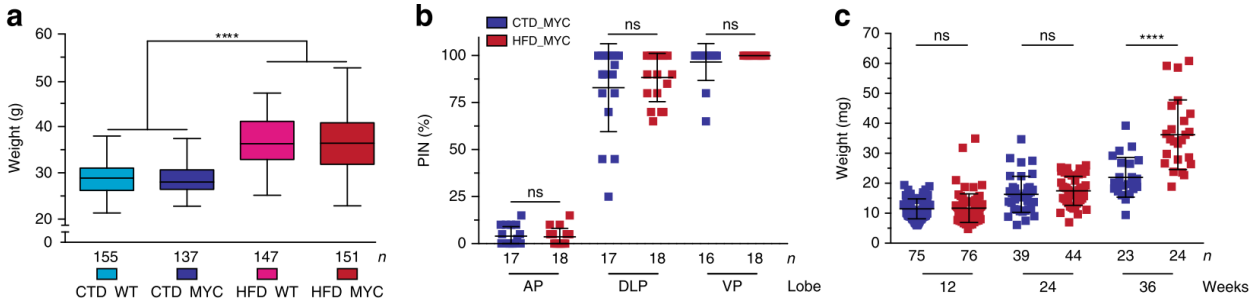

Figure 7: Mice on high-fat diet become obese and subsequently develop larger tumours.

A) Mice develop obesity by 12-weeks of age regardless of WT or Hi-MYC genotype. B) HFD-fed Hi-MYC mice do not experience an increased occurrence of PIN at 12 weeks of age but C) leads to greater tumour burden by 36 weeks of age [138]. Original figure modified and used under Creative Commons License 4.0. http://creativecommons.org/licenses/by/4.0/

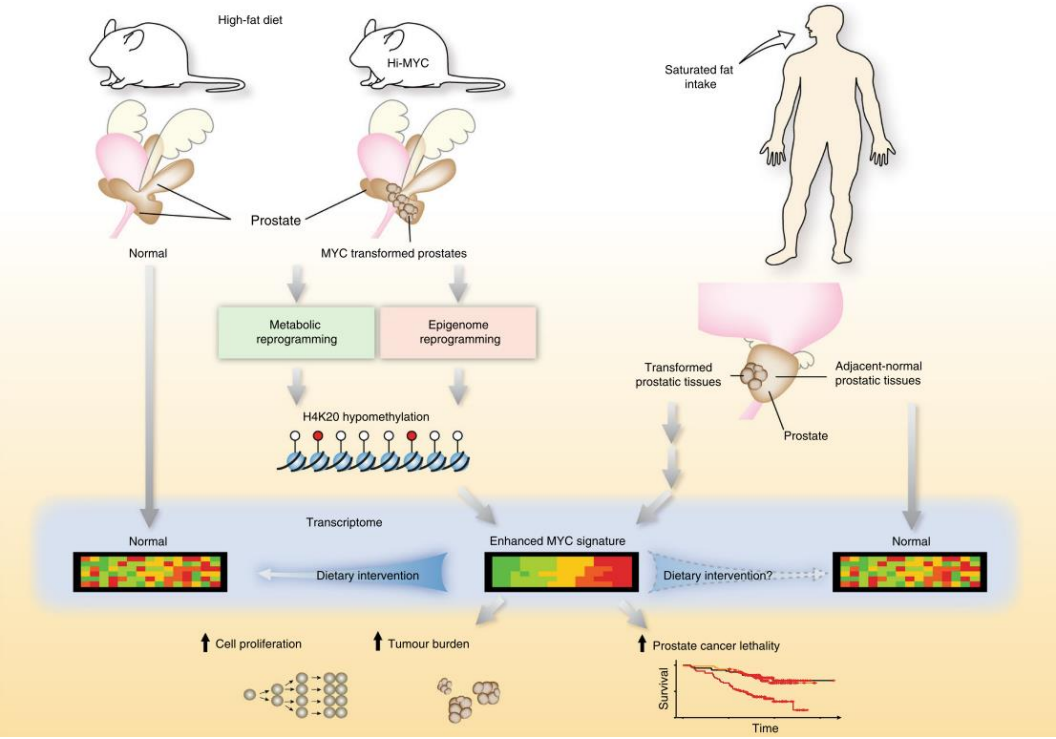

Figure 8: High-fat diet induces the MYC signature associated to prostate carcinogenesis and progression [138]. Original figure modified and used under Creative Commons License 4.0. http://creativecommons.org/licenses/by/4.0/

1.5 Research objectives

Rationale: prostate cancer is the most prevalent cancer in men and a leading cause of cancer-related mortality. The body of knowledge on genetic drivers of disease and their impact on the tumour microenvironment is incomplete. Evidence points to a key role of environmental factors such as diet, as contributing to the etiology of this disease. Indeed, epidemiological studies have reported that saturated fat intake and obesity are associated with increased prostate cancer progression and mortality, but the mechanistic underpinnings of this link remain elusive.

Interestingly, while the immune system has been recognized as an important component of carcinogenesis and progression, how genetic drivers and diet interact to create a disease-conducive microenvironment is unknown. Preliminary gene set enrichment analysis (GSEA) data, from the Hi-MYC FVB mouse model, demonstrated distinct tumour tissue IFN-α and IFN-γ signatures that are enriched by HFD [138].

Hypothesis: given that genetic drivers and diet impact the host inflammatory response, we hypothesize that the prostate tumour microenvironment is governed by the cancer cell-intrinsic mechanisms established by the combination of genetic drivers and extrinsic factors such as dietary patterns.

Objectives: based on the hypothesis that genetic drivers and diet promote prostate cancer by modulating the tumour microenvironment, we aim to pinpoint the underlying immune-related mechanisms supporting the development of an aggressive disease. We will achieve this objective by addressing the following three aims:

1) Characterize the impact of IFN-α on immune checkpoint ligand expression *in vitro*;

2) Determine the impact of genetic drivers and diet on tumour immune checkpoint ligand expression *in vivo*;

3) Compare the impact of genetic drivers and diet on cytokines of the tumour microenvironment.

Research design and methods: Our experimental design focuses on the use of two murine prostate cancer cell lines of C57BL/6 mouse background, representing oncogenic events central to human prostate carcinogenesis and progression, namely *Pten* tumour suppressor loss and combined *Pten* and *Rb1* tumour suppressor loss. Importantly, this approach provides clinically relevant prostate cancer models that can be manipulated in order to dissect mechanisms at the molecular level while remaining compatible with the use of immunocompetent mice as tumour

hosts (syngeneic model), a prerequisite to study the impact on the tumour microenvironment *in vivo*.

Contributions to the advancement of knowledge: The project addresses fundamental knowledge gaps in regard to the interplay between tumour genetic and diet-related mechanisms in modulating the tumour microenvironment to create conditions conducive to disease progression.

CHAPTER II

Methods

2.1 Cell culture

sKO and dKO cell lines (kindly provided by Dr. Leigh Ellis, Dana-Farber Cancer Institute) described in *Ku et al. Science. 2017* were kept in culture at 37° Celsius and 5% CO_2. Both cell lines are derived from spontaneous prostate tumours developed by mice of C57BL/6 genetic background. The sKO is driven by *Pten* loss and the dKO is driven by combined *Pten* and *Rb1* loss in the prostate epithelium. The PBCre4 transgene [139] was used to delete the floxed alleles. The cells were maintained in Dulbecco's Modified Eagle Medium (DMEM) (Wisent 319-015-CL) + 10% FBS (Life Technologies 12483020) and penicillin/streptomycin (Fisher Scientific SV30010). DMEM has higher concentrations of vitamins and amino acids than the minimal essential medium developed by Harry Eagle [140], making it suitable for the culturing of a broad range of adherent cell types.

2.2 IFN-α-stimulated pSTAT1 readout Western blot

6-well plates were used. The conditions were prepared in duplicate: 0 min (non-treated), 10 min (non-treated), 10 min (treated), 30 min (non-treated), and 30 min (treated). The dKO cells were counted using the Neubauer hemocytometer. The cells were resuspended in a volume of media that led to 50,000 cells being seeded per well when 2 ml of the suspension were added. The seeded cells were left in the incubator overnight.

For each condition with stimulation, 10 µl of IFN-α (BioLegend 752804) was added per 2 ml of suspension and kept in the incubator for the respective duration. The final concentration was 100 U/ml or 1.67 ng/ml of IFN-α per well. The cells were washed with 1 ml of PBS.

Triton-X lysis buffer had 1 phosphatase inhibitor tablet (ThermoFisher A32957) and 1 protease inhibitor tablet (ThermoFisher A32955) added fresh per 10 ml total of buffer. 120 µl of Triton-X lysis buffer (+) was added to each condition and to no more than 12 conditions at a time. This was left on ice an additional 2 minutes. Cells were scraped and transferred to Eppendorf tubes on ice. The tubes were left on ice an additional 5 minutes. Centrifugation was 10 min, 13000 rpm, 4˚C. The lysate was frozen at -80˚C.

Protein were quantified using the Pierce BCA protein assay (ThermoFisher A53225). The loading dye stock consisted of 900 µl 4x Laemmli buffer (Bio-Rad 161-0747) and 100 µl beta-mercaptoethanol (Bio-Rad 1610710)

Tris-glycine SDS-polyacrylamide gel electrophoresis was performed. 8% homemade acrylamide gels or pre-cast Mini-Protean TGX gels (Bio-Rad 456-8124) were used. 20 µg of sample was added per well. Molecular weight ladder (Bio-Rad 161-0373) was also loaded.

The nitrocellulose membrane and sponge paper stack were soaked with transfer buffer (Bio-Rad 1704271). Transfer was done using the Trans-Blot Turbo Transfer System (Bio-Rad 1704150). Ponceau reagent was added to the membrane. After confirming the transfer was successful, the membrane was rinsed with water.

The membrane was incubated on a shaker at room temperature for 1 hour with 5% skim milk in TBS.T. It was rinsed with water and split in half between the 75 kDa and 50 kDa bands. The top half was incubated with pSTAT1 (Cell Signaling 9167) 1:10,000 5%BSA-TBS overnight on the cold room rocker.

The bottom half was incubated with beta-actin (Cell Signaling 4970) 1:40,000 5%BSA-TBS overnight on the cold room rocker. The primary antibodies were collected, and 5% sodium azide was added to a final concentration of 0.02% (20 μl per 5 ml). 5 washes of 5 min with roughly 20 ml of TBS.T were performed.

Each membrane half was incubated with anti-rabbit secondary (Jackson ImmunoResearch 111-035-003) on a rocker at room temp for 1 hour. A 1:10,000 5%BSA-TBS.T mixture was used for pSTAT1. A 1:40,000 dilution was used for the β-actin-stained membrane. 5 washes were performed.

Each membrane was incubated for 5 minutes with 2 ml of Clarity Western enhanced chemiluminescence substrate (Bio-Rad 1705061). The substrate is a 1:1 mix of peroxide and enhancer. After the 5-minute incubation, the membranes were immediately taken to the dark room and Amersham Hyperfilm ECL (GE Healthcare 28906835) was exposed to the membranes for 30 seconds to 1 minute. The film was developed and the exposure time was adjusted if it was necessary. The film was scanned and saved as a TIFF format image.

The top half of the membrane was stripped for 20 min with 5 ml of stripping solution (2 litres – 200ml 10% sodium dodecyl sulfate, 3.76g glycine, completed with water and pH adjusted to 2 using hydrochloric acid) at room temperature. It was washed twice. The protocol was repeated from blocking onwards but with the total STAT1 antibody (Cell Signaling 14994).

ImageJ (NIH Bethesda, USA) was used for analysis. The intensity of the pSTAT1 bands were normalized by the actin values.

2.3 Immune checkpoint ligand expression of IFN-α-stimulated dKO cells

For each condition with stimulation, the final concentration was 100 U/ml or 1.67 ng/ml of IFN-α (BioLegend 752804) per well of 50,000 cells seeded the day before. Duration from treatment to harvesting varied (**Fig. 9**).

Washing was done with 500 ul of D-PBS and 150 ul of TrypLE Express Enzyme, no phenol red (Thermo Fisher Scientific 12604013) was added per well (pre-warm trypLE at 37˚C). This was kept in the incubator for 10 minutes and then it was checked for cell detachment.

150 ul of D-PBS was added to dilute the TrypLE, the cells were transferred to a 1.5 ml Eppendorf tube, and were centrifuged for 5 min at 300g. The supernatant was carefully aspirated and 200 ul of PBS- 50% fixation buffer (Biolegend 420801) prewarmed to room temperature was added. The cells were incubated on ice for 10 minutes. The samples were transferred from Eppendorfs to a 96-well plate. The cells were centrifuged at 300g for 5 min and the supernatant was aspirated. The cells were resuspended in 200 ul of PBS - 2% BSA, centrifuged, and washed again.

The cells were incubated with 100 ul of FC block (Invitrogen 14-0161-86) diluted 1:100 in 2%BSA-PBS for 20 min on ice. The compensation samples were prepared: one well with 200 ul of PBS for each antibody used. One drop each of positive and negative compensation beads (Invitrogen A10497) was added.

Afterwards, cells were centrifuged, aspirated, and resuspended in their respective antibody cocktail (**Table 1**). Each sample received half a test (volume that stains 1 million cells in 100 ul of buffer). Test size was calculated based on the concentration of the antibody (0.2 mg/ml means 5 ul is the test size). The compensation beads were simultaneously stained. 2.5 ul of the respective antibody was added to each compensation sample. After 30 min staining on ice, in the dark, the

unbound antibodies were removed by 2 washes with ice-cold PBS – 2% BSA. The samples were placed in individual polystyrene FACS tubes in preparation for flow cytometry.

Samples were acquired using a LSRFortessa X-20 Cell Analyzer (BDBiosciences 657669) and the FACS-DIVA software (5000 events for compensation beads). Instrument is maintained by the Immunophenotyping Platform at the Research Institute of the McGill University Health Centre (Montreal, Canada). Both the experiment and FCS 3.0 file formats were exported. The FlowJo program (Becton, Dickinson & Company) was used for analysis of the data.

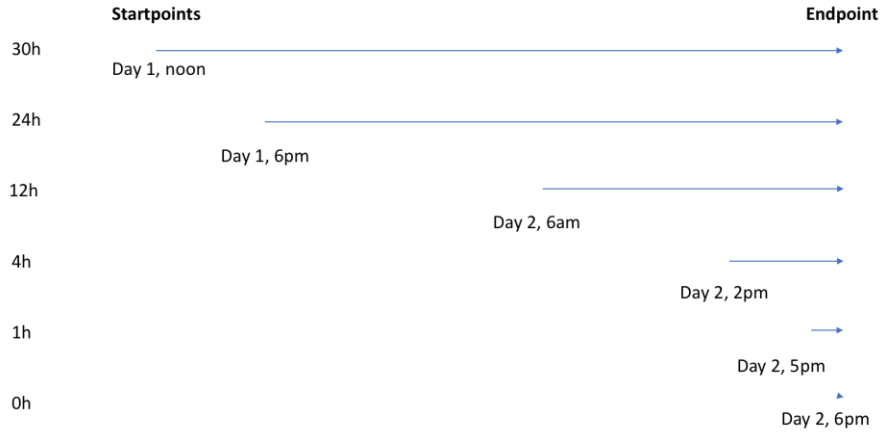

Figure 9: IFN-α stimulation timepoint schedule for synchronised collection of all samples.

Marker	Company	Catalog #	Fluorophore
CD273 (PD-L2)	BD Biosciences	740430	BV605
CD274 (PD-L1)	BD Biosciences	741014	BV786
CD40	BD Biosciences	562846	BV421
CD80	Biolegend	104734	PE/Cy7
CD86	BD Biosciences	564199	BUV395
Galectin-9	BD Biosciences	566028	BV421
H-2D^{b}	BD Biosciences	743540	BV786
H-2K^{b}	BD Biosciences	742864	BUV395
I-A/I-E	BD Biosciences	563413	BV605
OX40L	BD Biosciences	565214	BB515

Table 1: Antibodies used for flow cytometry analysis of *in vitro* and *in vivo* checkpoint marker expression.

2.4 Mice

C57BL/6 mice (The Jackson Laboratories 000664) are maintained in the Animal Resource Division of the Research Institute of the McGill University Health Centre (Montreal, Canada). Animals were received at 3 weeks of age and were immediately placed on CTD (Envigo TD.130838) or HFD (Envigo TD.06414). 10% of CTD calories come from fat while 60% of HFD calories come from fat. Over 90% w/w of the fat in the HFD comes from saturated, animal fat – lard. Mice were weighed three times per week until harvesting. All experiments involving mice had been approved (Protocol #7961).

2.5 Echo MRI

Fat and lean tissue proportion and mass were measured in mice at 9 weeks of age that had been fed control or HFD from 3 weeks of age. The purpose was to identify any HFD-caused changes in body composition by the time of subcutaneous tumour cell injection. Measurement was performed using the Bruker 7T MRI by the Small Animal Imaging Labs (SAIL) platform located at the Research Institute of the McGill Univesity Health Centre (Montreal, Canada).

2.6 C57BL/6 subcutaneous tumour injection

Sterile, phenol red-free Matrigel (Corning CB-40234C) tubes were placed on ice the night before the experiment. The sKO and dKO cell lines were cultured in T225 flasks with DMEM. Medium was aspirated and washing was done with PBS. Cells were detached with 3 ml of trypsin (Wisent 325-043-CL). Trypsin was quenched by adding 30 ml of full DMEM (containing 10% FBS). Cells were counted with a Neubauer hemocytometer. Cells were centrifuged for 5 min at 1,100 rpm. The medium was aspirated and washing of the cells was done with 20 ml sterile PBS. Cells were centrifuged and resuspended in DMEM without phenol red to a concentration of 1.5 million cells/100 µl. Cells were transferred to a sterile Eppendorf tube. An equal volume of Matrigel was added to the tube. Each mouse required one tube.

The 200 ul mixture was injected subcutaneously into the right flank of a 9-week old mouse that had been on the special control or HFD from 3 weeks of age. The mouse was anesthetized with 3% isoflurane and kept on a heated pad. Eye drops were added to avoid corneal drying. The mouse was placed back into the cage after the injection and monitored until awake and active.

Tumours were measured with digital calipers three times per week. The tumour volume in mm^3 was calculated by the formula: Volume = 4/3 x pi x $(width/2)^2$ x (length/2).

2.7 Harvesting samples from mice

Mice were sacrificed by first anesthetizing with 3% isoflurane and then cardiac puncture was performed. Cervical dislocation was performed after extracting blood. Serum was extracted (Sarstedt, 41.1378.005) from the blood. Liver and tumour sections were placed in Cassettes (Ultident 170-H1100) for formalin fixation and paraffin embedding. Fixation was done with formalin 10% for 48 hours at 4° Celsius. A tumour section was taken for flow cytometry analysis. It was collected in an Eppendorf tube containing 750 ul of complete medium and kept on ice. Another tumour section was taken for snap-freezing in liquid nitrogen and storage at -80° Celsius.

2.8 Tumour tissue dissociation

The fresh tumour section was minced as finely as possible with disposable scalpels (Thermo Fisher Scientific 08-927-5A). 1 ml was added of 5mg/ml collagenase II (Life Technologies 17101-015) for dKO cells or 5 mg/ml collagenase IV (Life Technologies 17104019) for sKO cells per 50 mg of tissue into a 15 ml Falcon tube. Collagenase II did not work well for the sKO tumour tissue, but collagenase IV was found to enhance tissue breakdown. The tissue was incubated for 45 minutes at 37°C. This short incubation was done to disrupt the extracellular matrix and make it easier for trypLE to release individual cells from the tissue [141]. It was washed with 10 ml of full DMEM media. Centrifugation at 1200 rpm for 5 min at 4°C was performed. This was followed by Resuspension with 0.5 ml of trypLE Express Enzyme, no phenol red (Thermo Fisher Scientific 12604013) for 5 min at 37°C. Two washes with 10 ml of DMEM plain medium were done. Cells were counted using Vi-CeLL XR Cell Viability Analyzer (Beckman Coulter 731050). Subsequent flow cytometry was performed in the same style as described previously.

2.9 Snap-frozen tissue preparation for multiplex

Samples had been kept at -80˚ Celsius. Np40-based lysis buffer used at a concentration of 50 µl per 10 mg of tumour.

The sample was minced with scalpels on the weigh boat. The tissue was gathered on the corner of the weigh boat and the respective lysis buffer volume was used to wash the pieces into the mortar. The tissue was homogenized with a mortar and pestle from Capitol Scientific Tissue Grinder Kit (ref. KIM-884900-0000) until no chunks were left. The ground glass surface mortar and pestle from the kit were used. Contents of the mortar were transferred to an Eppendorf tube. The sample was left for 30 min total in the lysis buffer and on ice before continuing. The samples were centrifuged for 10 minutes at 13000 rpm and 4° Celsius. The supernatant was transferred to a new Eppendorf tube. Total protein quantification was done with the BCA assay as previously described. A 20X dilution of each sample was prepared before performing the assay. 200 ul of working reagent was added to 10 ul of diluted sample using an automatic pipettor. The samples were shipped to Eve Technologies (Calgary, CA) for multiplexing: TGF-beta 3-Plex (TGFB1-3), Cytokine Array / Chemokine Array 44-Plex (MD44), Th17 Discovery 12-Plex (MDTH17-12), High Sensitivity T-Cell Discovery Array 18-plex (MDHSTC18), Procarta IFN 2-plex Array (MDIFNAB), Metabolic Array (MRDMET).

2.10 Luminex analyses

R software (R-project.org) and R Studio (rstudio.com) were used for downstream analysis. 91 analyte measurements were received, however 25 were removed due to redundancy (analyte measurement performed by more than one assay), technical issue (TIMP-1 was oversaturated as a sample and this affected the ability to measure), and complete lack of measurements (Glucagon

and EPO). Two mice from the sKO CTD group had to be excluded due to the fact that there was not enough tumour tissue to perform all of the assays for these mice.

2.11 Statistics

In vitro flow cytometry statistics were performed using Prism 8 (Graphpad Software, San Diego, USA). Multiple, unpaired *t*-tests were used to check significance of difference of checkpoint marker expression at specific timepoints between vehicle and IFN-α treated cells. Paired *t*-test was used to check significance of difference of checkpoint marker expression between vehicle and IFN-α treated cells across the timepoints.

In vivo statistics were performed using Prism 8 (Graphpad Software, San Diego, USA). D'Agostino and Pearson normality test was used to determine if each group of sKO CTD, sKO HFD, dKO CTD, and dKO HFD samples had a normal distribution for each data point measured. Unpaired *t*-test was used to check significance of difference if both groups had a normal distribution. Otherwise, the Mann-Whitney test (also known as Wilcoxon rank-sum test) was used.

Luminex statistical analysis was performed using R software (R-project.org). Shapiro-Wilk normality test was used to determine if each group of sKO CTD, sKO HFD, dKO CTD, and dKO HFD samples had a normal distribution for each checkpoint marker measured. Unpaired *t*-test was used to check significance of difference if both groups had a normal distribution. Otherwise, the Mann-Whitney test was used.

CHAPTER III

Results

3.1 *In vitro* IFN-α stimulation of dKO cells does not modulate checkpoint ligand expression

Given the evidence that genetic drivers and diet impact the host inflammatory response, we hypothesized that the prostate tumour microenvironment is governed by the cancer cell-intrinsic mechanisms established by the combination of genetic drivers and extrinsic factors such as dietary patterns. To study the tumour microenvironment, cell lines derived from genetically engineered mouse models bred in a common, immunocompetent, background (C57BL/6) were used [33]. The sKO (*Pten* loss) cell line models localized, early disease. Mice from which this cell line is derived, develop PIN by 6 weeks of age and invasive prostate adenocarcinoma by 9 weeks of age. However, the disease rarely progresses to a metastatic form. The dKO (*Pten* and *Rb1* loss) cell line models metastatic prostate cancer with neuroendocrine differentiation (synaptophysin and chromogranin A-expressing). Notably, the dKO is representative of the human disease through its ability to form bone metastases - in addition to lymph node, lung and liver metastases [33,142].

Given the enrichment of the IFN-α gene set RNA in the Hi-Myc model tumour tissue and the enhancement of that gene set under HFD [138], the impact of IFN-α signaling in the dKO was examined. dKO cells were treated *in vitro* with IFN-α and the impact of stimulation on the checkpoint ligand expression profile was examined (**Fig. 10-13**). Since the IFN-α signature could already be seen in a model of early disease, the dKO were used to check if the signature is still present in a more advanced form of prostate cancer. dKO cells were stimulated with 100 U/ml (1.67 ng/ml) of IFN-α (**Fig. 10**) according to established literature values [143,144]. Treatment was performed across a range of timepoints to identify how quickly checkpoint ligands are upregulated

in our model. Such information would indicate whether the cell has a predisposition towards expression of any particular checkpoints. The cells were detached from the well bottom with TrypLE to minimize damage to checkpoint ligands expressed on the cell surface before staining in preparation for flow cytometry (**Fig. 10**).

Gating of the flow cytometry result allowed examination of ligand expression by individual dKO cells (**Fig. 11A**), but confirmation of IFN-α stimulation was done using Western blotting. Samples for Western blotting were harvested at the same time as the flow cytometry samples. This ensured the Western blot served as a positive control for IFN-α-dependent signaling. 30 minutes incubation is recognized as providing sufficient IFN-α exposure to trigger peak stimulation in responsive cells [143]. IFN-α signals through the Janus kinase and Signal Transducer and Activator of Transcription (STAT) pathways. STAT1 is phosphorylated in cells stimulated with IFN-α. Phosphorylation of STAT1 was seen after 10 minutes of treatment and peaked at 30 minutes in the IFN-α-stimulated samples (**Fig. 11B**). With confirmation of IFN-α stimulation, the flow data was analyzed to identify any differences in checkpoint marker expression between the IFN-α and vehicle-treated groups in the form of percentage of marker-positive cells (frequency) and geometric mean fluorescence intensity of marker expression.

The frequency of expression (**Fig. 12**) and intensity of expression (**Fig. 13**) for CD274, CD80, and Galectin-9 varied between replicates and were not significantly different from the vehicle-treated group at individual timepoints. MHCI molecules H-2K^b and H-2D^b served as positive controls for the experiment due to their known increase in expression due to IFN-α stimulation [145]. This increase was observed in terms of expression frequency (**Fig. 12**), but not intensity (**Fig. 13**). Paired t-tests comparing IFN-α-treated and vehicle-treated replicates across timepoints shows a statistically significant difference for CD274 and CD80 expression frequency

(**Fig. 12**). However, the spread of the replicates of both the IFN-treated and vehicle-treated groups requires additional replicates to validate the significance of these results. Lack of IFN-α-mediated immune checkpoint ligand expression in the dKO could suggest it has a protective effect and limits tumour growth [146]. It is also possible that additional factors must be present to modulate checkpoint ligand expression and the tumour microenvironment as a whole must be recreated. The ensuing experiment examined the checkpoint ligand expression profiles *in vivo* (**Fig. 14**).

3.2 HFD leads to obesity in C57BL/6 mice and increased tumour growth in sKO and dKO

HFD increased the body mass of the C57BL/6 mice (**Fig. 15A**) and increased the body fat proportion (**Fig. 15B**). Interestingly, lean body mass also increased with HFD (**Fig. 15B**). The body mass increase was seen by 9 weeks of age, when the mice received the syngeneic tumour cell injection. Having ensured that we have a mouse responsive to diet, we next examined tumour engraftment.

The sKO and dKO cell lines had 100% engraftment in the C57BL/6 mice and formed tumours (**Fig. 16**). Tumour growth rate was found to be significantly increased by combination of *Pten* and *Rb1* loss or HFD (**Fig. 17**). On either CTD or HFD background, combined tumour suppressor loss significantly increases the growth rate. On either sKO or dKO background, HFD significantly increases tumour growth. Accordingly, the dKO tumours from mice on HFD grow the fastest.

By 13 weeks of age, when the tumours were harvested, the difference in mouse mass between the diet conditions was maintained and slightly more pronounced (**Fig. 15A**). To investigate the early tumour microenvironment, tumours were harvested at a mean size of 400 mm^3

(**Fig. 14**), a size usually devoid of uninformative necrotic regions typical of large tumours (i.e. 2000 mm^3).

3.3 Combined loss of *Pten* and *Rb1* reduces CD274 and CD80 expression *in vivo*

Tumour chunk processing and the flow cytometry analysis approach were designed for consistency and specificity. Tumour chunks selected for flow cytometry analysis were representative of the larger pool of harvested tumours (Fig 17B). The workflow design aimed to make the dissociation of these tumour chunks and preparation for flow cytometry analysis as similar as possible to the *in vitro* approach (**Fig. 18**). To match with the experimental setup *in vitro*, TrypLE was used to complete the dissociation and flow cytometry staining used the same antibodies for the checkpoint markers. The flow cytometry gating strategy removed debris, non-cancer cells, cell clumps, and dead cells to be able to specifically examine the checkpoint marker expression of individual sKO and dKO cells (**Fig. 19**). Robust GFP expression by the cancer cells [33] provided an additional level of stratification to ensure only the correct cells were included in the analysis.

Flow cytometry analysis indicates change in tumour genetic drivers influences checkpoint ligand expression, not change in diet (**Fig. 20**). Comparison of CTD and HFD checkpoint marker expression in mice with sKO or dKO tumours did not have significant differences (**Fig. 20 A and B**). dKO cells demonstrate significantly reduced expression frequency and expression intensity of CD80 and CD274 than sKO when compared in mice fed CTD or HFD (**Fig. 20 C and D**). This suggests that genotype has a prominent impact on immune checkpoint regulation of the tumour microenvironment. To note, the full influence of diet and genotype is unknown since only CD80 and PD-L1 were characterized for the sKO. Additionally, tumour control of the microenvironment consists of multiple mechanisms, not only checkpoint ligand expression.

3.4 Cytokine concentrations in the tumour microenvironment indicate genetic drivers and diet as potential modulators of immune infiltration and activation

With epidemiological and biological data pointing to an important role of diet in the modulation of the tumour microenvironment, Luminex was performed to measure cytokine and chemokine concentrations in the tumour chunks consisting of cancer cells along with infiltrated immune cells, fibroblasts, and other resident cells. This would help identify potential mechanisms that genetic drivers and diet use to modulate the tumour microenvironment.

Luminex provided concentration measurements for 66 analytes data and this can be analyzed with different approaches to elucidate any mechanisms regulating the tumour microenvironment. A broad examination of the data was first performed before narrowing our focus. The Spearman correlation of the mouse tumour samples indicates that samples cluster primarily by genetic driver than by diet (**Fig. 21A**). Spearman correlation of the individual analytes across experimental conditions shows TGF-β1,2,3 all correlate with CXCL9 and CXCL10. G-CSF and GM-CSF correlate with CXCL1,2,5 (**Fig. 21B**). Chemokine concentrations allow to extrapolate what kind of immune cells may be infiltrating the tumour microenvironment.

Cluster 4 of the unsupervised heatmap indicates the chemokines with the highest concentrations across tumours: CCL2, CCL12, CCL21, CXCL1, CXCL2, CXCL9 (**Fig. 22**). IL-33, an alarmin, is another member of cluster 4 of the unsupervised heatmap. The chemokines are involved in T cell and neutrophil movement and for induction of an inflammatory state. However, they are also implicated in supporting tumour development.

Examination of the 17 chemokines measured by Luminex identified strong genotype-driven differences in tumour concentrations of the chemokines (**Table 2**). Additionally, sKO and dKO chemokine tumour microenvironment concentrations change differently when the tumour is

exposed to HFD conditions. Results indicate increased concentration of chemokines involved in T cell migration in the dKO CTD when compared to the sKO CTD: CXCL9, CXCL10, CCL3, CCL5, CCL17, CCL19, CCL20, CCL22, and CX3CL1 are increased in the dKO. In the same comparison, chemokines involved in dendritic cell migration are increased in the dKO: CCL3, CCL11, CCL19, CCL20, and CX3CL1. While CXCL1, involved in neutrophil trafficking, is increased in the sKO. HFD attenuates the significant differences in chemokine levels that are driven by combined *Pten* and *Rb1* loss. This attenuation appears to be driven by diet-induced changes occurring in both cell lines. When comparing dKO on CTD to dKO on HFD, HFD potentially favours a myeloid-driven microenvironment as T cell-related markers decrease (CCL5, CCL17, CCL22) and macrophage and neutrophil makers increase (CXCL1 and CXCL2). When comparing sKO on CTD to sKO on HFD, HFD increases T cell-related markers (CCL3, CCL11, CCL12, CCL17, CCL19, CX3CL1), making the sKO more similar to the dKO on CTD. These results support the notion that the tumour genetic drivers shape the alteration of the tumour microenvironment in response to the diet.

Examination of fold change for the complete set of Luminex analytes identifies IL-11, VEGF, IL-6, TGF-β1,2,3, and several chemokines as significantly overexpressed in CTD dKO when compared against CTD sKO (**Fig. 23**). CCL19 encourages T cell trafficking to the lymph nodes, while CXCL9 promotes T cell extravasation into target tissues. CX3CL1 appears in both soluble and membrane-bound form to promote chemotaxis and extravasation, respectively. IL-11, IL-6, and TGF-β1,2,3 remain upregulated in the dKO under HFD (**Fig. 23A**). Based on the appearance of IL-33 in the unsupervised heatmap cluster of cytokines with the highest concentrations across tumour samples (**Fig. 22**), it is notable that IL-33 is increased more than two-fold in the dKO compared to the sKO regardless of diet (**Fig. 23B**).

To narrow the focus on a subset of cytokines more prominently associated with our genetic driver and diet-induced tumour microenvironment, principal component analysis was used to identify the variance between tumour samples and the analytes driving this variance (**Fig. 24**). The sKO and dKO tumour sample points cluster separately (**Fig. 24A**). In line with the Spearman correlation observations (**Fig. 21A**), there is less variation in the CTD dKO and HFD sKO groups (**Fig. 24B**). This points to the diet effect being modulated by the tumour genetic driver profile. Several chemokines were identified as driving the variance in the tumour samples from all four diet and genetic driver combinations, but the most prominent factors were IL-11, TGF-β1, VEGF, and IL-6 (**Fig. 24C**). The variance caused by IL-11 and TGF-β1 comes from the genetic drivers, while the variance caused by VEGF and IL-6 comes from the crosstalk of genetic driver with diet (**Fig. 23A**). The combination of cytokines identified may contribute to the mechanism by which genetic drivers and diet create a microenvironment conducive to tumour growth.

3.5 Results figures

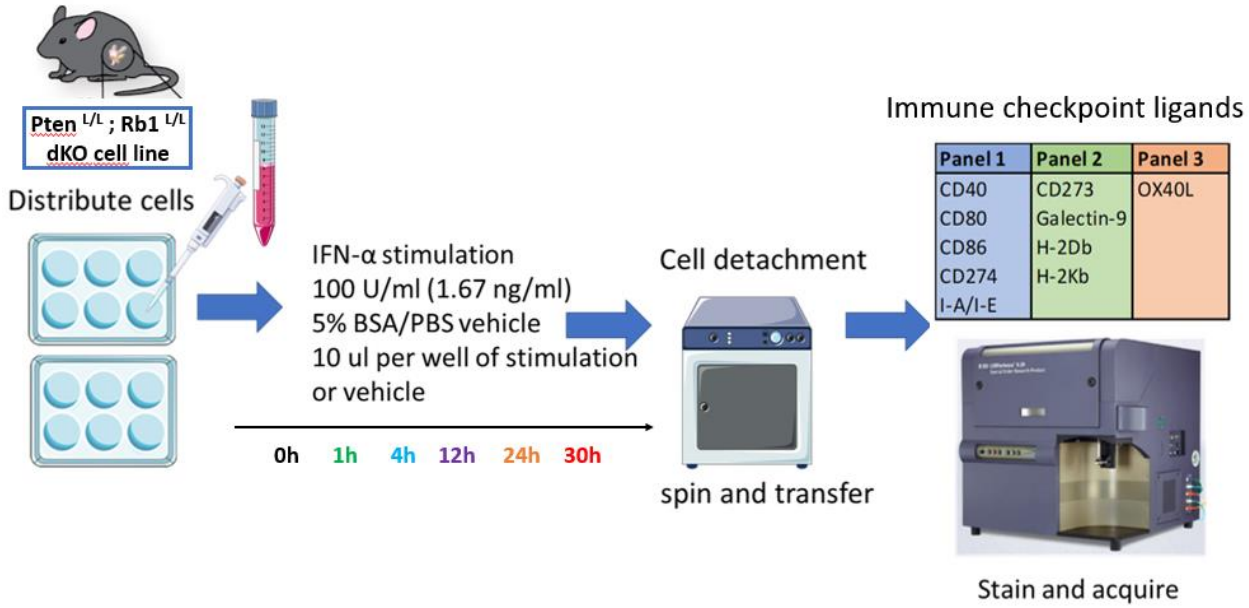

Figure 10: Flow cytometry workflow for the *in vitro* study of immune checkpoint ligand expression of the dKO cell line treated with IFN-α. 50,000 cells were seeded per well the day before the time course began. The time course examined the length of time needed for dKO checkpoint ligand expression. Cells were stained by fluorophore-bound antibodies and checkpoint marker expression was analyzed by flow cytometry.

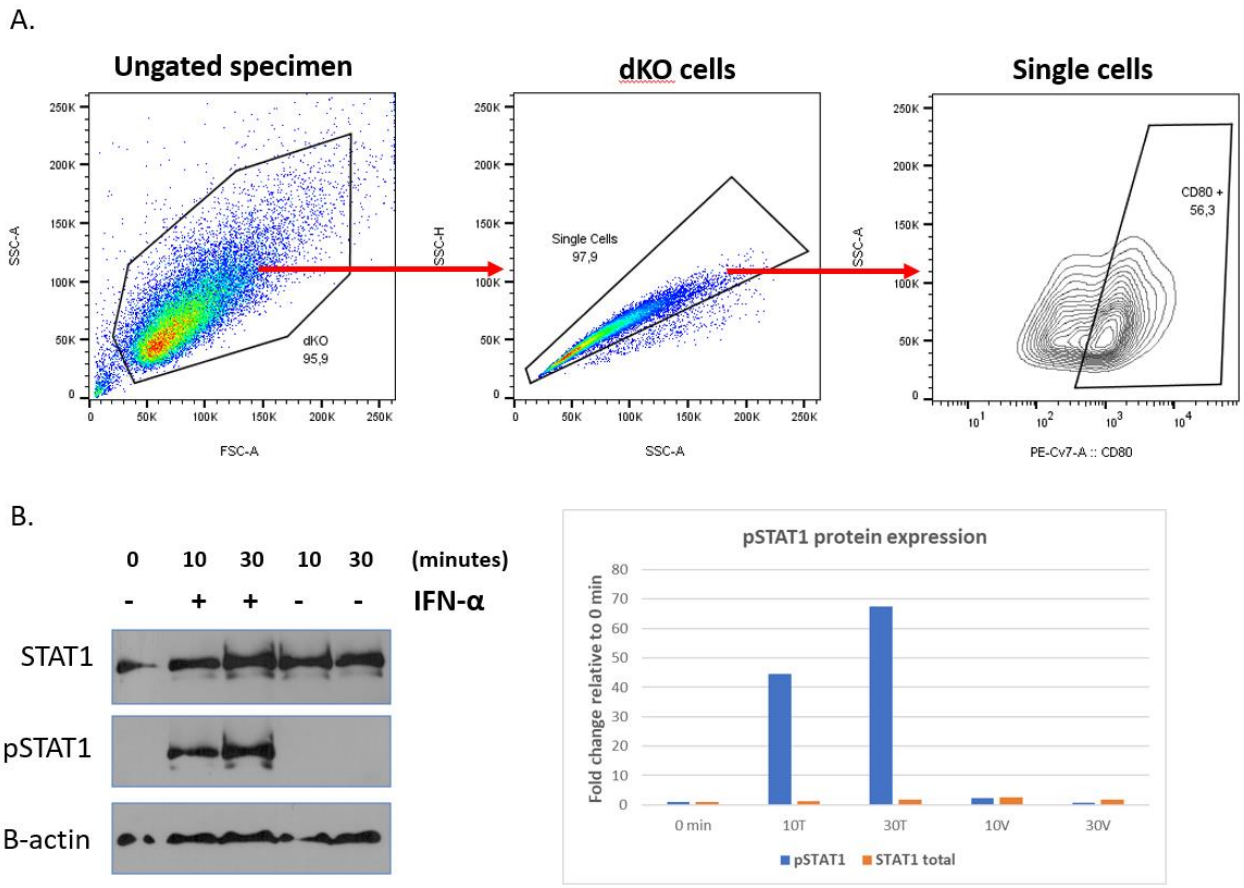

Figure 11: In vitro data analysis approach. A) gating strategy of *in vitro* flow cytometry results for the dKO cell line. Total events > dKO cells > single cells > checkpoint ligand +. B) Western blot confirming IFN-α treatment stimulated the dKO cells. Phosphorylation of STAT1 occurs only in IFN-α-treated conditions and peaks at 30 minutes duration of treatment.

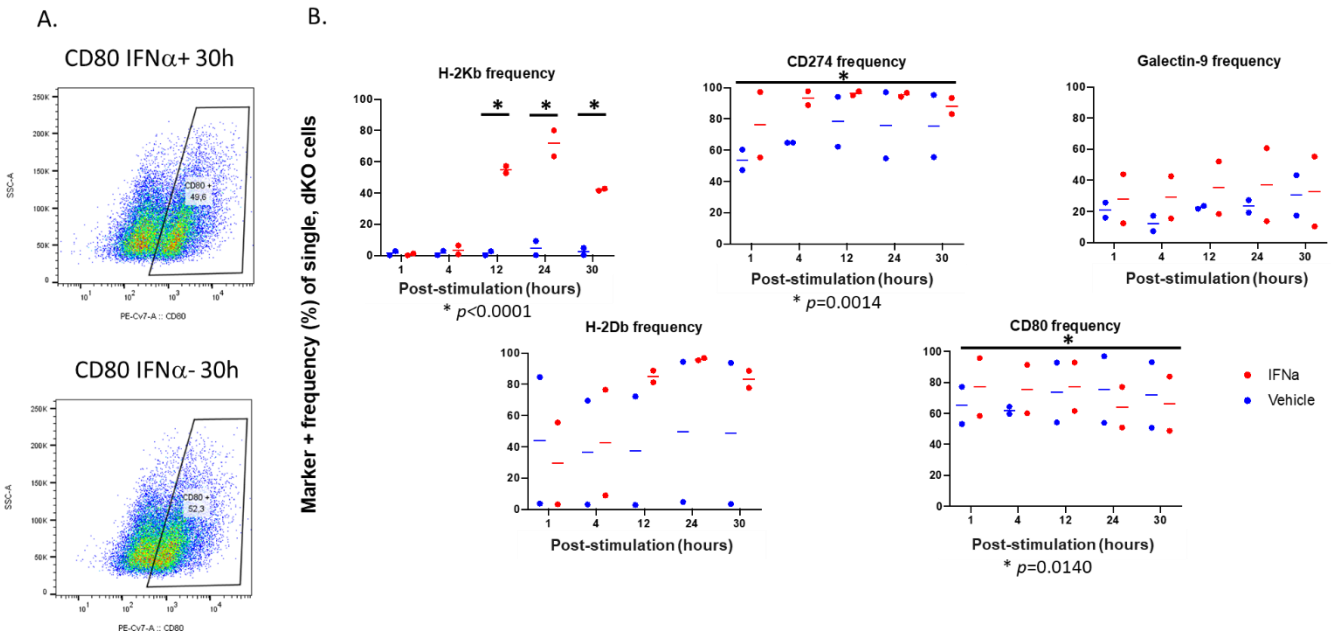

Figure 12: IFN-α modulation of checkpoint ligand expression frequency of dKO cells. A) Representative gating for positive fraction of cells in treated and non-treated conditions. B) Results of time course analysis for five checkpoint markers. H-2K^b and H-2D^b serve as positive controls. The difference between the set of IFN-α-treated timepoints and the set of vehicle-treated timepoints is statistically significant for CD274 (PD-L1) and CD80. Unstained sample checkpoint ligand population used as reference to gate positive population in stained sample. D'Agostino and Pearson normality test. Multiple t-tests analysis and paired t-test analysis performed. * refers to the *p*-value listed below graphs of panel B.

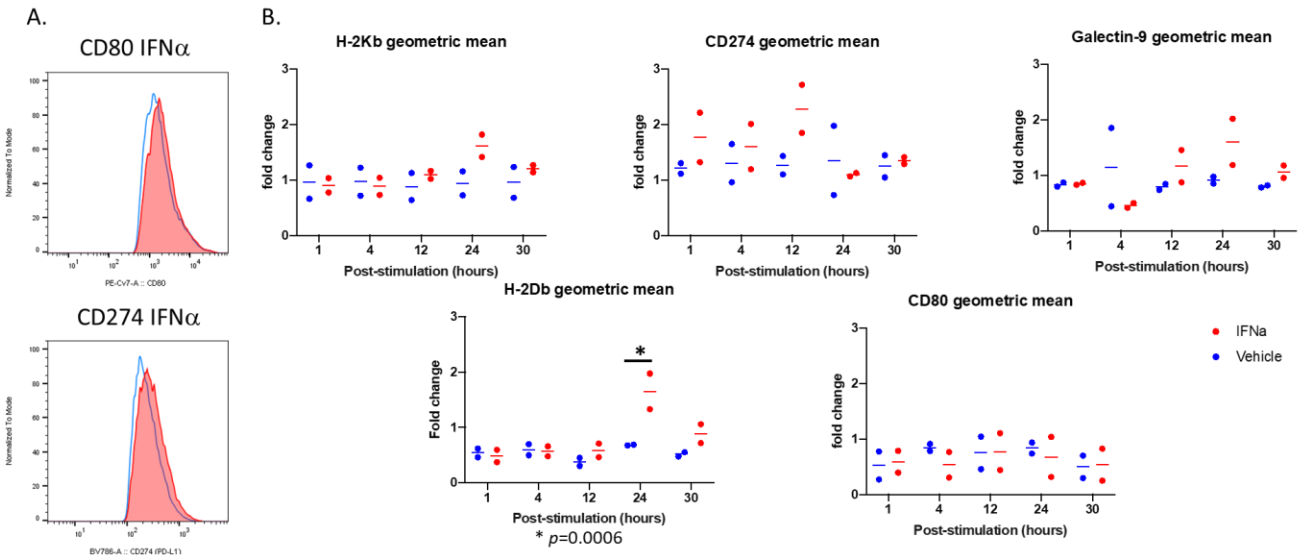

Figure 13: IFN-α modulation of checkpoint ligand expression intensity of dKO cells. A) Representative gating for positive fraction of cells in treated and non-treated conditions. B) Results of time course analysis for five checkpoint markers. Unstained sample checkpoint ligand population used as reference to gate positive population in stained sample. D'Agostino and Pearson normality test. Multiple t-tests analysis and paired t-test analysis performed. The geometric mean replicates were presented as fold change values to be able to compare the results from the different replicates since they were not passed through the flow cytometer together. Fold change = each replicate (vehicle and IFN-α) / average of vehicle replicates' geometric mean. * refers to the *p*-value listed below graphs of panel B.

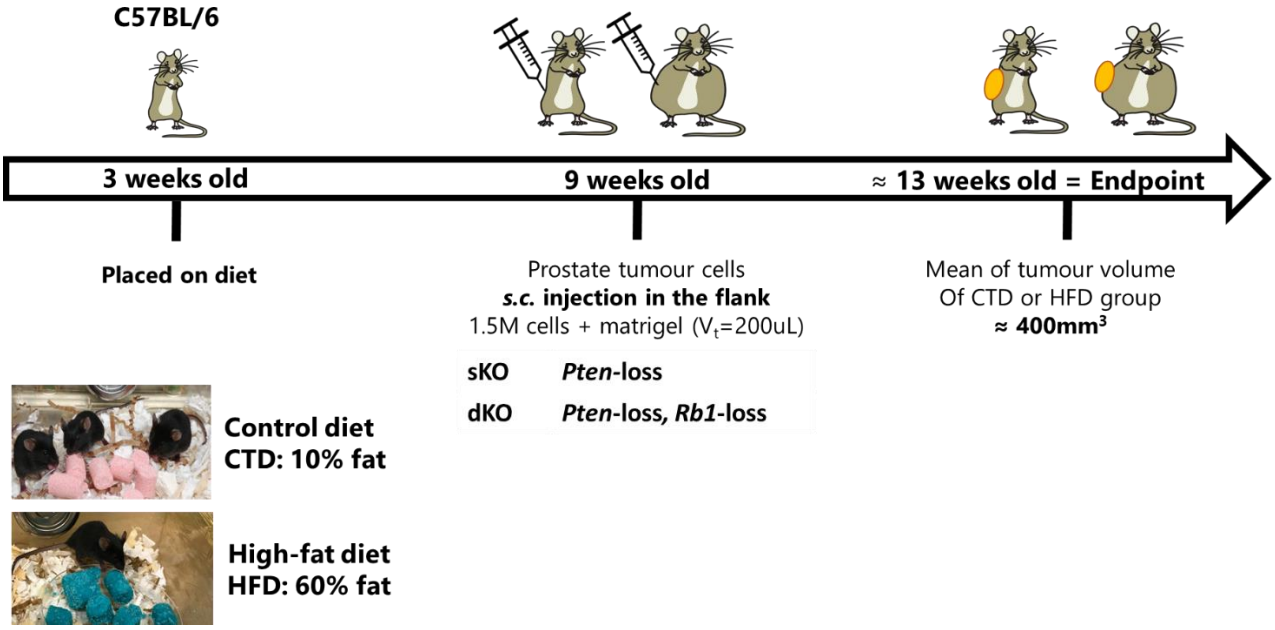

Figure 14: In vivo experimental design for studying tumour microenvironment modulation by genetic drivers and diet. C57BL/6 mice are switched to high-fat diet or control diet at 3 weeks of age. At 9 weeks of age, mice receive a subcutaneous injection in their right flank of sKO or dKO murine prostate cancer cells. Approximately 4 weeks later, one of the four conditions will reach a tumour mean volume of approximately 400 mm^3 and the mice are all harvested.

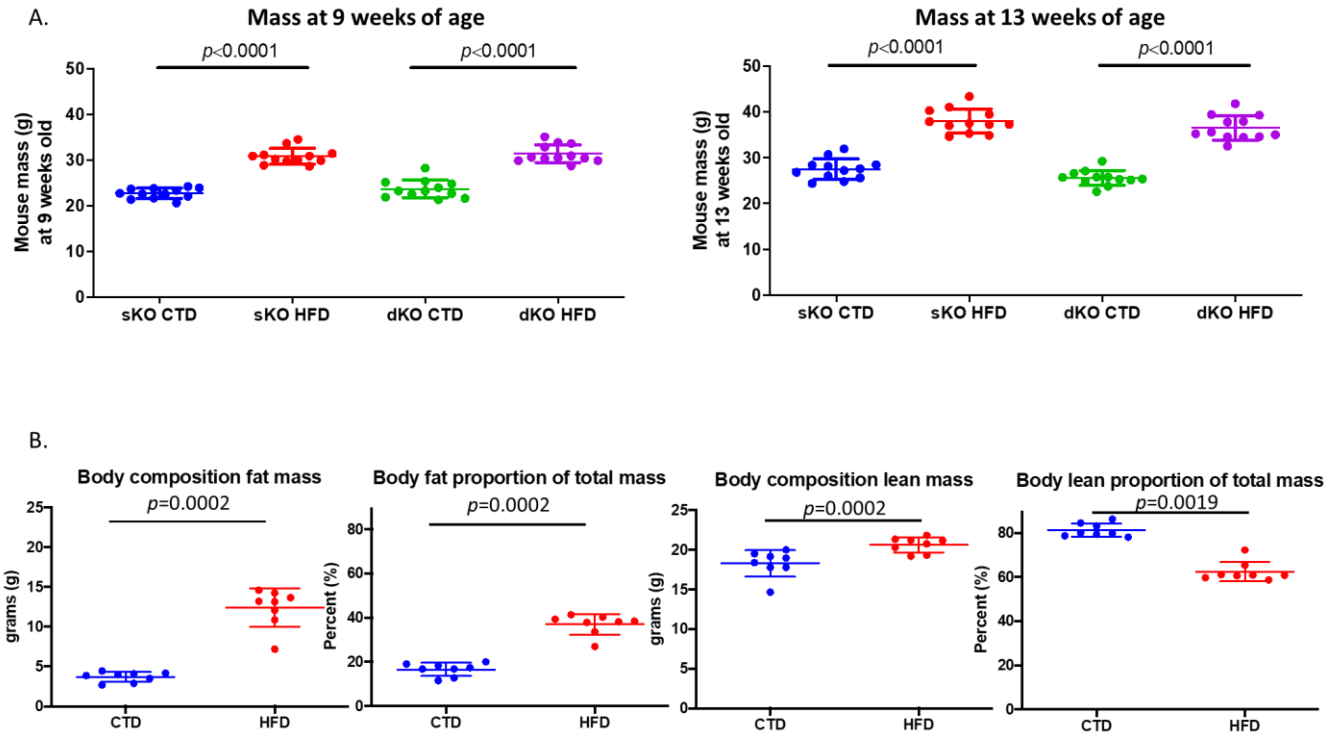

Figure 15: Increased body mass and body fat proportion in C57BL/6 mice on HFD. A) Mass gain, a hallmark of obesity, present in mice by age of injection (9 weeks). Differences in mass remain significant for the duration of the study. B) Body composition of 9-week-old C57BL/6 mice in diet study by EchoMRI. HFD increases both the fat mass and lean mass of mice. Fat makes up a larger proportion of body mass than on CTD. D'Agostino and Pearson normality test. Unpaired t-test or Mann-Whitney test.

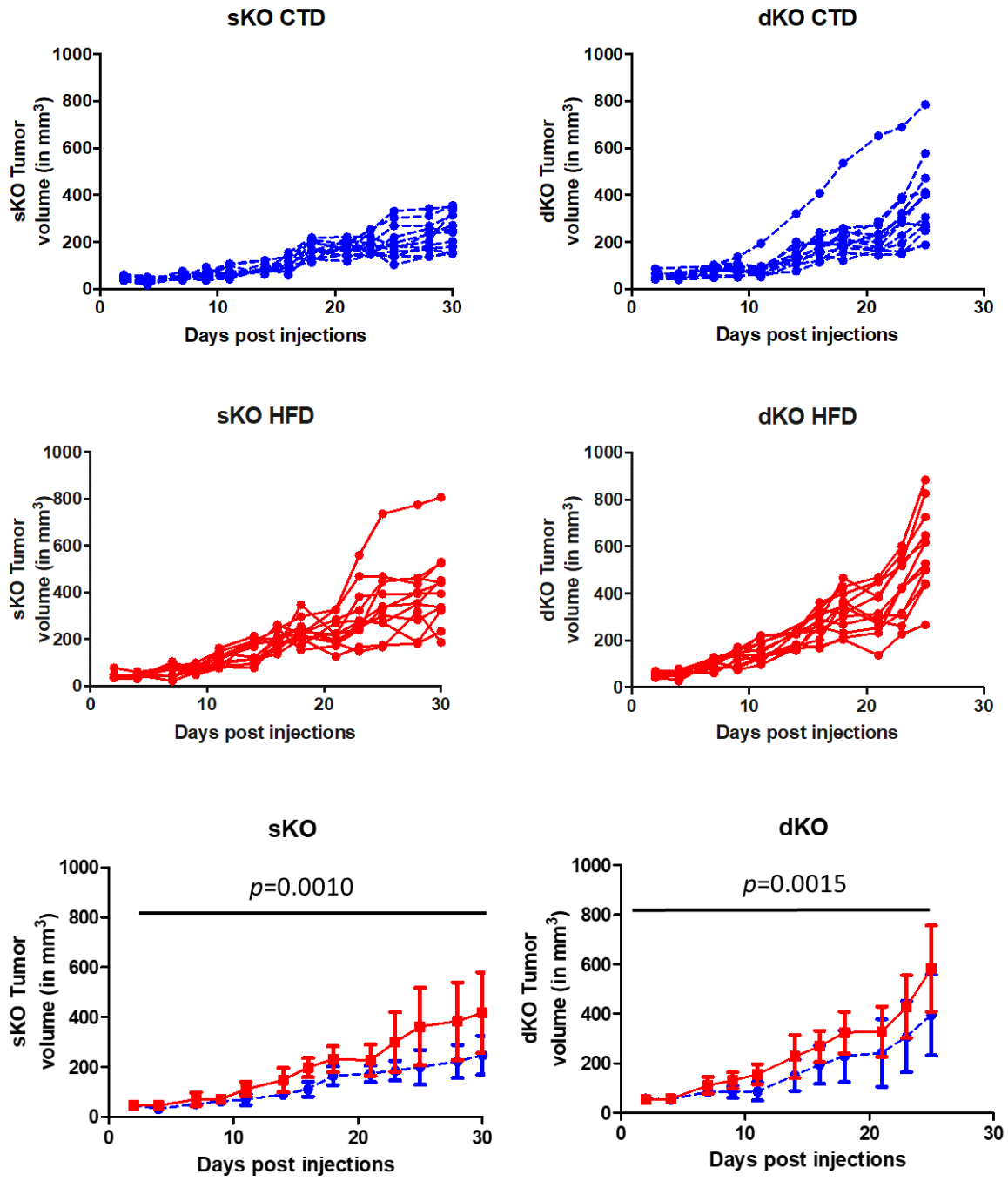

Figure 16: CTD or HFD-fed mouse sKO and dKO tumour growth curves. Tumours are growing in C57BL/6 mice regardless of genotype or diet. Combined tumour suppressor loss and HFD each lead to larger tumours. N = 12 for all conditions. Paired t-test. Mean and SD shown.

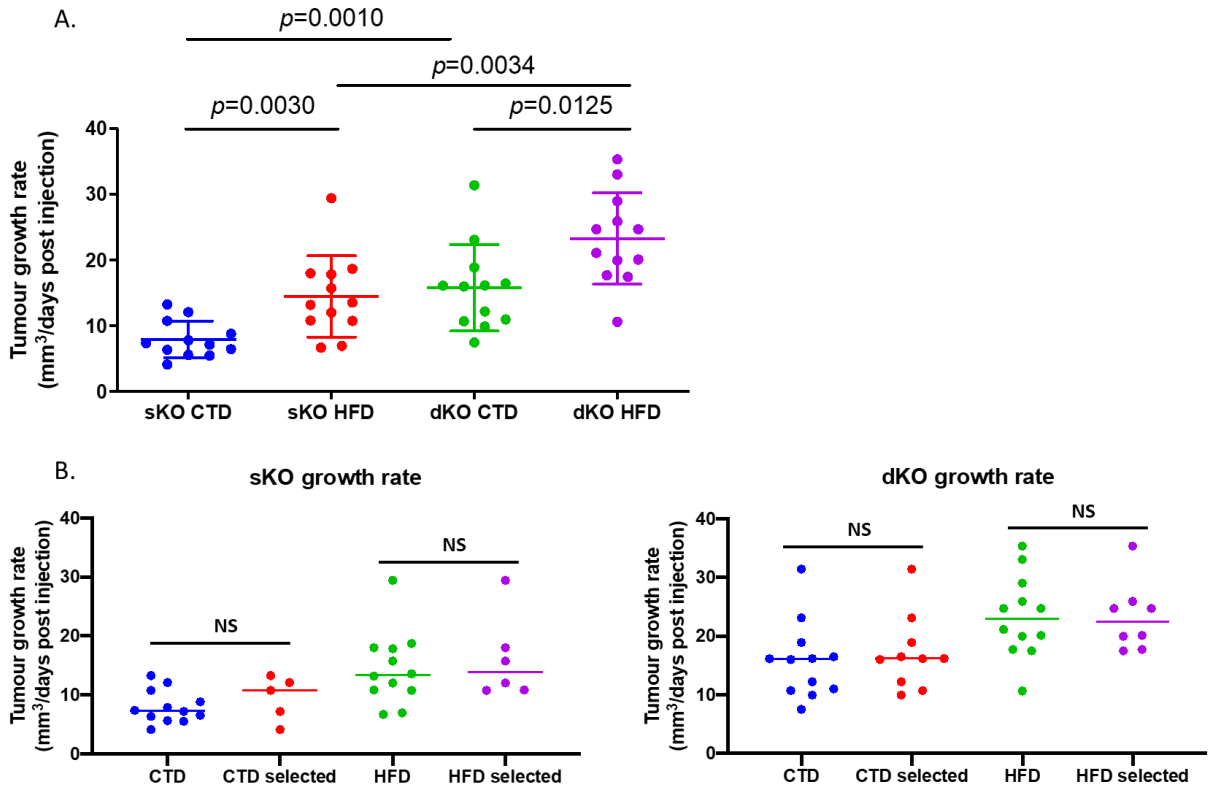

Figure 17: CTD or HFD-fed mouse sKO and dKO tumour growth rates. A) HFD increases tumour growth rate of both genotypes. dKO grow faster than sKO regardless of diet condition. N= 12 for each condition. D'Agostino and Pearson normality test. Unpaired t-test or Mann-Whitney test shown. 2-way ANOVA concludes genotype (p<0.0001) and diet (p=0.0002) influence tumour growth rate. B) Tumour growth rate of samples selected for flow cytometry analysis versus the tumour pool. Samples selected for analysis do not differ from the population. Selected N = 5 sKO CTD, 6 sKO HFD, 10 dKO CTD, 8 dKO HFD. D'Agostino and Pearson normality test. Unpaired t-test or Mann-Whitney test shown.

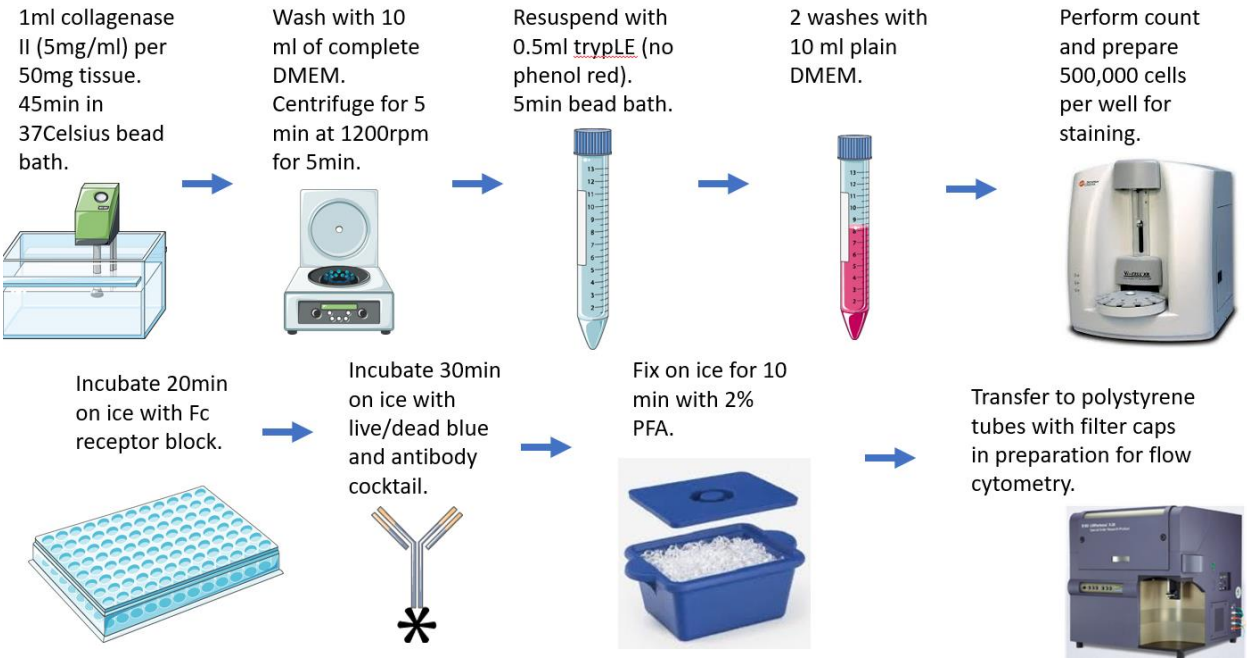

Figure 18: sKO and dKO tumour dissociation and staining. Workflow from dissociation of the tumour chunk to the capture of immune checkpoint ligand expression of individual cells.

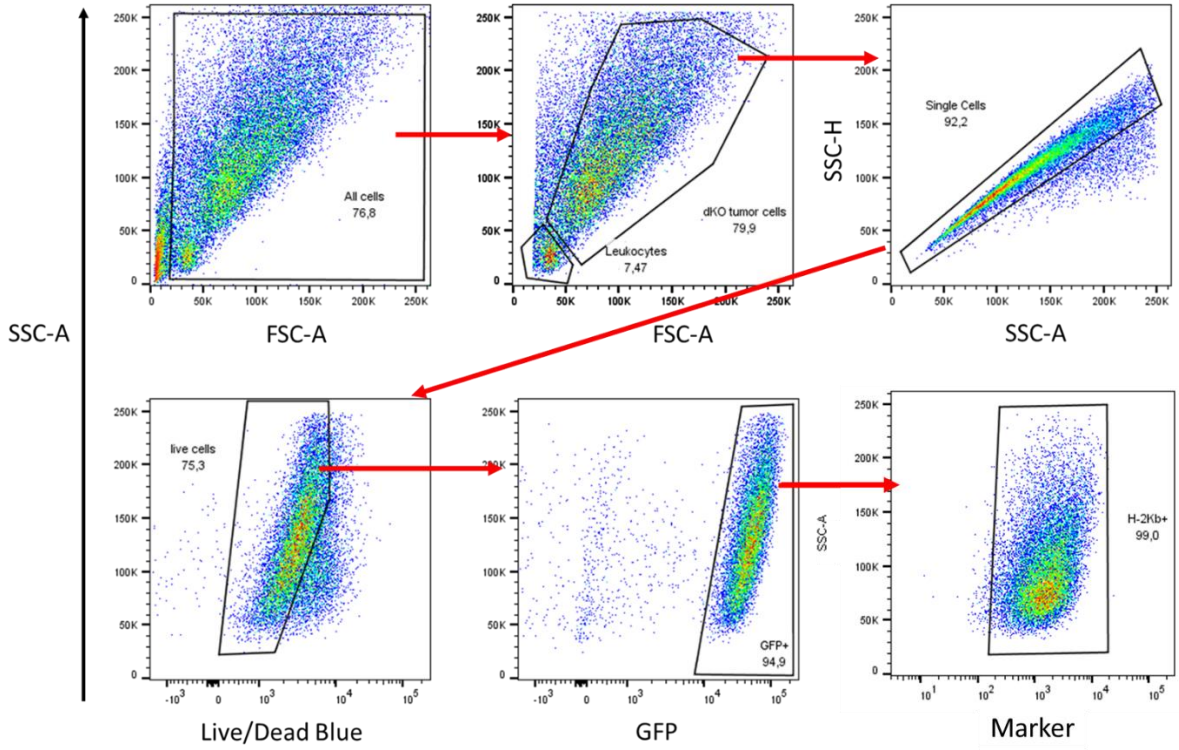

Figure 19: Gating strategy of in vivo flow cytometry results for identification of checkpoint ligand expression frequency and intensity in sKO and dKO cells from tumours of mice on CTD or HFD. Total events > cells > subpopulation of large tumour cells > single cells > live cells > GFP+ > checkpoint ligand +. Unstained sample checkpoint ligand population used as reference to gate positive population in stained sample.

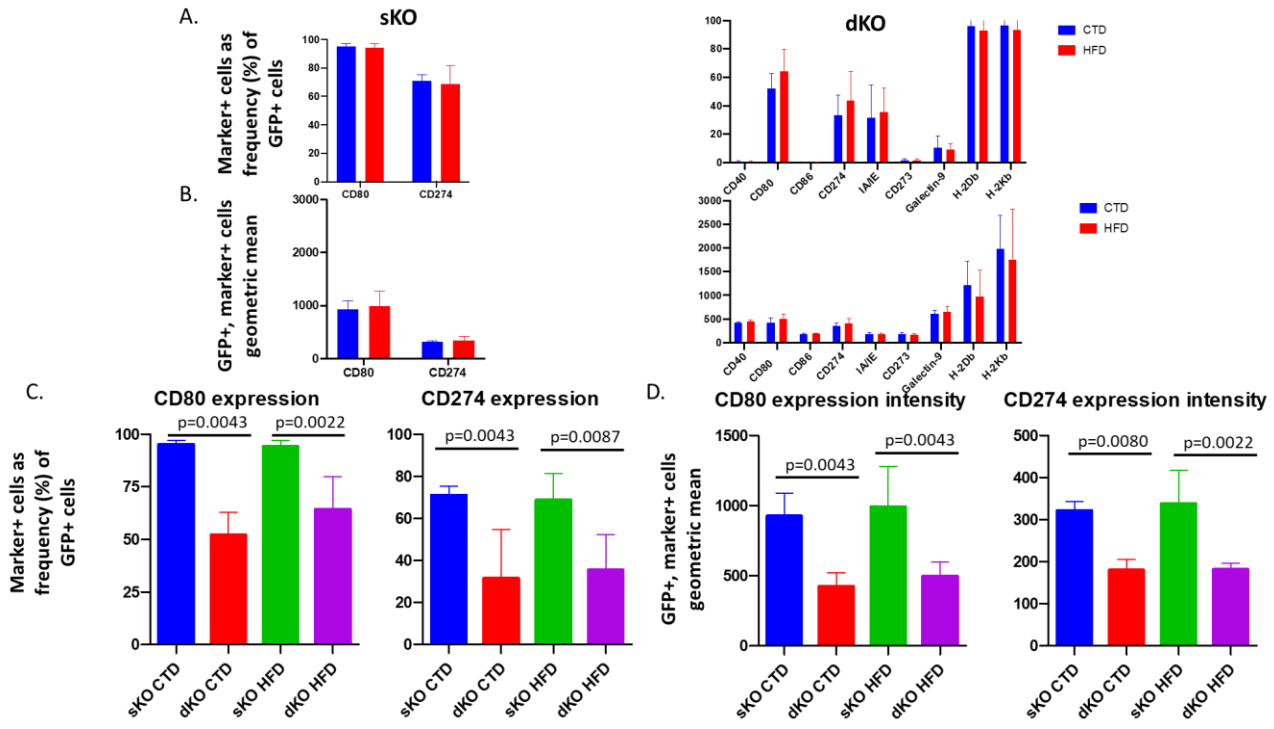

Figure 20: In vivo checkpoint ligand expression frequency and intensity is reduced in dKO cancer cells compared to sKO. A) Influence of diet on frequency of GFP+ (cancer) cells expressing the marker and B) intensity of marker expression by marker+ cancer cells. C) Influence of genotype on cancer cell marker expression frequency and D) marker expression intensity. D'Agostino and Pearson normality test. Unpaired t-test or Mann-Whitney test.

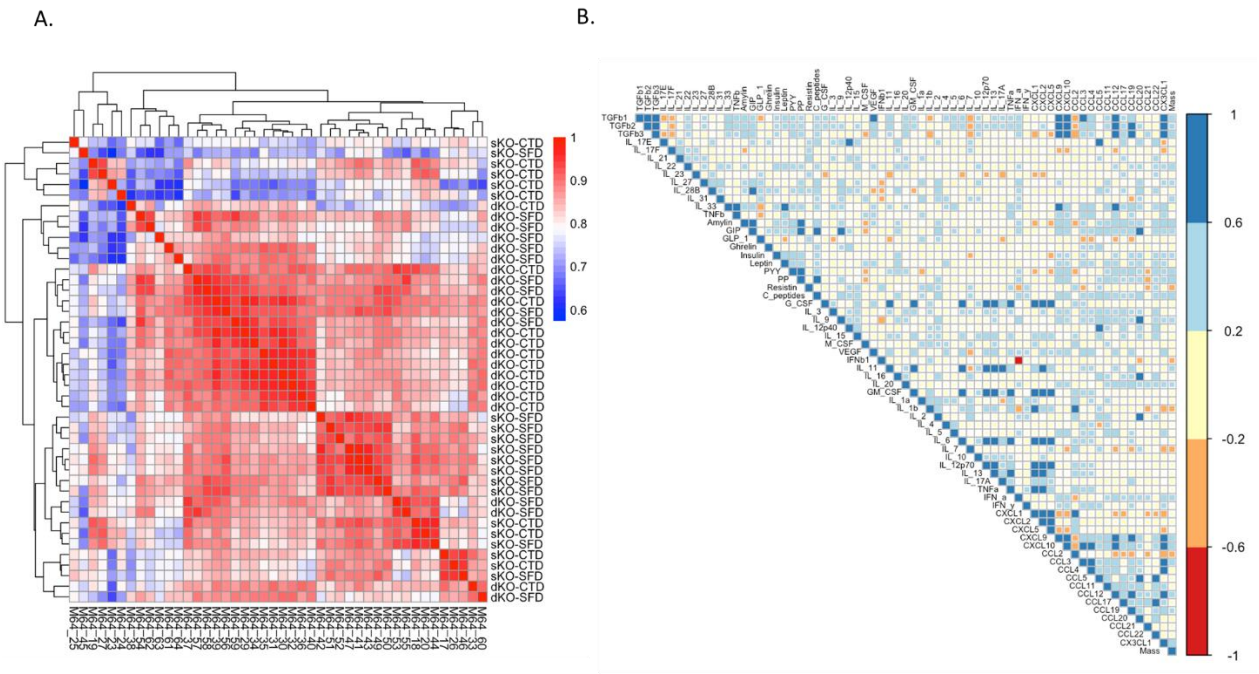

Figure 21: Luminex data correlation heatmaps for tumours and individual analytes. A) Correlation of the tumour chunks with each other based on the underlying analyte values recorded for each tumour. Tumours represented by genotype and diet. dKO CTD tumours correlate with each other and sKO HFD tumours correlate with each other. B) Correlation of analytes with each other across the four experimental conditions. CXCL9 and CXCL10 correlate with TGF-β1,2,3. CXCL1,2,5 correlate with G-CSF and GM-CSF. Spearman correlation.

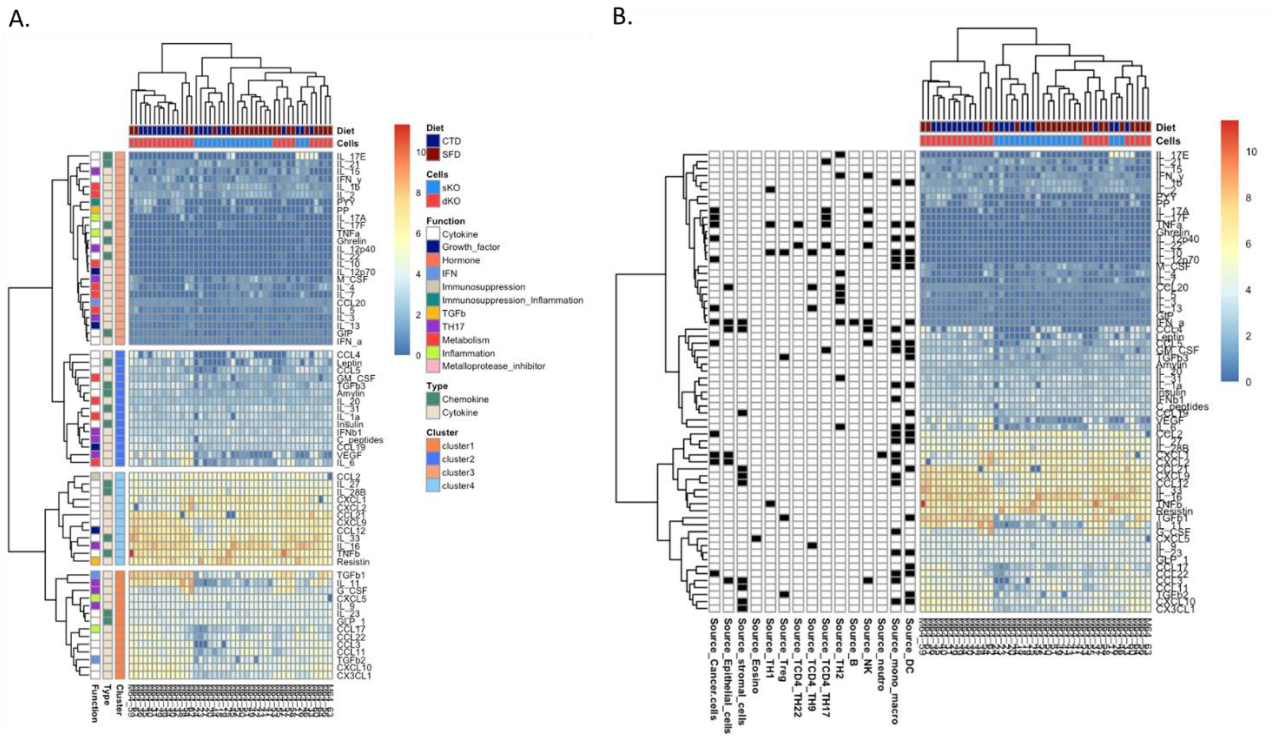

Figure 22: Unsupervised clustering of cytokine levels in sKO and dKO tumours. Created with R package pheatmap. (A) Annotated with analyte function and type. Cytokines have grouped into four clusters based primarily on cytokine concentration across the tumour samples. (B) Annotated with analyte sources.

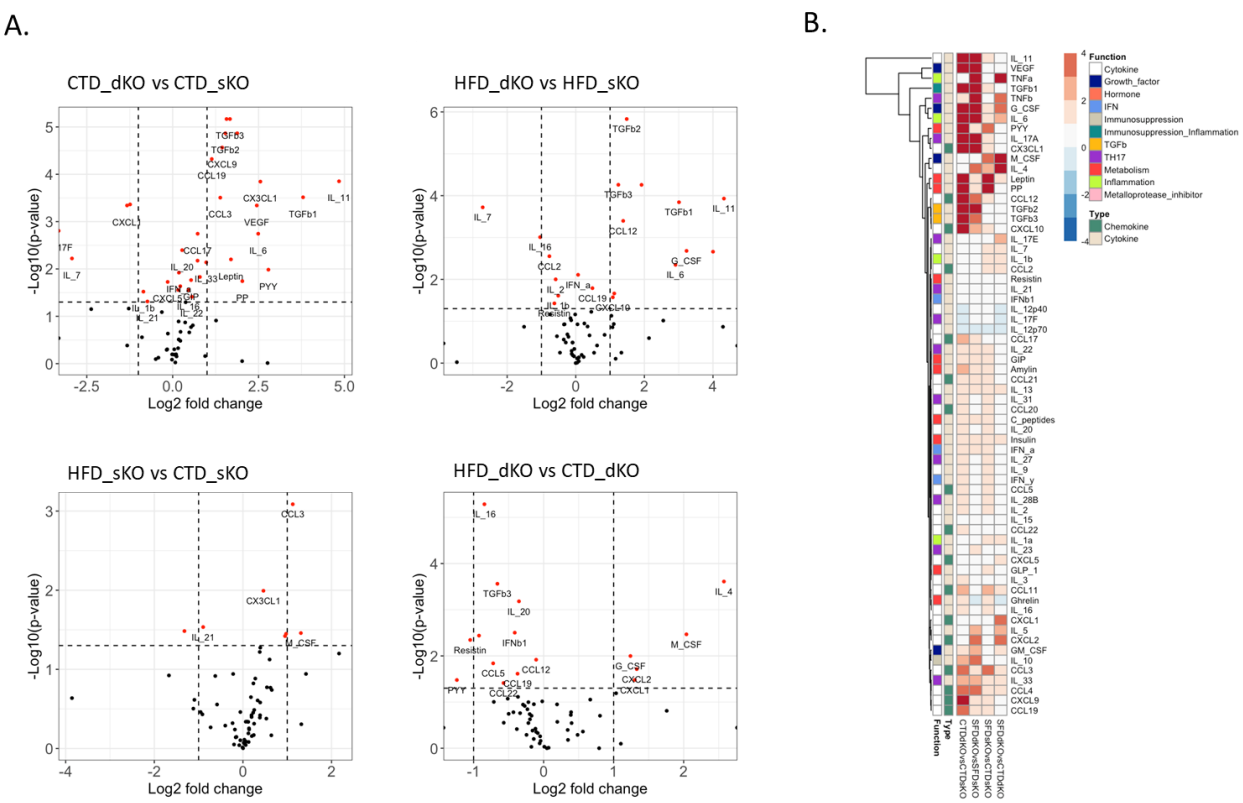

Figure 23: Genetic drivers and diet crosstalk modulates cytokine concentrations in the tumour microenvironment. A) Change of values from sKO to dKO under diet condition or change of values from CTD to HFD under genotype condition visualized by volcano plots. B) Heatmap presenting raw fold change values for each analyte under every condition comparison. Fold change based on mean values. Magnitude of fold change in volcano plots represented in Log base 2 format. *p*-values represented in –log base 10 format. Significant analytes must have a fold change of greater than 2 or less than 0.5 and a *p*-value less than 0.05. Unpaired t-test for normally distributed data or Wilcoxon rank-sum test otherwise.

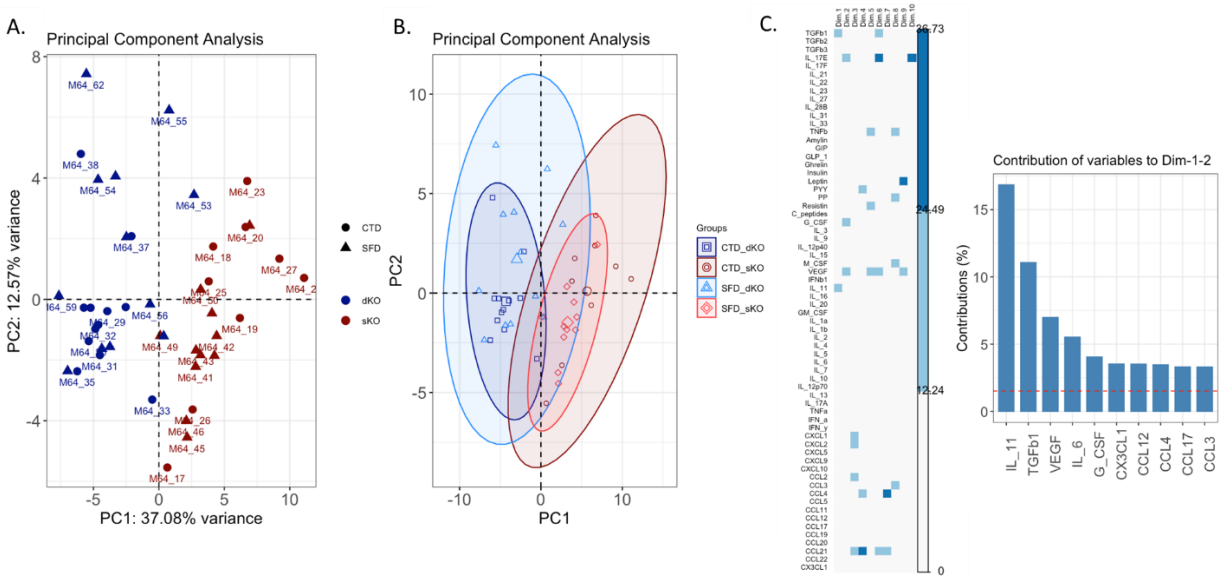

Figure 24: Principal component analysis of tumour samples shows clear separation between sKO and dKO that is driven by IL-11, TGF-β1, VEGF, and IL-6, among other analytes. (A). PCA plot point colour indicates genotype and shape indicates diet. (B) Plot emphasizes comparison of sample spread between the conditions through addition of concentration ellipses with mean point. (C). Summary of contributing cytokines to variance observed in each dimension with highlighting of top variance drivers for the main dimensions.

3.6 Results table

Analyte	Pca-expressed receptor	Function	dKO CTD / sKO CTD	dKO HFD / sKO HFD	sKO HFD / sKO CTD	dKO HFD / dKO CTD
IFNa (extrapolated values)			1.03	1.02	0.98	0.97
IFNγ			3.93	1.18	3.19	0.96
CXCL1 (KC)	CXCR2	Neutrophil trafficking	0.11	0.44	1.22	4.80
CXCL2 (MIP-2)	CXCR2	Neutrophil trafficking	0.48	1.42	1.66	4.93
CXCL5 (LIX) (fluorescence)	CXCR2	Neutrophil trafficking	0.92	0.98	0.91	0.97
CXCL9 (MIG)	CXCR3	Th1 response; Th1, CD8, NK trafficking	5.78	1.34	2.41	0.56
CXCL10 (Ip10)	CXCR3	Th1 response; Th1, CD8, NK trafficking	4.09	1.40	1.30	0.45
CCL2 (MCP-1)	CCR2	Inflammatory cytokine trafficking	0.29	0.27	1.54	1.43
CCL3 (MIP-1a)	CCR5	Macrophage and NK-cell migration; T - DC interaction	1.84	1.58	1.73	1.49
CCL4 (MIP-1b)	CCR5	Macrophage and NK-cell migration; T - DC interaction	1.54	1.76	1.42	1.61
CCL5 (RANTES)	CCR5	Macrophage and NK-cell migration; T - DC interaction	2.99	0.35	3.25	0.38
CCL11 (Eotaxin)		Eosinophils, basophils, Th2 cells, mast cells, dendritic cells	7.76	0.81	9.11	0.95
CCL12 (MCP-5)	CCR2	Eosinophils, monocytes, lymphocytes	10.79	2.48	2.22	0.51
CCL17 (TARC)		Th2 cells, Th17 cells, Treg cells, monocytes, basophils, CD4 and CD8 T cell	5.16	1.09	1.27	0.27
CCL19 (MIP-3b)	CCR7	T-cell and DC homing to LN	3.02	1.33	1.43	0.63
CCL20 (MIP-3a)		Th17 repsonses, B-cell, and DC homing to gut-associated lymphoid tissue	2.01	0.84	2.20	0.92
CCL21 (6ckine)	CCR7	T-cell and DC homing to LN	1.75	1.34	1.18	0.90
CCL22 (MDC)		Th2 response, Th2-cell migration, Treg migration	2.71	0.62	1.76	0.40
CX3CL1 (Fractalkine)		Monocytes macrophages, Th1 cells, DCs, NK cells	12.63	5.84	1.64	0.76

> 0.1 fold increase ($p < 0.05$)
> 0.1 fold decrease ($p < 0.05$)

Table 2: Luminex chemokine fold change summary indicates dKO have greater potential for immune cell infiltration than sKO. Chemokines are altered by genotypic drivers and diet, which indicates the potential alteration of the tumour immune infiltrate. Known prostate cancer chemokine receptors and classical function shown. Fold change comparison between genotypes in each diet condition and relative fold change comparison between switching each genotype from CTD to HFD. Cut-off for fold change of 0.1 in either direction and *p*-value less than 0.05. Median values from Mann-Whitney test used for fold change calculations.

CHAPTER IV

Discussion

4.1 Summary

The tumour microenvironment is a complex system that the tumour harnesses to sustain its continued development. Genetic drivers and environmental factors such as the diet have been recognized as contributing to the etiology of various cancers. Importantly, both cancer genetic drivers and diet have been shown to impact the host inflammatory response. The goal of this thesis is to pinpoint potential mechanisms by which genetic drivers and diet govern the tumour microenvironment in prostate cancer. To do so, it is important to understand the meaning of the results observed and discuss the conclusions that can be drawn from them. This will inform future directions in the aim to understand the prostate tumour microenvironment.

4.2 IFN-α stimulation of *Pten* and *Rb1*-driven prostate cancer cells

The purpose of the experiment was to learn, using the dKO cell line, whether stimulation with IFN-α in the context of prostate cancer driven by the combined loss of *Pten* and *Rb1* modulates the frequency and/or the intensity of immune checkpoint ligand expression. The purpose of the timepoints was to provide insight into the mechanism behind expression. Ligand expression may have to begin with gene transcription if there is no predisposition to ligand expression, or the ligand is just below the cell surface ready to be transported to the surface. The timepoints (**Fig. 10**) gave a sense of where the ligand is on this spectrum. Additionally, quantitative polymerase chain reaction (qPCR) of vehicle and IFN-stimulated dKO cells could be used to determine whether ligand expression requires mRNA transcription or mRNA translation. However, this interest is secondary to learning if IFN-α stimulates dKO cells to express checkpoint

ligands. Establishing the baseline expression level of checkpoint ligands on the dKO against expression on professional antigen presenting cells (pAPCs) would put into context any differences in checkpoint ligand expression seen with IFN-α stimulation.

H-2K^{b} serves as a positive control because MHCI expression is increased by IFN stimulation [61]. This is seen quite clearly in terms of frequency of expression (**Fig. 12**). However, a proportion of prostate cancers have dysregulation of IFN-mediated expression of MHCI [147], potentially explaining the lack of significant difference in H-2D^{b} expression (**Fig. 12**). Additionally, the lack of significant difference in expression intensity of the MHCI molecules under stimulation (**Fig. 13**) may be due to some dysregulation of the pathway that limits production or trafficking of the MHCI molecules to the cell surface. Characterization of MHCI expression due to IFN-α stimulation in the context of human pancreatic β cells demonstrates expression intensity should also increase [148]. However, expression intensity being a relative measure when acquired by flow cytometry, means that it is not possible to distinguish with this data (**Fig. 13**) if baseline expression intensity is high in dKO cells or IFN-signaling dysregulation prevents increased surface expression in stimulated cells. The other markers have large variations in frequency and intensity of expression between experimental replicates (**Fig. 12 and 13**). Additional replicates are needed to conclude that IFN-α modulates ligand expression of PD-L1 and CD80 in the dKO cell line *in vitro*. Important to note, the same cell batch was used for all replicates and the cell passage number is similar between experiments.

Several experimental modifications could be performed that may reduce the spread of the replicates in the vehicle and IFN-α treated groups.

- Live/dead staining and gating on GFP+ cells would provide a robust way to ensure that only healthy cells are being examined for ligand expression. The dKO (and sKO) are engineered to express GFP.
- Preparing only stained IFN-α-treated and vehicle-treated conditions and using fluorescence minus one controls (FMOs) as the reference for setting the ligand-positive gate instead of using unstained samples would significantly reduce the number of samples to be processed. FMOs also allow setting of more accurate gates than unstained samples alone since they account for spillover between detectors of the flow cytometer. However, compensation beads were used to account for any spillover in the data. The flow cytometry panels established for the experiment were specific to the Fortessa X20 flow cytometer and its combination of detectors and filters to minimize spillover.
- Removing the 3rd panel would reduce the number of samples by a third while losing only 1 of 10 checkpoint markers (OX40L). This would make the experiment much more manageable and reduces processing time. There are currently 72 unique samples per experiment with the 3 panels.
- Reducing the timepoints to 0h, 1h, 4h, and 12h would reduce the number of samples to process and still provide insight into the mechanism behind marker expression. H2-Kb expression frequency, which is expected to be increased at later time points, appears by the 12h timepoint.

It is possible that IFN-α is not an important component of the genetic driver and diet mechanism controlling checkpoint ligand expression in this prostate tumour model. While mice have larger tumours when fed HFD (**Fig. 17**), IFN-α and IFN-γ concentrations do not change due to the HFD (**Table 2**). This suggests that the interferons do not mediate the HFD-dependent tumour growth in tumours driven by *Pten* loss or combined *Pten* and *Rb1* loss – highlighting the crosstalk between genetic drivers and diet in prostate cancer. General observations have been made regarding the variation in functionality of the IFN signaling pathways between cancers from different patients and even within subclonal populations [147]. However, there has been recent focus on loss of IFN signaling in prostate cancer metastases [146]. There is a latency period between development of castration resistant prostate cancer and the emergence of bone metastases. This is attributed to a dormancy of prostate cancer cells that have already infiltrated the metastatic niche. It was demonstrated that loss of cancer cell intrinsic IFN signaling occurs in prostate cancer cells proliferating in bone [146]. With this loss, immunogenicity of these metastases also decreases, as evidenced by the loss of expression of Human Leukocyte Antigen (HLA)-related genes (HLA being the human form of MHC). Any HFD contribution specific to metastatic spread of prostate cancer appears to have to be mediated through another pathway. This suggests that genetic alterations of the prostate cancer influence how diet impacts the tumour microenvironment.

4.3 C57BL/6 model of *Pten* and combined *Pten* and *Rb1* -driven prostate cancer in the context of HFD

C57BL/6 mice fed HFD were significantly heavier and carried a higher body fat percentage than CTD-fed counterparts by 9 weeks of age when they are injected with the cancer cells (**Fig. 15**). sKO and dKO cell lines successfully engrafted in the C57BL/6 with all mice on CTD or HFD

developing tumours (**Fig. 16**). sKO and dKO tumours growing in HFD-fed mice grew larger (**Fig. 17**). This means that the model is a viable option for studying the combined effects of the HFD: the substrates and cofactors provided by the diet and the systemic inflammation driven by the increased visceral adipose tissue caused by the diet.

These results are consistent with the literature on *Pten* loss models. Mice with monoallelic *Pten* deletion experience prostatic intraepithelial neoplasia. Feeding HFD to these mice leads to neoplastic progression, angiogenesis, and inflammation [149]. Mice with homozygous Pten loss fed HFD present accelerated tumour growth and increased IL-6 secretion by tumour microenvironment macrophages. Additionally, there was an increase of the MDSC proportion and a skewing towards the immunosuppressive M2 macrophages versus the M1 [150].Similarly, the TRAMP mouse model, driven by pRb, p53, and PP2A inactivation, demonstrates that an increase in both dietary fat and dietary cholesterol significantly accelerates prostate tumour progression [135].

Myc oncogene driven prostate cancer models react similarly to HFD. The Hi-Myc model demonstrated that a low-fat diet delays tumour progression. Similarly, a calorie-restricted diet reduced the incidence of localized adenocarcinoma when compared to overweight mice (fed CTD) and obese mice (fed HFD). Mice fed the HFD developed increased body weight, liver steatosis, hyperinsulinemia, and hyperglycemia. Researchers also found that the MYC-driven metabolic and epigenetic reprogramming driving prostate carcinogenesis can be amplified by HFD [138].

HFD promotion of cancer progression appears consistent across tissue types. Melanoma, Lewis lung carcinoma, and breast cancer mouse models all demonstrated an increase in tumour growth and mouse obesity with HFD, regardless of whether the tumours were orthotopic or the genetic background of the mice [104]. Clearly, HFD promotes tumour progression not only in prostate

cancer, but across tissue types. Less clear is the mechanism by which diet leads to increased tumour growth and the variations in that mechanism between cancers of different tissue types.

4.4 Impact of genetic drivers and diet on tumour immune checkpoint ligand expression *in vivo*

HFD did not lead to the increase in checkpoint ligand expression (in either the sKO or dKO models) (**Fig. 20 A and B**) that was expected based on the gene expression data generated by the Hi-MYC FVB model of prostate cancer. While *Myc*-driven prostate cancer is a model of early stage disease like *Pten* loss-driven prostate cancer (sKO), combination loss of *Pten* and *Rb1* (dKO) is representative of a more advanced disease stage with neuroendocrine differentiation features. Results demonstrate that our C57BL/6-based tumour model is a valuable tool for continued research use, but it is important to note its limitation: it is not an orthotopic model. Modulation of ligand expression by HFD may only be visible in prostate cancer cells grown orthotopically. As an organ quite separate from the skin, it has a different biochemical environment and immune population to shape the tumour. The skin, besides lacking a high concentration of active androgen compounds, is a barrier organ and therefore has much higher baseline immune infiltration than internal organs such as the prostate. It is populated by Langerhans cells, macrophages, dermal dendritic cells, mast cells, and memory T cells [151].

These results are not in line with recently published data demonstrating diet-induced obesity leads to an increase in immune checkpoint expression, sensitizing tumours to immune checkpoint blockade [104]. Orthotopic murine B16-F0 melanoma data showed an increase in protein expression of several checkpoints, including PD-1, due to diet-induced obesity. Besides the tissue type, an important difference to note between the study presented in this thesis and that of the

paper is the age of the mice. Mice were roughly 13 weeks old by the end of our study while the mice utilized in the paper were 6 or 11 months old. This is an important distinction that refers back to the concept of inflammaging that was described in the introduction. Obesity, and also age, contribute to inflammaging – an immune aging effect causing T cell dysfunction. The authors noted that they did not see the heightened phenotypic exhaustion in the 6-month-old mice. The youth of our mice (significantly younger than in the paper) and the lack of HFD-modulated checkpoint ligand expression suggest that the T cell dysregulation induced by inflammaging that sensitizes a tumour to immune checkpoint blockade is caused by a combination of diet and age. For reference, C57BL/6 mice reach sexual maturity around 5 weeks of age, but they continue growing rapidly until 3 months of age. These mice are considered mature adults from 3 to 6 months of age, which corresponds to roughly the 20-30 year old age of a human being. Old age in mice is considered to be 18-24 months of age, corresponding to 56-69 years of age in humans [152]. Prostate cancer is much more common after the 5th decade of life. This suggests that perhaps more mature mice should be used to study the impact of the diet on prostate cancer.

This study also examined the role of genetic drivers on checkpoint ligand expression. Combined *Pten* and *Rb1* loss leads to reduced expression of both CD274 and CD80 regardless of the diet (**Fig. 20 C and D**). This suggests that in prostate cancer, an advanced tumour's control of the immune compartment of the microenvironment is potentially less dependent on checkpoint ligand expression. Possibly, other control mechanisms may evolve as the tumour develops to a more advanced stage. In advanced prostate cancer, enhancer of zeste homolog-2 (*EZH2*) is overexpressed [153]. A preprint article (**doi:** https://doi.org/10.1101/730135) led by Dr Leigh Ellis found that *EZH2* expression inversely correlates with inflamed T cell infiltration, IFN signaling, and PD-L1 expression. Patients lacking *EZH2* overexpression responded better to PD-1 blockade

while Hi-Myc mice with *Ezh2*$^{fl/fl}$ responded better to PD-1 blockade. According to the Prostate Cancer Foundation, immune checkpoint blockade is given only after other treatment options have been exhausted [95,96]. Immune checkpoint blockade clinical trials with prostate cancer patients stratified by genetic drivers could help change this. However, this does not clarify how tumour genetics and the diet of a prostate cancer patient will influence their response to ICB therapy. Metabolic alteration of the microenvironment is important to the mechanism by which the cancer cells control the immune compartment [154]. Further characterization of the tumour microenvironment is required to understand the mechanism at play and how genetics and diet establish this mechanism.

Additionally, the modest successes of immune checkpoint blockade therapy in prostate cancer may also be overcome by approaches that do not require the tumour to be well-infiltrated by immune cells and have immune suppression in the tumour microenvironment driven by checkpoint ligands. A novel approach similar to Sipuleucel-T, a treatment injecting prostate cancer patients with autologous dendritic cells loaded with prostatic acid phosphatase [94], is being proposed. The approach, successfully tested in mice, consists of injecting autologous dendritic cells loaded with PD-L1 immunogen to target cancer cells as they generally express much higher baseline levels of PD-L1 across tissue types even if that is not the dominant immune suppressive mechanism [155]. This approach leads to immune infiltration of the tumour microenvironment, which is especially needed in prostate cancer [156], by targeting the cancer cells and the immunosuppressive T reg cells. While murine data demonstrates inhibition of PD-L1+ tumour cells, it is important to remember that PD-L1- subpopulations may take over or the patient may experience immune-related adverse events due to the depletion of the signaling maintaining PD-1+ T reg cells. Additionally, antigen-presenting cells express PD-L1 and will be targeted by the newly developed

immune response. This may leave the body unable to respond to new subclonal outgrowths of the tumour. Improved immunotherapy options for prostate cancer will require a better understanding of the soluble molecules contributing to the mechanism prostate cancer cells use to control the immune infiltrate of the tumour microenvironment.

4.5 Modulation of microenvironment cytokines and chemokines by genetic drivers and diet

It has been demonstrated that secondary resistance to PD-1 blockade can be driven by signaling through the type I interferon receptor [157], rather than changes in checkpoint expression. This signaling induces nitric oxide synthase 2 (NOS2) and consequently, T reg and myeloid cell infiltration that leads to PD-1 blockade resistance. A similar mechanism of action may exist in prostate cancer resistance to immune checkpoint blockade and this may be reinforced by HFD. Jacquelot *et al* demonstrate that ligand expression levels are not necessarily correlated with blockade success [157]. By better understanding how tumour genetics and diet modulate tumour microenvironment cytokine concentrations, we can begin to look for other processes to target in addition to the ligand-receptor interactions of the immune checkpoint regulatory system.

The differences in cytokine and chemokine concentrations that are fueled by genetic drivers and diet in our model suggest that increasing or decreasing certain cytokines can decrease the tumour growth driven by those genetic drivers and diet. Physiologic concentrations of cytokines and chemokines serve to induce immune cell differentiation, maturation, and expansion as well as homing and retention in target tissues. A similar theory was put to the test in the form of injection of a cytokine/chemokine mixture in the metastases of patients with multiple cutaneous melanoma lesions. This injection led to increased CD8+ T cell infiltration in lesions (including non-injected) and durable regression of metastases (including non-injected) [158]. The

cytokine/chemokine mixture is the supernatant of the conditioned growth medium made from the *ex vivo* culture of autologous peripheral blood mononuclear cells exposed to various commercially available microbial antigens such as tuberculin. GM-CSF and IFN-α tended to be present in the unique cocktails that each patient with complete regression received. Several preclinical and clinical trials are testing chemokine and receptor inhibition as monotherapy or combined with existing treatments for a range of cancers including prostate [159]. Luminex results promote the notion that combined tumour suppressor loss and HFD modulate cytokine and chemokine concentrations to create a microenvironment conducive to prostate cancer growth. However, further research will be required to first identify the exact cytokine/chemokine combination driving tumour growth and then to elaborate a strategy to block it.

Luminex results show IFN-α and IFN-γ concentrations are unaffected by changes to genetic drivers or HFD while concentrations of other cytokines have pronounced changes (**Fig. 23**). Several relationships are suggested for potential cytokine involvement in regulation of the tumour microenvironment by the Luminex data and have been organized into 3 sections based on the potential sustaining factor:

Genetic driver (dKO vs sKO)

TGF-β1,2,3 correlation with CXCL9 and CXCL10 (**Fig. 21B**) suggests possible T reg-driven suppression of the immune response. TGF-β1,2,3 are increased in the dKO regardless of the diet, while CXCL9 and CXCL10 are increased in the dKO over the sKO when compared on CTD (**Table 2**). TGF-β promotes naïve T cell differentiation into T reg cells and is also produced by T reg cells to inhibit activated T effector cells (CD4+ and CD8+). T reg infiltration in prostate tumours has been found to be up to 10-fold higher than in normal prostate tissue [160]. Increased infiltration of T regs is associated with reduced PSA recurrence-free survival, advanced tumour

stage, and increased cellular proliferation [160]. CCL22, which is increased in the dKO under CTD conditions, has been shown to induce T reg cell migration in prostate cancer models [161]. With IL-6 significantly upregulated in the same direction between conditions, it is possible there is Th17 differentiation. While the role of Th17 cells in the cancer context is generally not well understood, it was believed that they may play a protective role [162]. More recent literature demonstrates that in an immunocompetent mouse model of prostate cancer, Th17-polarized cells contribute to tumour growth [163]. However, the lack of modulation of IL-17 concentrations (**Fig. 23**) make it more plausible that the T reg subset is the dominant T cell population and is shaped by the tumour genetics.

The IL-11/TGF-β1 signalling axis is known to recruit immune-suppressive fibroblasts and leads to chemoresistance. They are increased in the dKO over the sKO regardless of the diet (**Fig. 23A**). Relevant to our dKO HFD model, IL-11 is also involved in adipogenesis and neurogenesis. IL-11 activates Janus kinases in cancer and epithelial cells and along with TGF-β, is required for fibroblast activity. Notably, it was found to promote recruitment of immune suppressive lung cancer-associated fibroblasts and chemoresistance [164]. TGF-β1 stimulates collagen production through upregulation of IL-11. Dysregulation of these cytokines is associated with fibrotic diseases. TGF-β1 contributes to Th17 and induced T reg differentiation [61]. Th17 differentiation also requires IL6. T regs produce IL-11 to inhibit effector T cell activity and reduces MHCII expression (antigen presentation) in B cells and dendritic cells, which interferes with effector T cell maturation. TGF-β stops the cell cycle at the G1 phase to stop proliferation and induces differentiation or apoptosis. In cancer cells, the pathway is usually disrupted and cells continue to proliferate. Transformed cells produce more TGF-β, which acts on stromal cells, immune cells, and endothelial cells. Loss of TGF-β1 in adipose tissue of obese individuals leads to classically

activated (inflammatory) macrophages that create a state of chronic inflammation. Isoforms TGF-β2 and TGF-β3 may signal through the same receptor (TGF-βR1), however TGF-β1 is the most common and ubiquitously expressed. Combined tumour suppressor loss may lead to recruitment of cancer-associated fibroblasts in this prostate cancer model.

IL-33, upregulated in the dKO regardless of diet (**Fig. 23B**), acts as a danger-associated molecular pattern after release to the extracellular space of cells in the context of immunologic (not-silent) cell death such as necrosis or pyroptosis. IL-33 drives cytokine production in Th2 lymphocytes, mast cells, basophils, eosinophils, natural killer and natural killer T cells. IL-33 is also known to favour differentiation of immunosuppressive neutrophils [165]. IL-33 modulation is known to affect T cell subset differentiation and T reg cells have notable expression of the IL-33 receptor ST2 [166]. Obesity-associated inflammation is considered to be caused by a reduction of immunoregulatory cells in the visceral adipose tissue (VAT). IL-33 is critical for the development and maintenance of visceral adipose tissue T regs [167]. *In vitro* culturing of murine adipocytes with IL-33 induces IL-5 and IL-13 production, decreased expression of genes associated with adipogenesis and lipid metabolism, and reduced lipid storage. $ST2^{-/-}$ mice fed HFD had increased body weight and fat mass and impaired glucose regulation and insulin secretion compared to HFD WT controls. IL-33 treatment of obese, diabetic mice leads to reduced adiposity, lower fasting glucose levels, improved insulin tolerance, accumulation of Th2 cells and M2 macrophages in adipose tissue, and higher proportion of $ST2^{+}$ T regs in the visceral adipose tissue [168]. Combined tumour suppressor loss potentially leads to an increase in IL-33 to support T reg cells and tumour-associated neutrophils.

VEGF overexpression in the dKO (**Fig. 23**) may synergize with metalloproteinase production by neutrophils to promote angiogenesis [169]. VEGF is important for growth of blood

vessels from pre-existing vasculature (angiogenesis) by inducing endothelial cell mitogenesis and migration. VEGF is also a vasodilator and increases microvascular permeability. Cancer vascular leakage commonly leads to impaired drug delivery and facilitates the metastatic process.

Diet (HFD vs CTD)

M-CSF, instead of GM-CSF, upregulation under HFD conditions regardless of genotype (**Fig. 23**) suggests HFD contributes to the development of tumour-associated immune-suppressive macrophages [170]. These macrophages may also contribute to angiogenesis and tissue invasion [171]. Clinical trials are underway that look at combination treatment with ICB and inhibitors of the receptor (CSF1R) in several cancers including prostate [170].

Genetic driver / diet interaction

IL-6 contributes to the variance between tumour samples in our prostate cancer model, warranting examination of STAT3 signaling[31] in the sKO and dKO cells (**Fig. 24**). HFD enriches IL-6 concentrations in the dKO (**Fig. 23B**). IL-6 is known to cause androgen receptor-mediated gene activation, an important component of androgen-independent prostate cancer progression. HFD may increase IL-6 concentration in the dKO tumour microenvironment to directly support the development of cancer cell androgen independence and therefore resistance to androgen-targeting therapies.

G-CSF and GM-CSF correlation with CXCL1,2,5 (**Fig. 21B**) points to strong neutrophil recruitment and maturation. HFD leads to an increase of almost 500% of CXCL1 and CXCL2 in the dKO (**Table 2**). These molecules cause neutrophil trafficking from the bone marrow to the blood and maturation. Neutrophils account for 60 to 70% of white blood cells. Along with basophils and eosinophils, they form the polymorphonuclear cells[61]. Neutrophils are first responders capable of phagocytosis, degranulation, and forming extracellular traps (NETs). They

use pattern recognition receptors (Toll-like receptors) and opsonization receptors to sense. GM-CSF stimulates functional activity of mature neutrophils. Neutrophils also have angiogenic properties. Neutrophils are a rich source of the metallopeptidase MMP9 and do not express any of the metallopeptidase inhibitor (TIMP) molecules. The reactive oxygen species produced by neutrophils contributes to DNA damage, genome instability, and gene mutation in premalignant cells that contributes to oncogenic transformation. Neutrophils recruited to sites of chronic inflammation may promote carcinogenesis [169]. As ubiquitous tissue residents, neutrophils are found in prostate tissue, which commonly suffers from chronic inflammatory conditions. This could also lead to the recruitment of myeloid-derived suppressor cells [111]. It seems that combined tumour suppressor loss is necessary for HFD to lead to recruitment of potentially tumour-supporting neutrophils.

Based on the points above, *Pten* and *Rb1* tumour suppressor loss may synergize with HFD to suppress immune effector functions in the tumour microenvironment through the promotion of T reg, MDSC-neutrophil, and fibroblast populations (**Fig. 25**). These populations may synergize to create a highly immune-suppressed microenvironment. The distinction between neutrophils and myeloid-derived suppressor cells is not well defined. MDSCs may come from granulocytic or monocytic backgrounds. While granulocytic-MDSCs have been theorized to be a specific form of immature myeloid cell, they appear to share a similar morphology and cell surface marker profile as mature neutrophils [172]. The most prominent feature differentiating the two populations is the high suppressive capacity of the granulocytic-MDSCs. This suggests that the two groups may be one cell type capable of polarization based on the tumour microenvironment factors present. Cancer-associated fibroblasts have been found to establish a metabolic symbiosis with prostate

cancer cells. Fibroblasts are generally the major cellular stromal component of solid tumours, underscoring the significance of any metabolic relationship with the cancer cells. It was demonstrated that molecules and metabolites generated by fibroblasts are sensed by prostate cancer cells through the SIRT1/PGC-1α axis [173]. This leads to reshaping of mitochondrial functioning in the tumour cells. Additionally, fibroblasts are able to donate their mitochondria to the cancer cell to support an aggressive prostate cancer phenotype[173].

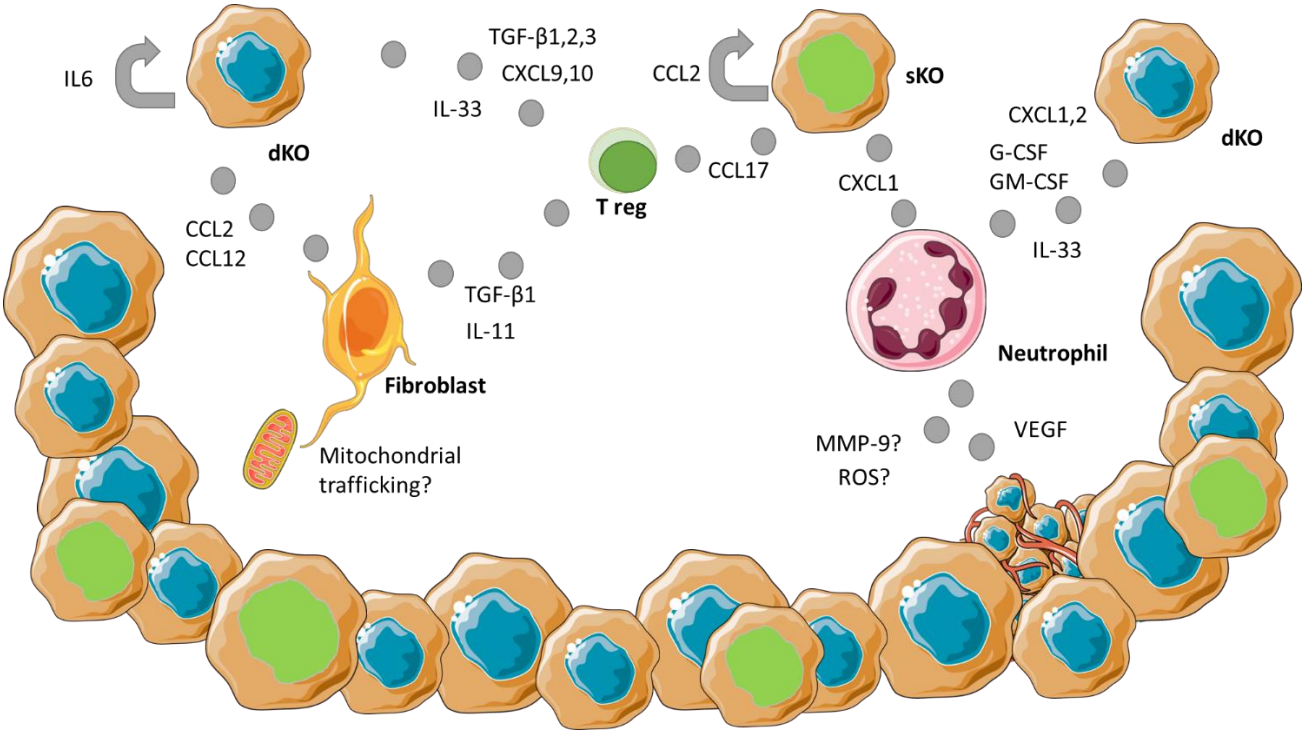

Figure 25: Potential mechanism for genetic driver cooperation with HFD in prostate cancer to promote tumour growth. T regs, immune-suppressive neutrophils, and fibroblasts are promoted to support the growth of the tumour through the cytokines and chemokines found in the tumour microenvironment. The sKO tumours have higher concentrations of IL-2 while the dKO have higher concentrations of IL-6, which contributes to androgen independence in advanced

disease. Neutrophils likely contribute to angiogenesis and the accumulation of genetic modifications in this model, while fibroblasts may contribute to the energetic and metabolic requirements of the cancer cells to maintain their rapid proliferation. Images from Servier were used in part to create this figure. Servier Medical Art by Servier is licensed under a Creative Commons Attribution 3.0 Unported License

In addition to the bullet points above, more support for this idea of immune suppressive cell types is found in cluster 4 of the unsupervised heatmap (**Fig. 22**) where several other chemokines had high concentrations. CCL2 autocrine signaling contributes to prostate cancer proliferation, but it is also needed for adherence and transmigration of neutrophils [174]. Together with CCL2, CCL12 serves as a chemoattractant for fibrocytes [175]. CCL21 and CXCL9 may be involved in T cell trafficking to lymph nodes and target tissues, respectively, in this tumour model. However, CCL21 is also known for neutrophil trafficking to the lymph nodes [176]. Neutrophils account for roughly two-thirds of the immune cell population. As first responders of the immune system, they are capable of phagocytosis, degranulation, and forming neutrophil extracellular traps (NETs). NETs are implicated in metastasis formation [177]. They express pattern recognition receptors (mainly toll-like receptors) and opsonization receptors. Neutrophils have also been noted to function as antigen presenting cells[178]. Such a wide range of capabilities makes the neutrophil a favourable candidate for performing functional assays in tumour cell-conditioned medium to assess its immunosuppressive capabilities and role in a potential suppressive immune cell mechanism by which genetic drivers and diet control the antitumour immune response in this model of prostate cancer.

Our data suggests injection of an *ex vivo*-derived cytokine/chemokine cocktail in prostate cancer may be as successful in altering prostate tumour growth as was seen with preliminary results in the literature for melanoma. Additionally, our data lends support to the targeting of specific soluble molecules particularly important in the prostate cancer context. The melanoma experiment had identified increased CD8+ T cell infiltration due to the cocktail treatment. To similarly identify changes in the immune infiltrate between conditions of our prostate cancer model, it is necessary to characterize the immune infiltrate in each of the four genetic driver and diet combinations. Flow cytometry of murine tumour chunks could identify populations of cells such as T cells, neutrophils, fibroblasts, and dendritic cells. Any cell population prominently affected by the tumour condition would be a good candidate for another round of flow cytometry for *in vivo* tumours to focus on establishing the functionality of that cell type in the tumour microenvironment. Identification of the key cell types driving the prostate cancer model would provide the basis for creating a unique cytokine cocktail to modulate tumour growth for prostate cancer stratified on genetic driver and diet status.

4.6 Role of Omega-3 fatty acids in shaping the tumour microenvironment

While the diet aspect of this thesis examines the role of increased fat intake, particularly saturated fat, complementary research has examined the role of Omega-3 fatty acids in prostate cancer development and progression using a cell line derived from the TRAMP mouse model [179]. The TRAMP prostate cancer mouse model is driven by pRb, p53, and PP2A inactivation caused by SV40 Large T and small t antigen expression in the prostate tissue [136]. Eugonadal and castrated C57BL/6 mice injected with TRAMP-C2 cancer cells experienced reduced tumour growth and increased overall survival when fed a diet with a higher proportion of Omega-3 fatty acids [137]. The

results suggest particular unsaturated fatty acids are more protective than others since the study compared Omega-3 against Omega-6. Since both are essential fatty acids, it is more relevant to discuss their ideal dietary ratio. Previous research similarly concluded that increasing the proportion of Omega-3 delays the progression of prostate cancer [180].

Eugonadal mice fed an Omega-3-enriched diet have a tumour microenvironment with increased concentrations of cytokines produced by Th1 and Th2-differentiated CD4+ T cells [179]. No difference is seen in overall CD4+ T cell infiltration due to the Omega-3 enrichment, however there are significantly fewer IL-10-producing CD4+ T cells in the Omega-3 condition. This suggests that another T helper cell population may expand due to the Omega-3-enriched diet as both effector and regulatory CD4+ T cells produce IL-10 [181].

Polyunsaturated fatty acids contribute to the regulation of inflammation. Toll-like receptor 4 (TLR4) signaling is recognized as one of the main drivers of systemic and chronic inflammation induced by obesity. Omega-3 polyunsaturated fatty acids attenuate TLR4 signaling to reduce the inflammation [182]. Arachidonic acid, an Omega-6 polyunsaturated fatty acid, is a precursor to several prostaglandins and leukotrienes that server as inflammatory mediators. However, evidence suggests increased intake in healthy adults does not correlate with a general increase in inflammatory markers [183]. This is in contrast with evidence that Omega-6 fatty acids may inhibit Omega-3 driven resolution of inflammation. Overall, this provides more support for examination of the Omega-6 to Omega-3 dietary ratio. *In vitro* treatment of starved sKO and dKO cells with varying ratios of Omega-6 to Omega-3 fatty acids followed by Luminex of the conditioned growth medium for potentially secreted metabolites could help characterize the substances that cells of the immune compartment encounter in the tumour microenvironment of prostate cancer. Characterization of the extent of tumour TLR4 signaling under the varying genetic driver and diet

conditions of this prostate cancer model may contribute to the existing literature on the role of metabolites in regulating prostate cancer inflammation.

4.7 Tumour control of the immune compartment of the microenvironment through metabolic dysregulation

Metabolic dysregulation concurrent with tumour development and progression modifies the microenvironmental immune response. The cell fate decisions and effector functions of immune cells is fueled by certain metabolic pathways: oxidative metabolism, glycolysis, and glutaminolysis [184]. In a study using melanoma and colon adenocarcinoma models, CD36 was found to be selectively upregulated in intratumour T reg cells and allowed the T regs to adapt to a lactic acid-enriched tumour microenvironment [185]. It is unknown how the metabolism of prostate cancer cells directly influences the immune cells that infiltrate the tumour microenvironment.

While a great number of solid tumours exhibit the Warburg effect, prostate cancer displays a different phenotype. Early prostate tumours rely on lipids rather than the increased glucose uptake seen with many malignancies [132]. It is only after significant disease progression where several mutations have accumulated that the Warburg effect appears in prostate tumours [132]. CD36 was shown to contribute to the increased fatty acid intake in human prostate cancer [186]. Deletion of *cd36* in a *Pten* loss murine prostate cancer model reduced fatty acid uptake and slowed progression of the disease. CD36 antibody therapy given to mice with patient-derived xenografts reduced the severity of prostate cancer, while combined inhibition of fatty acid uptake and de novo lipogenesis slowed proliferation of human cancer-based organoids better than individual treatment [186]. Interestingly, Omega-3 has been found to attenuate CD36 expression in endothelial cells [187].

Perhaps this contributes to the reduced TRAMP tumour growth seen in mice fed a diet with a higher proportion of Omega-3.

Identifying how the metabolic processes of prostate cancer cells influence the immune compartment of the tumour microenvironment will lead to increased understanding of cancer progression. Luminex specific for tumour tissue metabolites would identify key metabolites driven by tumour genetics and diet. Culturing T cells with these metabolites and examining their differentiation would help explain how genetic drivers and diet contribute to modulation of the immune compartment in the prostate tumour microenvironment.

4.8 Potential protective effect of creatine supplementation

It is also important to consider how other metabolites, such as creatine, may play a role in shaping the tumour microenvironment in prostate cancer. T cell maintenance and activation require large amounts of energy, which may be sparse in the tumour microenvironment where glucose, lipids, and amino acids may be preferentially taken up by rapidly dividing cancer cells. It is not well-understood how immune cells are metabolically regulated in the antitumour context. Creatine is a popular supplement among competitive athletes because this molecule buffers ATP levels in muscle cells through maintaining the high-energy phosphate levels needed to perform quick, powerful movements. However, it has also been found that T cells infiltrating the tumour microenvironment increase expression of the creatine transporter gene (*CrT*) [188]. Knocking out *CrT* leads to a deficiency of creatine in T cells and severely restricted antitumour immunity. Melanoma and colon adenocarcinoma mouse models demonstrate that creatine supplementation suppresses tumour growth and synergizes with PD-1/PD-L1 immune checkpoint blockade. Interestingly, HFD was found to suppress the positive effect of creatine supplementation on

skeletal muscle function mediated through the IGF1-PI3K-Akt-mTOR pathway [189]. However, it is not clear which fats mediate this effect nor how this translates to the cancer context. While not fully understood, manipulation of metabolic processes by supplementation or depletion of certain nutrients may allow modulation of tumour immune responses without the inherent risks of immune-related adverse events that plague current immunomodulatory approaches [185].

CHAPTER V

Conclusions

The goal of this thesis project was to pinpoint potential mechanisms sustaining the tumour microenvironment of prostate cancer through genetic drivers and HFD. The project aimed to build on the body of knowledge in the literature regarding the impact of diet on prostate carcinogenesis and progression established using the TRAMP, Hi-Myc, and prostate epithelium *Pten* loss mouse models of prostate cancer. Furthermore, it aimed to build the body of knowledge with regard to the integral role of the immune system in any potential mechanism mediating HFD impact on prostate cancer.

A model for the study of genetic driver and HFD impact on the prostate cancer tumour microenvironment was established. The concentration of 66 soluble molecules has been characterized under the genetic driver and diet conditions of this model. These molecules point to an immunosuppressed microenvironment supported by T regs, neutrophils, and fibroblasts. Flow cytometry of the tumour infiltrate will shed more light on this.

While the *in vitro* stimulation of dKO cells with IFN-α may have required another replicate for a strong conclusion regarding checkpoint ligand expression, Luminex data showed IFN-α and IFN-γ concentrations did not change in response to the diet. Interestingly, the literature indicates prostate cancer cells that have migrated to the bone metastatic niche begin to proliferate upon loss of intrinsic Type I IFN signaling [146]. Characterizing the immune checkpoint ligand expression profile of cancer cells in the metastatic niche would shed light on the value of different checkpoint blockade therapies for the specific treatment of metastatic prostate cancer.

The sKO and dKO tumour checkpoint ligand expression profiles did not change either in response to HFD. This attracted a closer look to the concept of inflammaging. Potentially advanced age is needed to establish a baseline level of T cell dysfunction that HFD can push over the edge to sensitise prostate cancer to immune checkpoint blockade.

On the other hand, the expression of CD80 and CD274 was reduced by combined *Pten* and *Rb1* tumour suppressor loss. This advanced stage of disease may be less reliant on checkpoints to control the effector immune cell subset – which would fit in nicely with the idea that certain cell types are driving immunosuppression rather than the tumour directly. If the sKO are more reliant on the checkpoints, this may support the notion of giving immune checkpoint blockade earlier in the course of treatment. Currently, pembrolizumab is given to prostate cancer patients after other standard treatment options have failed, including hormone therapy, surgery, and radiation [95].

REFERENCES

1. Medicine, J.H. Radical Prostatectomy. (2020).
2. Male anatomy.png. Vol. 2020 (commons.wikimedia.org, 2020).
3. Myers, R.P. Structure of the adult prostate from a clinician's standpoint. *Clinical anatomy (New York, N.Y.)* **13**, 214-215 (2000).
4. Lee, C.H., Akin-Olugbade, O. & Kirschenbaum, A. Overview of prostate anatomy, histology, and pathology. *Endocrinology and metabolism clinics of North America* **40**, 565-575, viii-ix (2011).
5. Society, C.C. Prostate Cancer. (2020).
6. Rybak, A.P., Bristow, R.G. & Kapoor, A. Prostate cancer stem cells: deciphering the origins and pathways involved in prostate tumorigenesis and aggression. *Oncotarget* **6**, 1900-1919 (2015).
7. Release notice - Canadian Cancer Statistics 2019. *Health promotion and chronic disease prevention in Canada : research, policy and practice* **39**, 255 (2019).
8. Siegel, R.L., Miller, K.D. & Jemal, A. Cancer statistics, 2020. *CA: a cancer journal for clinicians* **70**, 7-30 (2020).
9. Balk, S.P., Ko, Y.J. & Bubley, G.J. Biology of prostate-specific antigen. *Journal of clinical oncology : official journal of the American Society of Clinical Oncology* **21**, 383-391 (2003).
10. Institute, N.C. Prostate-Specific Antigen (PSA) Test. (2012, July 24).
11. Wu, S., Powers, S., Zhu, W. & Hannun, Y.A. Substantial contribution of extrinsic risk factors to cancer development. *Nature* **529**, 43-47 (2016).
12. Fradet, Y., Klotz, L., Trachtenberg, J. & Zlotta, A. The burden of prostate cancer in Canada. *Canadian Urological Association journal = Journal de l'Association des urologues du Canada* **3**, S92-s100 (2009).
13. Cao, Y. & Ma, J. Body mass index, prostate cancer-specific mortality, and biochemical recurrence: a systematic review and meta-analysis. *Cancer prevention research (Philadelphia, Pa.)* **4**, 486-501 (2011).
14. Zuccolo, L.*, et al.* Height and prostate cancer risk: a large nested case-control study (ProtecT) and meta-analysis. *Cancer epidemiology, biomarkers & prevention : a publication of the American Association for Cancer Research, cosponsored by the American Society of Preventive Oncology* **17**, 2325-2336 (2008).
15. Klein, E.A.*, et al.* Vitamin E and the risk of prostate cancer: the Selenium and Vitamin E Cancer Prevention Trial (SELECT). *Jama* **306**, 1549-1556 (2011).
16. Cui, Z., Liu, D., Liu, C. & Liu, G. Serum selenium levels and prostate cancer risk: A MOOSE-compliant meta-analysis. *Medicine* **96**, e5944 (2017).
17. Foerster, B.*, et al.* Association of Smoking Status With Recurrence, Metastasis, and Mortality Among Patients With Localized Prostate Cancer Undergoing Prostatectomy or Radiotherapy: A Systematic Review and Meta-analysis. *JAMA oncology* **4**, 953-961 (2018).
18. Jiang, J.*, et al.* The role of prostatitis in prostate cancer: meta-analysis. *PloS one* **8**, e85179 (2013).
19. Waalkes, M.P. & Rehm, S. Cadmium and prostate cancer. *Journal of toxicology and environmental health* **43**, 251-269 (1994).
20. Silva, J.F., Mattos, I.E., Luz, L.L., Carmo, C.N. & Aydos, R.D. Exposure to pesticides and prostate cancer: systematic review of the literature. *Reviews on environmental health* **31**, 311-327 (2016).
21. Heinzer, H. & Steuber, T. Prostate cancer in the elderly. *Urologic oncology* **27**, 668-672 (2009).
22. Saad, F. & McCormack, M. *Prostate Cancer*, (Annika Parance Publishing, 2012).
23. Worthington, J.F. Treatment for Prostate Cancer: External-Beam Radiation Therapy. Vol. 2020 (Prostate Cancer Foundation, 2020).

24. Herrera, F.G. & Berthold, D.R. Radiation Therapy after Radical Prostatectomy: Implications for Clinicians. *Frontiers in oncology* **6**, 117 (2016).
25. Radiation Therapy for Prostate Cancer. Vol. 2020 (American Cancer Society, 2019).
26. Oudard, S*., et al.* Cabazitaxel Versus Docetaxel As First-Line Therapy for Patients With Metastatic Castration-Resistant Prostate Cancer: A Randomized Phase III Trial-FIRSTANA. *Journal of clinical oncology : official journal of the American Society of Clinical Oncology* **35**, 3189-3197 (2017).
27. Vasaitis, T.S., Bruno, R.D. & Njar, V.C. CYP17 inhibitors for prostate cancer therapy. *The Journal of steroid biochemistry and molecular biology* **125**, 23-31 (2011).
28. Tran, C*., et al.* Development of a second-generation antiandrogen for treatment of advanced prostate cancer. *Science (New York, N.Y.)* **324**, 787-790 (2009).
29. Banerjee, P.P., Banerjee, S., Brown, T.R. & Zirkin, B.R. Androgen action in prostate function and disease. *American journal of clinical and experimental urology* **6**, 62-77 (2018).
30. Shen, M.M. & Abate-Shen, C. Molecular genetics of prostate cancer: new prospects for old challenges. *Genes & development* **24**, 1967-2000 (2010).
31. Chen, T., Wang, L.H. & Farrar, W.L. Interleukin 6 activates androgen receptor-mediated gene expression through a signal transducer and activator of transcription 3-dependent pathway in LNCaP prostate cancer cells. *Cancer research* **60**, 2132-2135 (2000).
32. Gurel, B*., et al.* NKX3.1 as a marker of prostatic origin in metastatic tumors. *The American journal of surgical pathology* **34**, 1097-1105 (2010).
33. Ku, S.Y*., et al.* Rb1 and Trp53 cooperate to suppress prostate cancer lineage plasticity, metastasis, and antiandrogen resistance. *Science (New York, N.Y.)* **355**, 78-83 (2017).
34. Lapointe, J*., et al.* Genomic profiling reveals alternative genetic pathways of prostate tumorigenesis. *Cancer research* **67**, 8504-8510 (2007).
35. Baca, S.C*., et al.* Punctuated evolution of prostate cancer genomes. *Cell* **153**, 666-677 (2013).
36. Ellwood-Yen, K*., et al.* Myc-driven murine prostate cancer shares molecular features with human prostate tumors. *Cancer cell* **4**, 223-238 (2003).
37. The Molecular Taxonomy of Primary Prostate Cancer. *Cell* **163**, 1011-1025 (2015).
38. Carver, B.S*., et al.* Aberrant ERG expression cooperates with loss of PTEN to promote cancer progression in the prostate. *Nature genetics* **41**, 619-624 (2009).
39. Wang, S*., et al.* Prostate-specific deletion of the murine Pten tumor suppressor gene leads to metastatic prostate cancer. *Cancer cell* **4**, 209-221 (2003).
40. Chen, Z*., et al.* Crucial role of p53-dependent cellular senescence in suppression of Pten-deficient tumorigenesis. *Nature* **436**, 725-730 (2005).
41. Dyson, N.J. RB1: a prototype tumor suppressor and an enigma. *Genes & development* **30**, 1492-1502 (2016).
42. Abate-Shen, C. & Shen, M.M. Molecular genetics of prostate cancer. *Genes & development* **14**, 2410-2434 (2000).
43. Armenia, J*., et al.* The long tail of oncogenic drivers in prostate cancer. *Nature genetics* **50**, 645-651 (2018).
44. Pan, D*., et al.* A major chromatin regulator determines resistance of tumor cells to T cell-mediated killing. *Science (New York, N.Y.)* **359**, 770-775 (2018).
45. Guertin, D.A*., et al.* mTOR complex 2 is required for the development of prostate cancer induced by Pten loss in mice. *Cancer cell* **15**, 148-159 (2009).
46. Hemmings, B.A. & Restuccia, D.F. PI3K-PKB/Akt pathway. *Cold Spring Harbor perspectives in biology* **4**, a011189 (2012).

47. Du, W. & Searle, J.S. The rb pathway and cancer therapeutics. *Current drug targets* **10**, 581-589 (2009).
48. Bezzi, M*., et al.* Diverse genetic-driven immune landscapes dictate tumor progression through distinct mechanisms. *Nature medicine* **24**, 165-175 (2018).
49. Charoentong, P*., et al.* Pan-cancer Immunogenomic Analyses Reveal Genotype-Immunophenotype Relationships and Predictors of Response to Checkpoint Blockade. *Cell reports* **18**, 248-262 (2017).
50. Li, T*., et al.* TIMER: A Web Server for Comprehensive Analysis of Tumor-Infiltrating Immune Cells. *Cancer research* **77**, e108-e110 (2017).
51. Hanahan, D. & Weinberg, R.A. The hallmarks of cancer. *Cell* **100**, 57-70 (2000).
52. Hanahan, D. & Weinberg, R.A. Hallmarks of cancer: the next generation. *Cell* **144**, 646-674 (2011).
53. Germano, G*., et al.* Inactivation of DNA repair triggers neoantigen generation and impairs tumour growth. *Nature* **552**, 116-120 (2017).
54. Turajlic, S*., et al.* Insertion-and-deletion-derived tumour-specific neoantigens and the immunogenic phenotype: a pan-cancer analysis. *The Lancet. Oncology* **18**, 1009-1021 (2017).
55. Azizi, E*., et al.* Single-Cell Map of Diverse Immune Phenotypes in the Breast Tumor Microenvironment. *Cell* **174**, 1293-1308.e1236 (2018).
56. Calcinotto, A*., et al.* IL-23 secreted by myeloid cells drives castration-resistant prostate cancer. *Nature* **559**, 363-369 (2018).
57. Munoz-Fontela, C., Mandinova, A., Aaronson, S.A. & Lee, S.W. Emerging roles of p53 and other tumour-suppressor genes in immune regulation. *Nature reviews. Immunology* **16**, 741-750 (2016).
58. Pauken, K.E. & Wherry, E.J. SnapShot: T Cell Exhaustion. *Cell* **163**, 1038-1038.e1031 (2015).
59. Efremova, M*., et al.* Targeting immune checkpoints potentiates immunoediting and changes the dynamics of tumor evolution. *Nature communications* **9**, 32 (2018).
60. Martinez-Lostao, L., Anel, A. & Pardo, J. How Do Cytotoxic Lymphocytes Kill Cancer Cells? *Clinical cancer research : an official journal of the American Association for Cancer Research* **21**, 5047-5056 (2015).
61. Jr, C.J., Travers, P., Walport, M. & Shlomchik, M. *Immunobiology: The Immune System in Health and Disease.*, (Garland Science, New York, 2001).
62. Pardoll, D.M. The blockade of immune checkpoints in cancer immunotherapy. *Nature reviews. Cancer* **12**, 252-264 (2012).
63. Guillerey, C., Huntington, N.D. & Smyth, M.J. Targeting natural killer cells in cancer immunotherapy. *Nature immunology* **17**, 1025-1036 (2016).
64. Aras, S. & Zaidi, M.R. TAMeless traitors: macrophages in cancer progression and metastasis. *British journal of cancer* **117**, 1583-1591 (2017).
65. Kolaczkowska, E. & Kubes, P. Neutrophil recruitment and function in health and inflammation. *Nature reviews. Immunology* **13**, 159-175 (2013).
66. Lei, X*., et al.* Immune cells within the tumor microenvironment: Biological functions and roles in cancer immunotherapy. *Cancer letters* **470**, 126-133 (2020).
67. Valkenburg, K.C. & Williams, B.O. Mouse models of prostate cancer. *Prostate cancer* **2011**, 895238 (2011).
68. Hoehn, W., Schroeder, F.H., Reimann, J.F., Joebsis, A.C. & Hermanek, P. Human prostatic adenocarcinoma: some characteristics of a serially transplantable line in nude mice (PC 82). *The Prostate* **1**, 95-104 (1980).

69. Craft, N., Shostak, Y., Carey, M. & Sawyers, C.L. A mechanism for hormone-independent prostate cancer through modulation of androgen receptor signaling by the HER-2/neu tyrosine kinase. *Nature medicine* **5**, 280-285 (1999).
70. Mombaerts, P.*, et al.* RAG-1-deficient mice have no mature B and T lymphocytes. *Cell* **68**, 869-877 (1992).
71. Yonou, H.*, et al.* Establishment of a novel species- and tissue-specific metastasis model of human prostate cancer in humanized non-obese diabetic/severe combined immunodeficient mice engrafted with human adult lung and bone. *Cancer research* **61**, 2177-2182 (2001).
72. D'Antonio, J.M.*, et al.* Loss of androgen receptor-dependent growth suppression by prostate cancer cells can occur independently from acquiring oncogenic addiction to androgen receptor signaling. *PloS one* **5**, e11475 (2010).
73. Binnewies, M.*, et al.* Understanding the tumor immune microenvironment (TIME) for effective therapy. *Nature medicine* **24**, 541-550 (2018).
74. Elia, A.R., Caputo, S. & Bellone, M. Immune Checkpoint-Mediated Interactions Between Cancer and Immune Cells in Prostate Adenocarcinoma and Melanoma. *Frontiers in immunology* **9**, 1786 (2018).
75. Strasner, A. & Karin, M. Immune Infiltration and Prostate Cancer. *Frontiers in oncology* **5**, 128 (2015).
76. Vitkin, N., Nersesian, S., Siemens, D.R. & Koti, M. The Tumor Immune Contexture of Prostate Cancer. *Frontiers in immunology* **10**, 603 (2019).
77. Nardone, V.*, et al.* Tumor infiltrating T lymphocytes expressing FoxP3, CCR7 or PD-1 predict the outcome of prostate cancer patients subjected to salvage radiotherapy after biochemical relapse. *Cancer biology & therapy* **17**, 1213-1220 (2016).
78. Lundholm, M.*, et al.* Secreted Factors from Colorectal and Prostate Cancer Cells Skew the Immune Response in Opposite Directions. *Scientific reports* **5**, 15651 (2015).
79. Johansson, A.*, et al.* Mast cells are novel independent prognostic markers in prostate cancer and represent a target for therapy. *The American journal of pathology* **177**, 1031-1041 (2010).
80. Shafique, K.*, et al.* Systemic inflammation and survival of patients with prostate cancer: evidence from the Glasgow Inflammation Outcome Study. *Prostate cancer and prostatic diseases* **15**, 195-201 (2012).
81. Berger, M.F.*, et al.* The genomic complexity of primary human prostate cancer. *Nature* **470**, 214-220 (2011).
82. Heninger, E.*, et al.* Inducible expression of cancer-testis antigens in human prostate cancer. *Oncotarget* **7**, 84359-84374 (2016).
83. Zaidi, M.R. & Merlino, G. The two faces of interferon-gamma in cancer. *Clinical cancer research : an official journal of the American Association for Cancer Research* **17**, 6118-6124 (2011).
84. Mandai, M.*, et al.* Dual Faces of IFNgamma in Cancer Progression: A Role of PD-L1 Induction in the Determination of Pro- and Antitumor Immunity. *Clinical cancer research : an official journal of the American Association for Cancer Research* **22**, 2329-2334 (2016).
85. Di Franco, S., Turdo, A., Todaro, M. & Stassi, G. Role of Type I and II Interferons in Colorectal Cancer and Melanoma. *Frontiers in immunology* **8**, 878 (2017).
86. Ferrantini, M., Capone, I. & Belardelli, F. Interferon-alpha and cancer: mechanisms of action and new perspectives of clinical use. *Biochimie* **89**, 884-893 (2007).
87. Albacker, L.A.*, et al.* Loss of function JAK1 mutations occur at high frequency in cancers with microsatellite instability and are suggestive of immune evasion. *PloS one* **12**, e0176181 (2017).

88. Budhwani, M., Mazzieri, R. & Dolcetti, R. Plasticity of Type I Interferon-Mediated Responses in Cancer Therapy: From Anti-tumor Immunity to Resistance. *Frontiers in oncology* **8**, 322 (2018).
89. Katlinski, K.V.*, et al.* Inactivation of Interferon Receptor Promotes the Establishment of Immune Privileged Tumor Microenvironment. *Cancer cell* **31**, 194-207 (2017).
90. Solorzano, C.C.*, et al.* Administration of optimal biological dose and schedule of interferon alpha combined with gemcitabine induces apoptosis in tumor-associated endothelial cells and reduces growth of human pancreatic carcinoma implanted orthotopically in nude mice. *Clinical cancer research : an official journal of the American Association for Cancer Research* **9**, 1858-1867 (2003).
91. Dunn, G.P., Koebel, C.M. & Schreiber, R.D. Interferons, immunity and cancer immunoediting. *Nature reviews. Immunology* **6**, 836-848 (2006).
92. Greenwald, R.J., Freeman, G.J. & Sharpe, A.H. The B7 family revisited. *Annual review of immunology* **23**, 515-548 (2005).
93. Harrington, K.J.*, et al.* Clinical development of talimogene laherparepvec (T-VEC): a modified herpes simplex virus type-1-derived oncolytic immunotherapy. *Expert review of anticancer therapy* **15**, 1389-1403 (2015).
94. Kantoff, P.W.*, et al.* Sipuleucel-T immunotherapy for castration-resistant prostate cancer. *The New England journal of medicine* **363**, 411-422 (2010).
95. Antonarakis, E.S.*, et al.* Pembrolizumab for Treatment-Refractory Metastatic Castration-Resistant Prostate Cancer: Multicohort, Open-Label Phase II KEYNOTE-199 Study. *Journal of clinical oncology : official journal of the American Society of Clinical Oncology* **38**, 395-405 (2020).
96. PCF. Immunotherapy for Prostate Cancer. Vol. 2020 (Prostate Cancer Foundation).
97. Sharma, P. & Allison, J.P. The future of immune checkpoint therapy. *Science (New York, N.Y.)* **348**, 56-61 (2015).
98. Friedman, C.F., Proverbs-Singh, T.A. & Postow, M.A. Treatment of the Immune-Related Adverse Effects of Immune Checkpoint Inhibitors: A Review. *JAMA oncology* **2**, 1346-1353 (2016).
99. Subudhi, S.K.*, et al.* Clonal expansion of CD8 T cells in the systemic circulation precedes development of ipilimumab-induced toxicities. *Proceedings of the National Academy of Sciences of the United States of America* **113**, 11919-11924 (2016).
100. Gao, J.*, et al.* VISTA is an inhibitory immune checkpoint that is increased after ipilimumab therapy in patients with prostate cancer. *Nature medicine* **23**, 551-555 (2017).
101. Fridman, W.H., Pages, F., Sautes-Fridman, C. & Galon, J. The immune contexture in human tumours: impact on clinical outcome. *Nature reviews. Cancer* **12**, 298-306 (2012).
102. Kwon, E.D.*, et al.* Ipilimumab versus placebo after radiotherapy in patients with metastatic castration-resistant prostate cancer that had progressed after docetaxel chemotherapy (CA184-043): a multicentre, randomised, double-blind, phase 3 trial. *The Lancet. Oncology* **15**, 700-712 (2014).
103. Topalian, S.L.*, et al.* Safety, activity, and immune correlates of anti-PD-1 antibody in cancer. *The New England journal of medicine* **366**, 2443-2454 (2012).
104. Wang, Z.*, et al.* Paradoxical effects of obesity on T cell function during tumor progression and PD-1 checkpoint blockade. *Nature medicine* (2018).
105. Elgueta, R.*, et al.* Molecular mechanism and function of CD40/CD40L engagement in the immune system. *Immunological reviews* **229**, 152-172 (2009).
106. Croft, M., So, T., Duan, W. & Soroosh, P. The significance of OX40 and OX40L to T-cell biology and immune disease. *Immunological reviews* **229**, 173-191 (2009).

107. Li, H.*, et al.* Tim-3/galectin-9 signaling pathway mediates T-cell dysfunction and predicts poor prognosis in patients with hepatitis B virus-associated hepatocellular carcinoma. *Hepatology (Baltimore, Md.)* **56**, 1342-1351 (2012).
108. Zhang, J.M. & An, J. Cytokines, inflammation, and pain. *International anesthesiology clinics* **45**, 27-37 (2007).
109. Luckheeram, R.V., Zhou, R., Verma, A.D. & Xia, B. CD4(+)T cells: differentiation and functions. *Clinical & developmental immunology* **2012**, 925135 (2012).
110. Marcuzzi, E., Angioni, R., Molon, B. & Cali, B. Chemokines and Chemokine Receptors: Orchestrating Tumor Metastasization. *International journal of molecular sciences* **20**(2018).
111. Xu, L., Kitade, H., Ni, Y. & Ota, T. Roles of Chemokines and Chemokine Receptors in Obesity-Associated Insulin Resistance and Nonalcoholic Fatty Liver Disease. *Biomolecules* **5**, 1563-1579 (2015).
112. de Oliveira, S.*, et al.* Cxcl8 (IL-8) mediates neutrophil recruitment and behavior in the zebrafish inflammatory response. *Journal of immunology (Baltimore, Md. : 1950)* **190**, 4349-4359 (2013).
113. Schadendorf, D.*, et al.* IL-8 produced by human malignant melanoma cells in vitro is an essential autocrine growth factor. *Journal of immunology (Baltimore, Md. : 1950)* **151**, 2667-2675 (1993).
114. Tokunaga, R.*, et al.* CXCL9, CXCL10, CXCL11/CXCR3 axis for immune activation - A target for novel cancer therapy. *Cancer treatment reviews* **63**, 40-47 (2018).
115. Janssens, R., Struyf, S. & Proost, P. The unique structural and functional features of CXCL12. *Cellular & molecular immunology* **15**, 299-311 (2018).
116. Saha, A.*, et al.* Proinflammatory CXCL12-CXCR4/CXCR7 Signaling Axis Drives Myc-Induced Prostate Cancer in Obese Mice. *Cancer research* **77**, 5158-5168 (2017).
117. Shurin, G.V.*, et al.* Loss of new chemokine CXCL14 in tumor tissue is associated with low infiltration by dendritic cells (DC), while restoration of human CXCL14 expression in tumor cells causes attraction of DC both in vitro and in vivo. *Journal of immunology (Baltimore, Md. : 1950)* **174**, 5490-5498 (2005).
118. Lu, Y.*, et al.* Monocyte chemotactic protein-1 (MCP-1) acts as a paracrine and autocrine factor for prostate cancer growth and invasion. *The Prostate* **66**, 1311-1318 (2006).
119. O'Hayre, M., Salanga, C.L., Handel, T.M. & Allen, S.J. Chemokines and cancer: migration, intracellular signalling and intercellular communication in the microenvironment. *The Biochemical journal* **409**, 635-649 (2008).
120. Schmall, A.*, et al.* Macrophage and cancer cell cross-talk via CCR2 and CX3CR1 is a fundamental mechanism driving lung cancer. *American journal of respiratory and critical care medicine* **191**, 437-447 (2015).
121. Rani, A., Dasgupta, P. & Murphy, J.J. Prostate Cancer: The Role of Inflammation and Chemokines. *The American journal of pathology* (2019).
122. Aberg, J.A. Aging, inflammation, and HIV infection. *Topics in antiviral medicine* **20**, 101-105 (2012).
123. Choe, S.S., Huh, J.Y., Hwang, I.J., Kim, J.I. & Kim, J.B. Adipose Tissue Remodeling: Its Role in Energy Metabolism and Metabolic Disorders. *Frontiers in endocrinology* **7**, 30 (2016).
124. Wieser, V.*, et al.* Adipose type I interferon signalling protects against metabolic dysfunction. *Gut* **67**, 157-165 (2018).
125. Eder, K., Baffy, N., Falus, A. & Fulop, A.K. The major inflammatory mediator interleukin-6 and obesity. *Inflammation research : official journal of the European Histamine Research Society ... [et al.]* **58**, 727-736 (2009).
126. Calle, E.E. & Kaaks, R. Overweight, obesity and cancer: epidemiological evidence and proposed mechanisms. *Nature reviews. Cancer* **4**, 579-591 (2004).

127. Grosso, G.*, et al.* Possible role of diet in cancer: systematic review and multiple meta-analyses of dietary patterns, lifestyle factors, and cancer risk. *Nutrition reviews* **75**, 405-419 (2017).
128. Weroha, S.J. & Haluska, P. The insulin-like growth factor system in cancer. *Endocrinology and metabolism clinics of North America* **41**, 335-350, vi (2012).
129. Shimizu, H.*, et al.* Cancers of the prostate and breast among Japanese and white immigrants in Los Angeles County. *British journal of cancer* **63**, 963-966 (1991).
130. Van Blarigan, E.L.*, et al.* Fat intake after prostate cancer diagnosis and mortality in the Physicians' Health Study. *Cancer causes & control : CCC* **26**, 1117-1126 (2015).
131. Vander Heiden, M.G., Cantley, L.C. & Thompson, C.B. Understanding the Warburg effect: the metabolic requirements of cell proliferation. *Science (New York, N.Y.)* **324**, 1029-1033 (2009).
132. Eidelman, E., Twum-Ampofo, J., Ansari, J. & Siddiqui, M.M. The Metabolic Phenotype of Prostate Cancer. *Frontiers in oncology* **7**, 131 (2017).
133. Labbe, D.P.*, et al.* Role of diet in prostate cancer: the epigenetic link. *Oncogene* **34**, 4683-4691 (2015).
134. Shabbeer, S., Williams, S.A., Simons, B.W., Herman, J.G. & Carducci, M.A. Progression of prostate carcinogenesis and dietary methyl donors: temporal dependence. *Cancer prevention research (Philadelphia, Pa.)* **5**, 229-239 (2012).
135. Llaverias, G.*, et al.* A Western-type diet accelerates tumor progression in an autochthonous mouse model of prostate cancer. *The American journal of pathology* **177**, 3180-3191 (2010).
136. Greenberg, N.M.*, et al.* Prostate cancer in a transgenic mouse. *Proceedings of the National Academy of Sciences of the United States of America* **92**, 3439-3443 (1995).
137. Berquin, I.M.*, et al.* Modulation of prostate cancer genetic risk by omega-3 and omega-6 fatty acids. *The Journal of clinical investigation* **117**, 1866-1875 (2007).
138. Labbe, D.P.*, et al.* High-fat diet fuels prostate cancer progression by rewiring the metabolome and amplifying the MYC program. *Nature communications* **10**, 4358 (2019).
139. Wu, X.*, et al.* Generation of a prostate epithelial cell-specific Cre transgenic mouse model for tissue-specific gene ablation. *Mechanisms of development* **101**, 61-69 (2001).
140. Eagle, H. Amino acid metabolism in mammalian cell cultures. *Science (New York, N.Y.)* **130**, 432-437 (1959).
141. Eirew, P., Stingl, J. & Eaves, C.J. Quantitation of human mammary epithelial stem cells with in vivo regenerative properties using a subrenal capsule xenotransplantation assay. *Nature protocols* **5**, 1945-1956 (2010).
142. Labbe, D.P.*, et al.* TOP2A and EZH2 Provide Early Detection of an Aggressive Prostate Cancer Subgroup. *Clinical cancer research : an official journal of the American Association for Cancer Research* **23**, 7072-7083 (2017).
143. Radaeva, S.*, et al.* Interferon-alpha activates multiple STAT signals and down-regulates c-Met in primary human hepatocytes. *Gastroenterology* **122**, 1020-1034 (2002).
144. Jost, E., Roos, W.P., Kaina, B. & Schmidberger, H. Response of pancreatic cancer cells treated with interferon-alpha or beta and co-exposed to ionising radiation. *International journal of radiation biology* **86**, 732-741 (2010).
145. Keskinen, P., Ronni, T., Matikainen, S., Lehtonen, A. & Julkunen, I. Regulation of HLA class I and II expression by interferons and influenza A virus in human peripheral blood mononuclear cells. *Immunology* **91**, 421-429 (1997).
146. KL, O., LJ, G., DJ, Z. & al, e. Prostate cancer cell-intrinsic interferon signaling regulates dormancy and metastatic outgrowth in bone. *EMBO reports* (2020).

147. Bander, N.H.*, et al.* MHC class I and II expression in prostate carcinoma and modulation by interferon-alpha and -gamma. *The Prostate* **33**, 233-239 (1997).
148. Coomans de Brachene, A.*, et al.* IFN-alpha induces a preferential long-lasting expression of MHC class I in human pancreatic beta cells. *Diabetologia* **61**, 636-640 (2018).
149. Liu, J.*, et al.* High-calorie diet exacerbates prostate neoplasia in mice with haploinsufficiency of Pten tumor suppressor gene. *Molecular metabolism* **4**, 186-198 (2015).
150. Hayashi, T.*, et al.* High-Fat Diet-Induced Inflammation Accelerates Prostate Cancer Growth via IL6 Signaling. *Clinical cancer research : an official journal of the American Association for Cancer Research* **24**, 4309-4318 (2018).
151. Richmond, J.M. & Harris, J.E. Immunology and skin in health and disease. *Cold Spring Harbor perspectives in medicine* **4**, a015339 (2014).
152. flurkey, K., Currer, J. & Harrison, D. The Mouse in Aging Research. in *The Mouse in Biomedical Research* (ed. Fox, J.) 637-672 (American College Laboratory Animal Medicine, Burlingtion, MA, 2007).
153. Varambally, S.*, et al.* The polycomb group protein EZH2 is involved in progression of prostate cancer. *Nature* **419**, 624-629 (2002).
154. Reina-Campos, M., Moscat, J. & Diaz-Meco, M. Metabolism shapes the tumor microenvironment. *Current opinion in cell biology* **48**, 47-53 (2017).
155. Chen, J.*, et al.* A Novel Anti-PD-L1 Vaccine for Cancer Immunotherapy and Immunoprevention. *Cancers* **11**(2019).
156. Bilusic, M., Madan, R.A. & Gulley, J.L. Immunotherapy of Prostate Cancer: Facts and Hopes. *Clinical cancer research : an official journal of the American Association for Cancer Research* **23**, 6764-6770 (2017).
157. Jacquelot, N.*, et al.* Sustained Type I interferon signaling as a mechanism of resistance to PD-1 blockade. *Cell research* (2019).
158. Valentine, F.T., Golomb, F.M., Harris, M. & Roses, D.F. A novel immunization strategy using cytokine/chemokines induces new effective systemic immune responses, and frequent complete regressions of human metastatic melanoma. *Oncoimmunology* **7**, e1386827 (2018).
159. Mollica Poeta, V., Massara, M., Capucetti, A. & Bonecchi, R. Chemokines and Chemokine Receptors: New Targets for Cancer Immunotherapy. *Frontiers in immunology* **10**, 379 (2019).
160. Flammiger, A.*, et al.* High tissue density of FOXP3+ T cells is associated with clinical outcome in prostate cancer. *European journal of cancer (Oxford, England : 1990)* **49**, 1273-1279 (2013).
161. Miller, A.M.*, et al.* CD4+CD25high T cells are enriched in the tumor and peripheral blood of prostate cancer patients. *Journal of immunology (Baltimore, Md. : 1950)* **177**, 7398-7405 (2006).
162. Wilke, C.M.*, et al.* Th17 cells in cancer: help or hindrance? *Carcinogenesis* **32**, 643-649 (2011).
163. Duan, Z.*, et al.* Th17 cells promote tumor growth in an immunocompetent orthotopic mouse model of prostate cancer. *American journal of clinical and experimental urology* **7**, 249-261 (2019).
164. Tao, L.*, et al.* Cancer-associated fibroblasts treated with cisplatin facilitates chemoresistance of lung adenocarcinoma through IL-11/IL-11R/STAT3 signaling pathway. *Scientific reports* **6**, 38408 (2016).
165. Liang, Y.*, et al.* IL-33 induces immunosuppressive neutrophils via a type 2 innate lymphoid cell/IL-13/STAT6 axis and protects the liver against injury in LCMV infection-induced viral hepatitis. *Cellular & molecular immunology* **16**, 126-137 (2019).
166. Alvarez, F., Fritz, J.H. & Piccirillo, C.A. Pleiotropic Effects of IL-33 on CD4(+) T Cell Differentiation and Effector Functions. *Frontiers in immunology* **10**, 522 (2019).

167. Griesenauer, B. & Paczesny, S. The ST2/IL-33 Axis in Immune Cells during Inflammatory Diseases. *Frontiers in immunology* **8**, 475 (2017).
168. Han, J.M.*, et al.* IL-33 Reverses an Obesity-Induced Deficit in Visceral Adipose Tissue ST2+ T Regulatory Cells and Ameliorates Adipose Tissue Inflammation and Insulin Resistance. *Journal of immunology (Baltimore, Md. : 1950)* **194**, 4777-4783 (2015).
169. Liang, W. & Ferrara, N. The Complex Role of Neutrophils in Tumor Angiogenesis and Metastasis. *Cancer immunology research* **4**, 83-91 (2016).
170. Cannarile, M.A.*, et al.* Colony-stimulating factor 1 receptor (CSF1R) inhibitors in cancer therapy. *Journal for immunotherapy of cancer* **5**, 53 (2017).
171. Noy, R. & Pollard, J.W. Tumor-associated macrophages: from mechanisms to therapy. *Immunity* **41**, 49-61 (2014).
172. Aarts, C.E.M. & Kuijpers, T.W. Neutrophils as myeloid-derived suppressor cells. *European journal of clinical investigation* **48 Suppl 2**, e12989 (2018).
173. Ippolito, L.*, et al.* Cancer-associated fibroblasts promote prostate cancer malignancy via metabolic rewiring and mitochondrial transfer. *Oncogene* **38**, 5339-5355 (2019).
174. Reichel, C.A.*, et al.* Ccl2 and Ccl3 mediate neutrophil recruitment via induction of protein synthesis and generation of lipid mediators. *Arteriosclerosis, thrombosis, and vascular biology* **29**, 1787-1793 (2009).
175. Moore, B.B.*, et al.* The role of CCL12 in the recruitment of fibrocytes and lung fibrosis. *American journal of respiratory cell and molecular biology* **35**, 175-181 (2006).
176. Beauvillain, C.*, et al.* CCR7 is involved in the migration of neutrophils to lymph nodes. *Blood* **117**, 1196-1204 (2011).
177. Park, J.*, et al.* Cancer cells induce metastasis-supporting neutrophil extracellular DNA traps. *Science translational medicine* **8**, 361ra138 (2016).
178. Vono, M.*, et al.* Neutrophils acquire the capacity for antigen presentation to memory CD4(+) T cells in vitro and ex vivo. *Blood* **129**, 1991-2001 (2017).
179. Gevariya, N.*, et al.* Omega-3 fatty acids decrease prostate cancer progression associated with an anti-tumor immune response in eugonadal and castrated mice. *The Prostate* **79**, 9-20 (2019).
180. Apte, S.A., Cavazos, D.A., Whelan, K.A. & Degraffenried, L.A. A low dietary ratio of omega-6 to omega-3 Fatty acids may delay progression of prostate cancer. *Nutrition and cancer* **65**, 556-562 (2013).
181. Trinchieri, G. Interleukin-10 production by effector T cells: Th1 cells show self control. *The Journal of experimental medicine* **204**, 239-243 (2007).
182. Rogero, M.M. & Calder, P.C. Obesity, Inflammation, Toll-Like Receptor 4 and Fatty Acids. *Nutrients* **10**(2018).
183. Innes, J.K. & Calder, P.C. Omega-6 fatty acids and inflammation. *Prostaglandins, leukotrienes, and essential fatty acids* **132**, 41-48 (2018).
184. Ganeshan, K. & Chawla, A. Metabolic regulation of immune responses. *Annual review of immunology* **32**, 609-634 (2014).
185. Wang, H.*, et al.* CD36-mediated metabolic adaptation supports regulatory T cell survival and function in tumors. *Nature immunology* **21**, 298-308 (2020).
186. Watt, M.J.*, et al.* Suppressing fatty acid uptake has therapeutic effects in preclinical models of prostate cancer. *Science translational medicine* **11**(2019).
187. Madonna, R.*, et al.* Omega-3 fatty acids attenuate constitutive and insulin-induced CD36 expression through a suppression of PPAR alpha/gamma activity in microvascular endothelial cells. *Thrombosis and haemostasis* **106**, 500-510 (2011).

188. Di Biase, S.*, et al.* Creatine uptake regulates CD8 T cell antitumor immunity. *The Journal of experimental medicine* **216**, 2869-2882 (2019).
189. Ferretti, R.*, et al.* High-fat diet suppresses the positive effect of creatine supplementation on skeletal muscle function by reducing protein expression of IGF-PI3K-AKT-mTOR pathway. *PloS one* **13**, e0199728 (2018).